The technical design, dynamic simulation and analysis of a wind-powered hydrogen energy system

Emma Croiset van Uchelen *29-11-2019*

TU Delft VATTENFALL

Delft University of Technology

The technical design, dynamic simulation and analysis of a wind-powered hydrogen energy system

Case study: Hemweg 8

---

by

Emma Croiset van Uchelen

To obtain the degree of Master of Science at the Delft University of Technology, to be defended publicly on November 29, 2019

Student number:	4209087	
Project duration:	February 1, 2019 – November 29, 2019	
Thesis committee:	Prof. dr. A. J. M. van Wijk,	TU Delft, supervisor
	Ir. K. Visser,	TU Delft
	Dr. D. J. Scholten,	TU Delft

TU Delft

Abstract

To comply with the 2020 targets for reducing greenhouse gas GHG emissions, the government of the Netherlands ordered to close the coal-fired power plant at Hemweg 8 by the end of the year 2019 and Vattenfall aims to utilise this valuable location in the harbour of Amsterdam for production of green hydrogen and other renewable alternatives.

The objective of this research project was to analyse multiple technical designs, using dynamic simulation, of a wind-powered energy system to produce hydrogen for mobility and industries at the Hemweg 8 location.

The technical characteristics of hydrogen production, storage and transport were analysed in the case study of the Hemweg and a general evaluation of the issues that are relevant regarding the introduction of a wind-powered energy system was conducted. The wind turbines located near the Hemweg were used as a renewable energy source. The present and future hydrogen demands were evaluated and a growing demand for hydrogen is expected. Thereafter, different demand scenarios were determined for the present time and in 2030. A system comparison was made to verify if a wind-powered hydrogen energy system is indeed a viable option for the Hemweg location. Therefore, 4 different system configurations have been evaluated: a hydrogen-energy system with an Alkaline electrolyser and a polymer electrolyte membrane PEM electrolyser, both at 1 MW and 2 MW. All systems have been evaluated for two moments in time: the present time and the year 2030. For the present time, technologies were used that are readily on the market. For the 2030 scenario, expected advancement in technologies were included.

The energy demand is met using wind energy. In case the energy supply is too low, grid electricity is used to provide additional supply. The hydrogen is transported in compressed form and transported at 200 bar to different industries and to fuelling stations for fuel cell electric vehicles ($FCEV$) and hydrogen-powered ships. The wind-powered hydrogen energy systems were modelled in MATLAB and SIMULINK to calculate the amount of hydrogen each electrolyser can produce and how much electricity of the wind turbine is used. When there is lower demand for hydrogen, the electrolysers do not work at nominal load all the time, leading to a higher efficiency. In order to include the change in efficiency, the Alkaline and the PEM electrolyser were both dynamically modelled in detail for each scenario.

An economic analysis of each system-configuration was performed. Important factors that influence the amount of hydrogen output and the levelised cost of the hydrogen are: the running time, partial load performance, output pressure and the share of renewable energy used. The economic analysis and system comparison show that the Alkaline electrolyser with a size of 2 MW produces hydrogen at the lowest levelised cost for the present scenario. For the 2030 scenario, the PEM electrolyser at a 2 MW size is the lowest in levelised cost and is competitive with green hydrogen production prices found on the market. For the present scenario, the hydrogen production cost of the system is 3.8 €/kg and the dispensing price for $FCEV$ is 6.7 €/kg, when working full-time at nominal load. The production cost and the dispensed hydrogen fuel cost price for the future scenario will reduce to 3.2 €/kg and 5.1 €/kg, respectively, which makes the hydrogen a competitive fuel in comparison to the fuel price of gasoline.

From the research findings, it was concluded that the $WACC$ and the cost of electricity supplied by the wind turbine have a large impact and the $CAPEX$ of the electrolyser has a minor impact on the levelised cost of hydrogen. A hydrogen energy system at the Hemweg, powered by wind and grid electricity, is accessed as technological feasible and cost competitive.

Preface

The past ten months I conducted my graduation research in collaboration with Vattenfall. This thesis is my deliverable of my graduation research for the Master of Sustainable Energy Technology at the Delft University of Technology. Through my research, I've conducted multiple technical designs of a wind-powered hydrogen energy system. With the help of dynamic simulations, the designs were economically analysed and recommendations have been made for the Hemweg location in Amsterdam. Working on my thesis, has given me the pleasure to gain great insight into the fundamentals of electrolysers and hydrogen-powered energy systems and an insight into the challenges and opportunities the energy transitions brings for Vattenfall.

Since high school I have been involved in sustainable projects and renewable energy has always been a great interest of mine. During the final year of my bachelor in Civil Engineering, I decided to change my current path and switch to Mechanical Engineering, to subsequently conduct my master in Sustainable Energy Technology because I wanted to contribute to a more sustainable future. I followed the track specialised in Storage, Solar- and Wind-Energy. In this track I was first introduced to hydrogen and its great potential.

Firstly, I would like to express my gratitude to professor Ad van Wijk from the TU Delft for helping me during my research. His enthusiasm and critical questions have encouraged me to think outside the box and has learned me to reflect on my work from an academic angle. Secondly, I would like to thank my other thesis committee member, assistant professor Scholten from the TU Delft for his time in the final stage of my research to read my report and to join the thesis committee. Thirdly I would like to express my gratitude to assistant-professor Visser for the interesting meetings we had, introducing me with sodium-borohydrides and the possibilities for hydrogen-fuelled ships.

It has been very inspiring for me to see the energetic attitude of the employees of Vattenfall in confronting and tackling the challenges that come with the energy transition. I would like to thank Jos van der Valk from Vattenfall Amsterdam for showing me around at the Vattenfall office and for helping me with all my questions and requests. Furthermore, I would like to thank Arne Jacobsen from Vattenfall Hamburg for helping me with the technical aspects of my research and reviewing the technical details of my thesis. Finally, I would like to thank Jacques van der Dool from Vattenfall Amsterdam. During our monthly lunch meetings, he has helped me to reflect on my work and has kept me up to date on the latest developments around hydrogen within Vattenfall. The past ten months have been a very educational and exciting journey for me and I would like to thank him with emphasis for his guidance and support.

Emma Croiset van Uchelen
Delft, November 2019

Contents

List of Figures

List of Tables

Abbreviations

AEC Alkaline Electrolyser Cell

AF Annuity Factor

APX Amsterdam Power Exchange

atm Atmospheric Pressure

$CAPEX$ Capital Expense

CCS Carbon Capture and Storage

CSD Compression

CTV Crew Transfer Vessel

E^0_{cell} Minimal Cell Voltage

E_{act} Anodic and Cathodic Overpotential

E_{con} Concentration Overvoltage

E_{ohm} Overvoltage caused by Ohmic Resistance

E_{op} Operating Voltage

E_t Thermoneutral Cell Voltage

F Faradayconstante

$FCEV$ Fuel Cell Electric Vehicle

GHG Green House Gas

H Hydrogen

HDW Howaldtswerke-Deutsche Werft

HFS Hydrogen Fuelling Station

HHV Higher Heating Value

$HICE$ Hydrogen Internal Comustion Engine

HP High Pressure

I Current through the Conductor

IC Investment Cost

K Kelvin

KOH Potassium Hydroxide

$LH2$ Liquid Hydrogen

LHV Lower Heating Value

$LOHC$ Liquid Organic Hydrogen Carriers

LP Low Pressure

M Molar

MOF Metal-Organic Frameworks

MP Medium Pressure

$NH3$ Ammonia

$O\&M$ Operating & Maintenance Cost

$OPEX$ Operating Expense

PEM Polymer Electrolyte Membrane

$PEMEC$ Polymer Electrolyte Membrane Electrolyser Cell

PSA Pressure Swing Adsorption

ΔQ Heat

R Resistance of the Conductor

$SLCoE_{H2}$ System Levelised Costs of Hydrogen

SMR Steam Methane Reforming

$SOEC$ Solid Oxide Electrolyser Cell

$SOFC$ Solid Oxide Fuel Cell

$WACC$ Weighted Average Cost of Capital

$ZEM - SHIP$ Zero Emission Ship

Chapter 1

Introduction

The Paris climate agreement of 2015 aims to limit temperature increase to well below 2 degrees Celsius above pre-industrial levels. [17] In order to meet the intentions that were set, all 195 countries that signed the agreement, including the Netherlands, have to undertake take ambitious efforts to combat climate change and reduce green house gas (GHG) emissions. [18] At the end of 2015, in the Urgenda Climate Case against the Dutch Government, Dutch citizens stated that their government has a legal duty to prevent climate change. The District Court of the Hague declared the Dutch policy to reduce GHG emissions not fit for purpose and the District Court ruled that there was a gap between the national emission targets and the Paris Agreement targets. As a result, the District Court ordered the government to adjust its policy to achieve a 25% reduction of GHG emissions by 2020 with reference to 1990. This led to another decision by the Dutch government this year, concerning a power plant belonging to Vattenfall Netherlands.

Since 1953, Vattenfall (Formerly Nuon) owns a power station based at the Hemweg location in the harbour of Amsterdam. This power station currently consists of the coal plant based at Hemweg 8 (630MW) and the gas plant at Hemweg 9 (435MW). [19] In March this year, the government decided to close Hemweg 8 earlier than the previously agreed closure date in 2024. The accelerated closure of the power plant must help the Ministry to comply with the court ruling in the Urgenda Climate Case. The coal plant will be closed by the end of this year (2019). The location of Hemweg 8 is near the Port of Amsterdam and in 2020 a new wind farm will be opened close to the Hemweg by Vattenfall in collaboration with NS. [20] The obligatory closing of Hemweg 8 creates new opportunities for the land use of this valuable location. Vattenfall aims to develop sustainable alternatives for a fossil-free transition at the Hemweg location.[19]

Many technologies already exist that can help succeed the transition to a low-carbon economy with a low, or a non-existing, output of GHG emissions. The use of renewable energy sources such as wind and solar power, is growing. [21] The electricity created by wind and solar power is highly fluctuating during the days and with the seasons. This fluctuation causes an imbalance in the grid and a need for energy storage when the renewable energy sources are producing a surplus of electricity on a short term base (day and night) and on a long term base (weeks and seasons). Using hydrogen as an energy carrier is an option for storing electricity on a long term base. Hydrogen can also be used as a replacement for fossil fuels in the transport sector. Future applications of hydrogen as a fuel for airplanes, ships, buses and cars are being explored. As the Netherlands has to undertake actions to reduce the GHG emissions, it is of interest for Vattenfall and the TU Delft to be part of the transition to a low carbon economy and to explore how this would have to take place.

In the future, the Hemweg site will serve as a fossil-free 'hub' for electricity and heat. In addition, alternative fuels such as green hydrogen and synthetic kerosene will be produced at the Hemweg site. Vattenfall aims to provide green fuels to the aviation industry, the shipping industry and the mobility sector. When the new wind farm creates a surplus of electricity, this could be stored in the form of hydrogen and possibly be used as a green fuel. How such a wind to hydrogen energy system would work at the Hemweg site and if it would be economically feasible needs to be analysed.

Chapter 2

Research Methodology

2.1 Objective

The objective of this research is to analyse multiple technical designs, using dynamic simulation of a wind-powered energy system - at the Vattenfall location Hemweg 8 - to produce hydrogen for mobility and industries.

2.2 Research Question and Sub Questions

- **How can a cost competitive hydrogen energy system be designed at the Hemweg location, using available wind power, ensuring reliability of hydrogen supply at all times?**
  - Which characteristics of technologies for production, storage and fuelling of hydrogen are relevant?
  - Which electrolyser is the best option for this case study: A *PEM* electrolyser or an Alkaline electrolyser?
  - How much green hydrogen can be produced and is that amount sufficient to meet the demand of consumers?
  - Can a wind to hydrogen energy system on the Hemweg location be cost competitive compared to alternative hydrogen energy systems?

2.3 Report Outline

In order to answer the research questions, a description of the case study, energy system designs, dynamic modelling, energy balance and cost analysis of the energy systems is provided in the report. The following structure is used for the report: after introducing the objective and research questions, the methodology and scope of the research is explained. In chapter 3 an introduction to hydrogen and the characteristics of all technologies involved will be given. Chapter 4 describes the case study and the designs for the possible system configurations. Chapter 5 describes how the system components were modelled and how the energy is balanced. Chapter 6 presents the modelling results. In chapter 7, an economic analysis for every energy system configuration is carried out. Finally, the research approach is discussed and the answers of the research questions, followed by recommendations for further research, are provided in chapter 8.

2.4 Methodology

The research will be performed in seven steps:

1. Firstly, a literature study will be done to identify important characteristics of the technologies utilised for production, transport, storage and fuelling of hydrogen. Different technologies will be analysed for various system configurations.

2. The electricity supply from the wind park will be estimated with the collected wind data.

3. The technical aspects from hydrogen-powered ships and other consumers will be considered, to make a relevant estimation of the hydrogen demand for two moments in time: a present and 2030 scenario.

4. Multiple energy system configurations will be designed and for each energy system configuration, technologies for production, storage, transport and fuelling will be selected.

5. The different system configurations proposed will be modelled. The softwares MATLAB and Simulink will be used to match the demand and supply and calculate efficiency and losses. For every system configuration the required electricity and the amount of hydrogen produced will be determined. The results of each system configuration will be compared and discussed.

6. An economic analysis for every energy system configuration will be carried out in Excel and the levelised cost of hydrogen for every system configuration will be calculated for the two time frames.

7. Ultimately, conclusions and recommendations will be provided. The results of the research will consist of a model in MATLAB, an excel sheet with the economic analysis and a report with the findings and conclusions. The results will give insight in how a cost competitive hydrogen energy system can be designed at the Hemweg location using available wind power.

Chapter 3

Hydrogen as a Future Energy Carrier

In this chapter a general introduction to hydrogen is given, after which the fundamentals and possibilities of green hydrogen production are discussed and compared. Next, the storage methods for hydrogen are described and categorised. The final section of this chapter discusses how hydrogen can be used as a fuel.

3.1 General Introduction to Hydrogen

Hydrogen is a chemical element with symbol H. The hydrogen atom is the most abundant element in the universe. The atom H consists of a proton and an electron, making it the lightest element in the universe. [22] However, the hydrogen gas molecule does not occur in nature and can only be produced by a chemical process. Hydrogen is one of three gases (Helium, Hydrogen and Neon) which have negative Joule-Thomson coefficients at normal temperature and pressure conditions. This means that when hydrogen is compressed the temperature of the molecule lowers. Subsequently, when hydrogen's pressure is reduced, its temperature rises. Basic physical properties of hydrogen are shown in table 3.1:

Properties	
Molar Mass	2.02 g/mol
Lower Heating Value by Volume	10.8 MJ/nm^3
Lower Heating Value by Mass	120 MJ/kg
Higher Heating Value by Volume	12.75 MJ/nm^3
Higher Heating Value by Mass	142 MJ/kg
Vapour Density [a]	0.0899 kg/nm^3

[a] At standard conditions for temperature and pressure.

Table 3.1: Physical properties of hydrogen

Hydrogen can be used for many applications such as: welding, annealing, petroleum refining, glass purification, aerospace applications, fertiliser production, methanol production, hydrogen peroxide production, heat-treating metals, steel production, synthetic fuel production, pharmaceuticals and as a coolant in power plant generators. Besides all these uses, hydrogen has the potential to have a significant role in realising the energy transition. Hydrogen can be used as a clean energy carrier, meaning an energy carrier without carbon emissions. At present, the prospects for hydrogen as an energy carrier are being researched, as electrification is growing in transport and other sectors. Hydrogen could replace fossil fuels in different areas, e.g. mobility and heating. Furthermore, hydrogen could be a suitable alternative for long-term seasonal energy storage since batteries have much lower energy density than hydrogen and the chemical energy in batteries degrades more quickly over time. [15]

3.2 Green Hydrogen Production

Hydrogen can be produced using several chemical methods that require energy sources such as nuclear energy, fossil fuels and renewable energy. Currently, 96% of the hydrogen in the world is produced using fossil fuels with natural gas as the main raw feed-stock. [1] Figure 3.1 shows the hydrogen production methods and the corresponding energy sources. The methods for hydrogen production are often divided into three different categories; grey, blue or green. Grey hydrogen is hydrogen which is produced with the use of fossil fuels. The most common form of grey hydrogen production is steam methane reforming (SMR). Blue hydrogen is also produced with fossil fuels but the CO2 that is produced during the process is captured and stored, preventing it from entering the atmosphere. This procedure is called carbon capture and storage (CCS). Green hydrogen is produced without fossil fuels and can be produced with electrolysis. In electrolysis electricity is used to split water into hydrogen and oxygen. The hydrogen from electrolysis is only considered green if the electricity that is used for the electrolysis process is from a renewable energy source such as solar, biomass or wind energy. To make appropriate choices concerning what type of electrolyser is best to use, the technological aspects of electrolysis will be discussed.

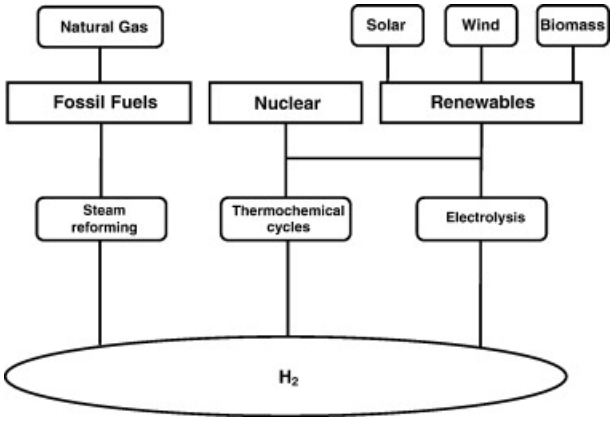

Figure 3.1: Main hydrogen production methods [1]

3.2.1 Concept and Fundamentals of Water Electrolysis

Electrolysers are made out of individual cells and central system units, referred to as "balance of plant". Electrolyser cells consist out of a cathode and an anode, separated by an electrolyte. During the process of electrolysis, electricity is used to split water into hydrogen and oxygen. The cathode is where reduction (gain of electrons) takes place and the anode is where oxidation (loss of electrons) takes place. In figure 3.2 the basic arrangement of an electrolyser is shown.

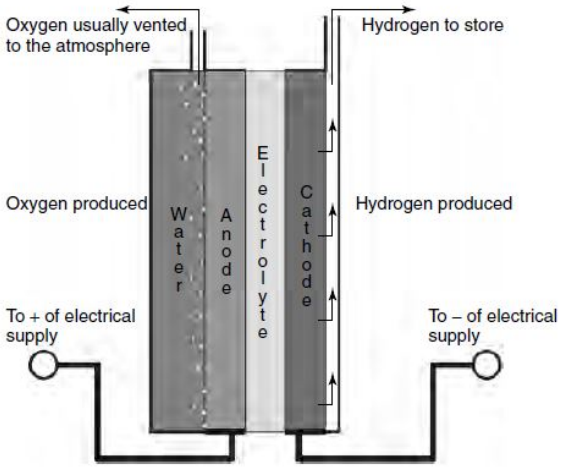

Figure 3.2: Simplified electrolyser [2]

At the anode (the positive electrode), the water is oxidised - electrons are removed - and oxygen is created via the reaction:

$$2H_2O \longrightarrow O_2 + 4e^- + 4H^+ \tag{3.1}$$

At the cathode (the negative electrode), hydrogen ions combine with electrons, which are supplied by an external circuit. Consequently, hydrogen is formed via the reaction:

$$4H^+ + 4e^- \longrightarrow 2H_2 \tag{3.2}$$

The overall chemical reaction of the water electrolysis can be expressed as:

$$2H_2O \longrightarrow O_2 + 2H_2 \tag{3.3}$$

The change in enthalpy (ΔH) represents the necessary energy that is needed to accomplish the electrolysis. The necessary energy can partly be supplied by heat (ΔQ) from the environment and partly by the change in Gibbs energy (ΔG), which is supplied electrically. Thus, the change in enthalpy equals the Gibbs energy + heat, which is expressed as:

$$\Delta H = \Delta G + \Delta Q \tag{3.4}$$

In a temperature range of 0-1000$°C$, the overall energy demand for the electrolysis (ΔH) varies a little between 283.5 and 291.6 $kJ/mol\ H_2$. [3] ΔH rises slowly with temperature and the heat demand ΔQ rises strongly with temperature, which reduces the demand for electrical energy ΔG at higher temperatures as shown in figure 3.3. The higher the temperature the lower the ratio of ΔG to ΔH is. Thus, the high temperature electrolysis requires less electricity to produce hydrogen than low temperature electrolysis. Heat production by internal losses can be utilised for the electrolysis, which makes the process more efficient at higher temperatures.

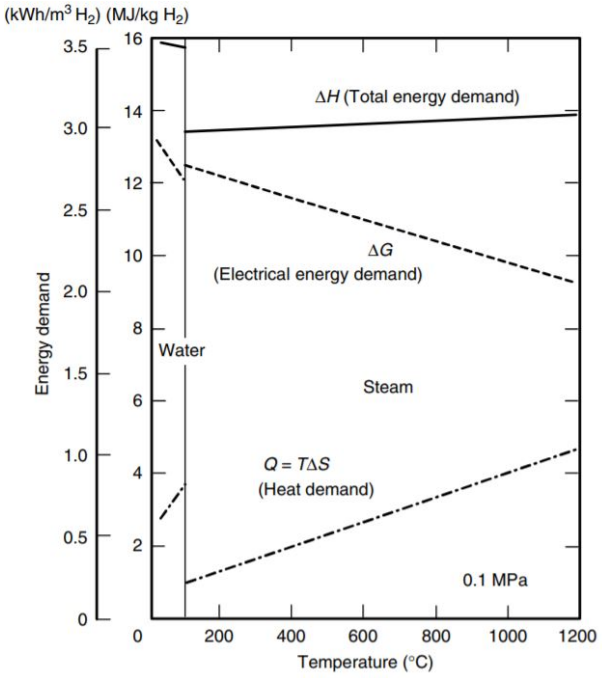

Figure 3.3: Enthalpie (ΔH), Gibbs energy (ΔG) and thermal energy (ΔQ) as a function of temperature of an ideal electrolysis process [3]

Standard conditions is defined as a temperature of 298.15 K (25$°C$), a pressure of 1 atm, and a Molarity of 1.0 M for both the anode and cathode solutions. The minimum necessary cell voltage for the start-up of electrolysis, E^0_{cell}, also called reversible cell voltage, is expressed under standard conditions with the following equation:

$$E^0_{cell} = \frac{\Delta G}{nF} \tag{3.5}$$

With n being the number of electrons transferred and F is the Faraday constante which is 96485 C/mol. The reversible voltage is equal to 1.23 V and ΔG is 237.2 kJ/mol, at standard conditions. E^0_{cell} decreases with rising temperature as shown in figure 3.4. Within the temperature range of 0-1000°C, E^0_{cell} varies in the range of 1.25-0.91 V. [3] It is an endothermic process as the process requires heat, under reversible conditions, or it will cool itself down.

Joule heating, also known as ohmic heating or resistive heating, is a process in which heat is produced. Joule heating results from electrons moving through conductors and ions moving through the electrolyte. This heat can become significant enough to produce an overall heating effect within the electrolysis cell, even with an endothermic process going on at the same time. The thermoneutral cell voltage, E_t, is the voltage at which the joule heating provides enough heat to maintain the temperature of the cell during electrolysis. E_t gives the minimum voltage necessary for electrolysis in an ideal cell without any heat integration. This is called an isothermal process because the temperature remains constant. Under standard conditions the thermoneutral cell voltage is expressed with the following equation:

$$E_t = \frac{\Delta H}{nF} \tag{3.6}$$

With n being the number of electrons transferred, F in C/mol and ΔH in kJ/mol. To prevent heat integration to take place, the overall energy demand ΔH (including the heat ΔQ) of the electrolysis is supplied electrically. E_t is approximately 1.47-1.48 V, which is equal to 284-286 $kJ/mol\ H^2$, at standard conditions and feed with liquid water below 100°C. Any cell that operates at a voltage of greater magnitude than E_t will generate more heat than is needed for electrolysis. A cell that operates at a lower voltage will need heat in order to maintain the temperature. A cell that operates at the thermoneutral cell voltage will need neither heating nor cooling to remain at a temperature. When steam is supplied instead of liquid water, E_t decreases to 1.26-1.29 V (243-249 $kJ/mol\ H^2$). This means that steam electrolysis can reduce the minimum electrical energy consumption E_t with 41 kJ/mol. Steam electrolysis can replace valuable electrical energy in the form of hydrogen by evaporation of water.

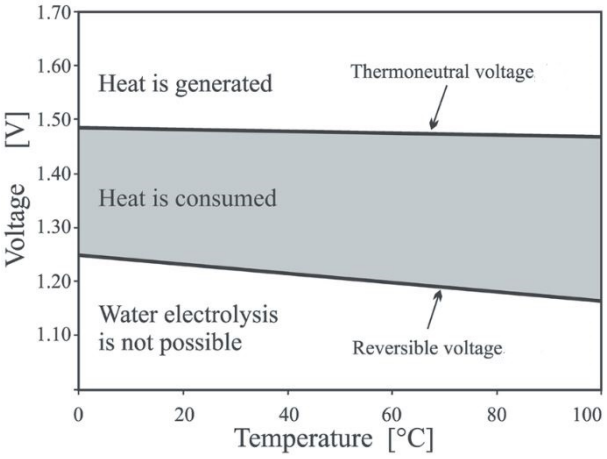

Figure 3.4: Reversible and thermoneutral voltage for electrolysis as a function of temperature at a pressure of 1 atm [4]

In figure 3.4 the thermoneutral cell voltage and the reversible voltage as a function of temperature are shown. Electrolysers are operated above E_t due to the over-voltages. [3] For all electrolysers, the operating cell voltage for thermoneutral operations is moderately higher than E_t because of losses or over-voltages. Operation at a voltage level above E_t heats up the module and external cooling of the cells is required for low temperature electrolysers. The operating voltage or actual voltage E_{op} of an electrolyser can be expressed as:

$$E_{op} = E_0 + E_{ohm} + E_{act} + E_{con} \tag{3.7}$$

With E^0_{cell} being the reversible cell voltage, E_{ohm} being the over-potential caused by ohmic resistance, E_{act} being the anodic and cathodic over-potentials and E_{con} being the concentration over-potential caused by mass transport, all expressed in V. The over-potentials should be kept low in order to maximise the efficiency and to minimise the production of heat. However, the lower the over-potential the slower the reaction will proceed. [23] The three different over-potentials of over-voltages briefly explained:

- **Activation Loss**. The activation loss is represented by the over-potential in the anode and cathode E_{act}, created as a result of polarisation effects, including low activity of the electrodes in the electrolyte. The over-potential in the electrodes increases logarithmically with current density as given by the Tafel relation:

$$E_{act} = a + b \times ln(i) \tag{3.8}$$

Where a and b are constants, and i is the current density in A/cm^2. The over-potential at the electrodes can be minimised by selecting electrode materials with high electro-catalytic activity, maximising the contact area between the electrodes and the liquid and increasing the temperature and pressure to enhance the reaction rate. When operating at higher current densities, the over-voltage is increased.[4]

- **Ohmic Loss**. The term E_{ohm} represents the energy losses related to ohmic drops within the electrolytic cell. These occur mainly at the electrodes, metal-metal joints, electrical lead wires and inside the electrolyte. [4] The ohmic over-voltage can be lowered by optimising the cell design, for instance: The distance between the electrodes could be minimised and the resistance of the electrolyte could be reduced (by increasing the temperature). The ohmic over-voltage changes according to Ohm's law:

$$E_{ohm} = R \times I \tag{3.9}$$

Where R is the resistance (in Ω) of the conductor and I the current in A.

- **Concentration Loss**. The concentration loss or over-voltage is caused by mass transfer losses, caused by the decrease in reactant concentration at the surface of the electrodes. At maximum current, the reactant concentration at the catalyst surface is approximately zero, as soon as the reactants are supplied to the surface, they are consumed. Concentration loss starts being very important at higher currents, while at low currents it is negligible. The concentration over-potential is expressed as:

$$E_{con} = \frac{R \times T}{2F} \times ln(1 - (\frac{I}{I_L})) \times I \tag{3.10}$$

With R being the gas constant equal to 8.3145 $J/Kmol^{-}1$, T being the temperature in K, F being the Faraday's constant, I being the current used in A and I_L is the limiting current at the point where the gas is consumed at an equal rate as the maximum power supply.

A polarisation curve shows the voltage loss for different currents, as shown in the graph below:

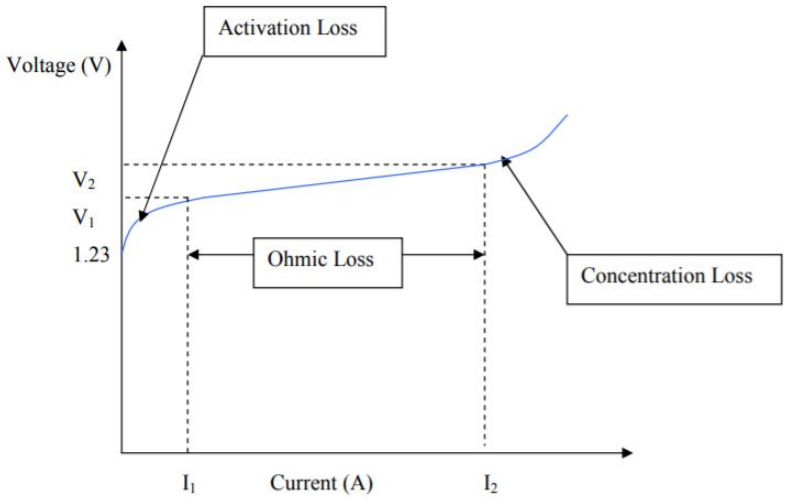

Figure 3.5: Polarisation curve [5]

The three different regions of Activation loss, Ohmic loss and Concentration loss are clearly shown in the voltage current graph. As can be seen for each loss or overpotential there is a voltage loss at different currents. According to Faraday's law, the current density is proportional to the hydrogen production rate. This however

only works for electrolysis in an ideal situation, in other cases the Faraday efficiency η_F has to be taken into account. η_F is defined as the ratio of the actual to the theoretical production rate of hydrogen. This variation is created by cross permeation of the produced gases and parasitic current losses. Cross-permeation is the process of hydrogen and oxygen being produced at both sides of the electrode, permeating through the electrolyte and then mixing together at the counter electrode. Cross-permeation increases with higher temperature and pressure and decreases at low current densities which causes a decreased gas production. [3] The parasitic current is an unintended current flow that increases at low electric resistance which is caused by high temperatures and lower current density. Which makes it especially relevant for high-temperature electrolysers. The Faraday efficiency of low temperature electrolysers is reported to be close to 100% at nominal current density. [3] Electrolysers can have two different designs: The unipolar and the bipolar design. The unipolar electrolyser consists of electrodes connected in parallel. The bipolar design is more common and in the bipolar design the electrolysis cells are connected in series. Hydrogen is produced at one side of the cell and oxygen at the other. The total hydrogen production rate in Nm^3/h for bipolar modules is defined as:

$$\dot{V}_{H2} = \eta_F \frac{n_c I}{2F} \times [22.414 \times 3.6 \frac{Nm^3/h}{mol/s}] \tag{3.11}$$

Where η_F is the Faraday efficiency, n_c is the number of electrolysis cells electrically connected in series, I is the current in A and F is the Faraday constant.
The efficiency of an electrolyser is expressed with the following equation:

$$\eta_{HHV} = \frac{\dot{V}_{H2} \times HHV_{H2}}{P_e} \tag{3.12}$$

Where HHV_{H2} is the higher heating value of hydrogen (3.54 $kWh/Nm3$), $\dot{V}_{H2}$ is the hydrogen production rate in Nm^3/h and P_{el} is the electrical energy consumption in kW. The heating value is the amount of heat produced by a complete combustion of a fuel. The efficiency of low temperature electrolysis is often provided based on the HHV.

Using higher of lower heating value is fairly arbitrary. When liquid water exists in the combustion products, which is the case for low temperature electrolysis, the higher heating value HHV is commonly used. Both the HHV and the lower heating value (LHV) are defined as the amount of heat released when the fuel (initially at $25°C$) is combusted and the products have returned to a temperature of $25°C$. For the HHV, the heat of condensation of the water is included in the total measured heat and is is assumed that all water vapour condenses. [24] The LHV assumes that all water vapour formed by combustion remains in vaporised state. [25] The LHV is determined by subtracting the heat of vaporisation of water that is generated during the combustion of the fuel, from the higher heating value and is 3.00 $kWh/Nm3$.[3] Thus, the efficiency of an electrolyser using the LHV is defined as:

$$\eta_{LHV} = \frac{3.00}{3.54} \times \eta_{HHV} \tag{3.13}$$

Using the LHV can result in a system efficiency of over a 100%, which is thermodynamically impossible. The higher heating value accounts for all the energy available and using the HHV will never result in an efficiency which is above 100%. That is the reason why from now on, the HHV will be used in this report for all efficiency's, unless indicated otherwise.

The efficiency of the electrolysis process increases when the over-potentials decrease. This happens when:

- The current density decreases.
- The temperature increases.
- The pressure slightly decreases.

Different types of electrolysers are distinguished due to the different type of electrolyte material utilised. There are currently three different types of electrolyser cells mainly is use; the Proton Exchange Membrane (PEM) Electrolyser Cells, the Alkaline Electrolyser Cells (AEC) and the Solid Oxide Electrolyser Cells ($SOEC$).

3.2.2 PEM Electrolyser

A PEM electrolyser cell ($PEMEC$) was first utilised by General Electric in the 1960s. [3] The $PEMEC$ uses an ionically conductive solid polymer as electrolyte, which makes the $PEMEC$ a very compact device. In figure

3.6 a basic layout of a $PEMEC$ is shown. The electrolyte and the two electrodes are in between two bipolar plates. A proton exchange membrane separates the two half-cells. The corrosive acidic environment of the proton exchange membrane requires the electrodes to be made out of noble metals such as iridium for the anode and platinum for the cathode. [3] The $PEMEC$ operates at low temperature of approximately $70 - 90°C$.

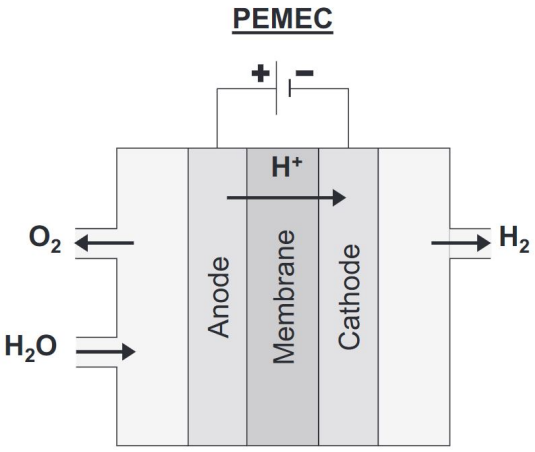

Figure 3.6: Simplified $PEMEC$ electrolyser [6]

When a potential difference (voltage) from an external circuit is applied between the two electrodes, the water molecules split into protons (H^+), electrons (e^-) and oxygen (O_2) at the anode. The H^+ ions travel through the polymer, which conducts protons, towards the cathode where they combine with an electron to become a neutral H atom. The H atoms combine and become H_2 at the cathode:

$$Cathode : 4H^+ + 4e^- \longrightarrow 2H_2 \tag{3.14}$$

$$Anode : 2H_2O \longrightarrow O_2 + 4H^+ + 4e^- \tag{3.15}$$

The $PEMEC$ has a very low cross-permeation, yielding hydrogen with a very high purity that is typically higher than 99.99%. [26] The design of the $PEMEC$ is very compact because of the solid electrolyte and high current density operation. The solid electrolyte makes high pressure operation of the electrolysis possible. A high pressure is allowed between the electrodes which can reach high pressures of 85 bar [3], with a few exceptions reaching up to 350 bar, but only on cell level and never on bigger scale [27]. The highest commercial output pressure is found to be 40 bar. [28][29]

A comparison of multiple studies was conducted by A. Buttler and H. Spliethoff [3], where the I-U-curves for commercial AEC, $PEMEC$ and $SOEC$ are summarised. The commercial $PEMEC$ shown in figure 3.7 typically reach current densities up to 2 A/cm^2. This corresponds to a specific hydrogen production rate of 8.4 Nm^3/m^2 cell area, which is a lot higher than for AEC. At nominal current density, 2 A/cm^2, the efficiency varies between 50-76%, which is within the same range as AEC, however with a higher current density. As shown in figure 3.7, the efficiency increases at lower current densities (partial load performance), similar as the AEC.

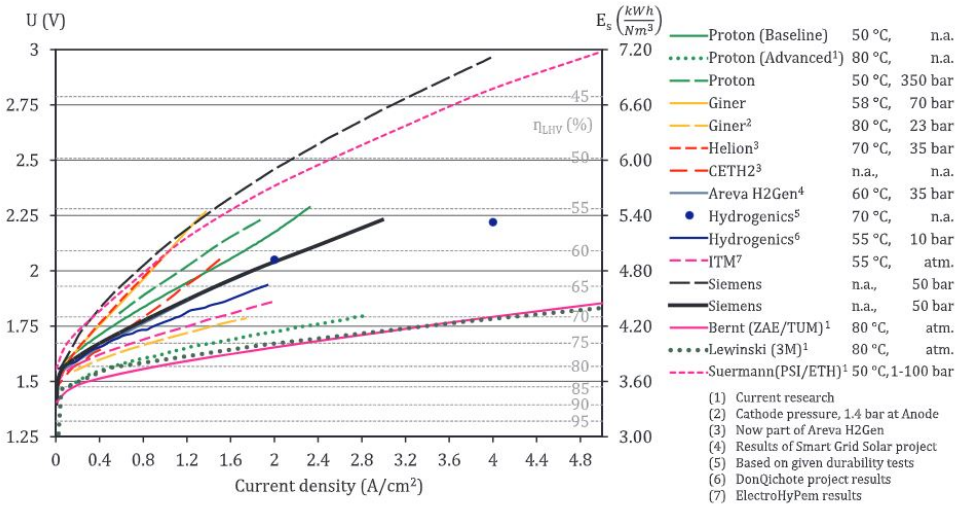

Figure 3.7: Overview of I-U-curves of PEM electrolysers [3]

3.2.3 Alkaline Electrolysers

Alkaline Electrolyser Cells *AEC* have been used since 1920 for large-scale industrial applications of MW-scale. [6] In an *AEC* hydroxide ions (OH^-) are transported from the cathode to the anode through the electrolyte with hydrogen being generated at the cathode side. The principle layout of an *AEC* is shown in figure 3.8.

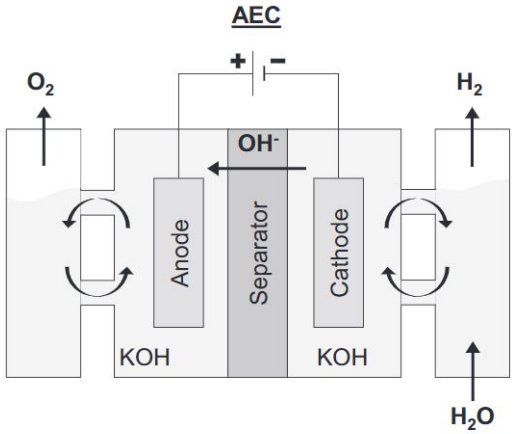

Figure 3.8: Simplified *AEC* electrolyser [6]

The electrodes, separated by a diaphragm, are placed in a liquid electrolyte. Usually, the electrolyte is a liquid alkaline solution of sodium or potassium hydroxide (KOH). The *AEC* operates at low temperatures of around 100 – 150°C. At the partial reactions at the electrodes H_2 and H_2O are formed:

$$Cathode : 2H_2O + 2e^- \longrightarrow 2OH^- + H_2 \tag{3.16}$$

$$Anode : 2OH^- \longrightarrow \frac{1}{2}O_2 + H_2O + 2e^- \tag{3.17}$$

Water is consumed at the cathode side and water is produced at the anode side. The *AEC* systems are durable and have relatively low capital costs due to non-noble metals such as nickel for the electrodes. The hydrogen quality is typically in the range of 99.5-99.9%. [3] The output pressure can reach a maximum of 30 bar. [3]The I-U-curve for commercial *AEC* is shown in figure 3.9. The commercial *AEC* reach current densities up to 0.45 A/cm^2 (with a few exceptions further explained in [3]), which corresponds to a specific production rate of 1.9 Nm^3/m^3 of hydrogen. The efficiency, at nominal current density (0.4 A/cm^2), varies between 60-75%,

which corresponds to a specific energy consumption of 4-5 kWh/Nm^3. In partial load operation - with lower current density - the efficiency is increased. At 0.1 A/cm^2 the efficiency is approximately 73-86% However, these other parts of the system will not be fully utilised, which lowers the overall efficiency of the system.

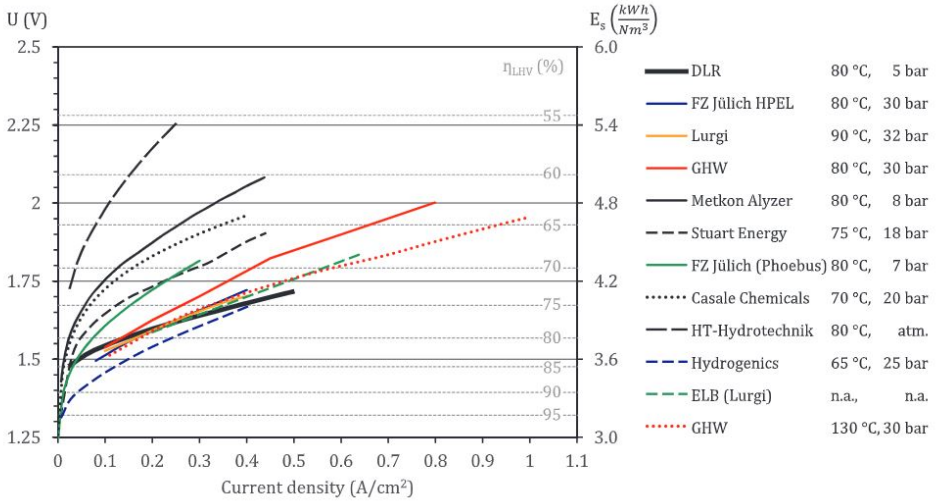

Figure 3.9: Overview of I-U-curves of alkaline electrolysers [3]

3.2.4 Solid Oxide Electrolyser

Solid oxide electrolyser cells ($SOEC$) were first developed in the 1970s and are commercialised only recently. [3] [30] $SOEC$ consists of electrodes and an electrolyte of a solid ceramic material that selects negatively charged oxygen ions (O^{2-}) to conduct through the electrolyte. The $SOEC$ operates at a temperature of 700 - 900°C. [3] That the $SOEC$ operates at such a high temperature results in a high efficiency caused by improved kinetics and can effectively utilise available heat to decrease the amount of electrical energy that is needed. A simplified layout of a $SOEC$ electrolyser is shown in figure 3.10.

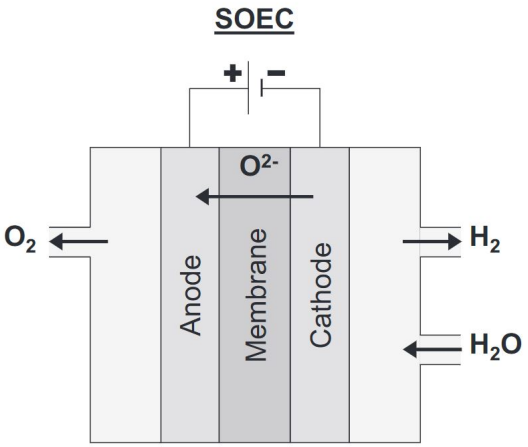

Figure 3.10: Simplified $SOEC$ electrolyser [6]

At the partial reactions at the electrodes H_2 and O_2 are formed:

$$Cathode : 2H_2O + 4e^- \longrightarrow 2O^{2-} + 2H_2 \tag{3.18}$$

$$Anode : 2O^{2-} \longrightarrow O_2 + 4e^- \tag{3.19}$$

Water combines with electrons supplied by the external circuit and forms hydrogen gas and negatively charged oxygen ions at the cathode. The oxygen ions pass through the solid ceramic membrane and form oxygen gas

and electrons at the anode, which are supplied to the external circuit. The *SOEC* offers some interesting applications such as the ability to produce syngas, a fuel gas mixture consisting primarily of H_2, CO, and often some CO_2. Another interesting application is the reversible operation increasing the utilisation capacity. However, the *SOEC* is still at a research stage and has been used only for small applications. In figure 3.11 the I-U-curves of multiple *SOEC* are shown. These are more difficult to determine due to dependence on factors such as the steam conversion rate, which rises at higher current densities and lower feed flow, and factors such as the feed composition and sweep gas on the oxygen side. [3] Because *SOEC* are still in a research state the curves presented provide only an approximation of the performance. The limitations of the current density are caused by degradation issues, which have to be reduced first before *SOEC* can be used commercially at high current densities. As can be seen in the graph, there is potential for the *SOEC* to operate at very high current densities at thermoneutral cell voltage.

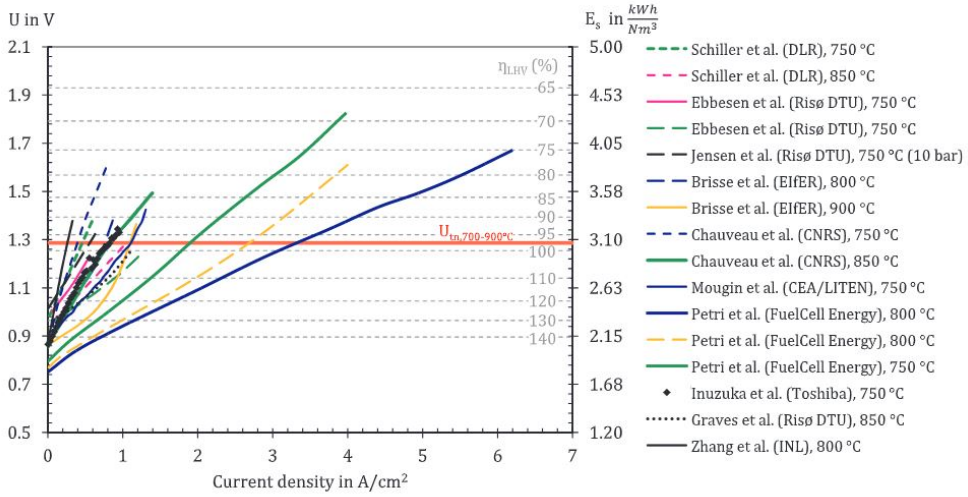

Figure 3.11: Overview of I-U-curves of solid oxide electrolysers [3]

As the energy system will be designed for the near future, the *SOEC* will be left out of this research. The *SOEC* is still in a research phase and only very small-scale systems are offered on the commercial market. *AEC* have been available on MW-scale (up to 6 MW) for a long time and *PEMEC* has been scaling up in recent years up to 2 MW. [3] The *SOEC* could be interesting for Vattenfall research within the R&D department and keep a close eye on the market developments. For this specific scope of building a wind to hydrogen system within the coming few years, it is more useful to focus on the established technologies and research incremental adjustments or additions for the system. A possible addition could be the Battolyser.

3.2.5 Battolyser

The Battolyser is still a new concept, invented by professor Mulder and his research group of the TU Delft. A Battolyser is an integrated battery and electrolyser concept combined, based on a nickel-iron battery. The battery provides storage capacity for electricity. When a surplus of renewable electricity is available the battery is charged and when there is a need for electricity the battery is discharged. Most conventional batteries will be destroyed rapidly by overcharging or deep discharging. [31] When the battery in the Battolyser is reaching its maximum capacity, hydrogen will be produced from the excess electricity. It is a combination of short-term battery storage and long-term hydrogen storage. The TU Delft and Vattenfall are planning on realising a model of 15 kW at the Magnumcentrale of Vattenfall in Eemshaven in 2019. [32] The Battolyser has not yet been developed for larger applications of kW or MW scale. The Battolyser consist of two electrodes containing: $Fe(OH)_2$ and $Ni(OH)_2$. The electrolyte is made out of KOH and conducts OH^- ions. When charged the negative electrode reduces $Fe(OH)_2$ to Fe:

$$Cathode : Fe(OH)_2 + 2e^- \longrightarrow Fe + 2OH^- \tag{3.20}$$

The positive electrode contains $Ni(OH)_2$ and when charged it releases a proton:

$$Anode : Ni(OH)_2 + OH^- \longrightarrow NiOOH + H_2O + e^- \tag{3.21}$$

When the battery is fully charged, the electrodes that formed into Fe and $NiOOH$ work as catalyst for the following reactions at the positive electrode and the negative electrode, respectively:

$$Anode : 4OH^- \longrightarrow O_2 + 2H_2O + 4e^- \tag{3.22}$$

$$Cathode : 2H_2O + 2e^- \longrightarrow H_2 + 2OH^- \tag{3.23}$$

A ceramic polymer composite diaphragm is used to separate the hydrogen and oxygen gas while the OH ions are transferred between the electrodes. [31] Until now, the Battolyser is used with a maximum temperature of $40°C$, to prevent potential long-term stability issues of the electrode made out of iron. [31] Nickel and iron are earth abundant elements, and no catalysts constructed out of noble metals have to be used. The heat losses in the charging process are used for the electrolysis which makes the Battolyser very efficient. The electrolyser efficiency of the Battolyser is approximately 80-90%. [7] The partial and total efficiencies are demonstrated in figure 3.12. The green area is the electrical energy output, while the hydrogen output is represented by the blue area. The white area displays the energy losses. The overall charge that is inserted, either discharges the battery or produces hydrogen. Total and partial energy efficiencies of the battery and the electrolyser are given by dividing the relevant area's by the total inserted energy. The Battolyser is still in a research and development phase, therefore no commercial data is available. However it could be interesting in the future to explore the possibility of using a Battolyser to balance demand and supply.

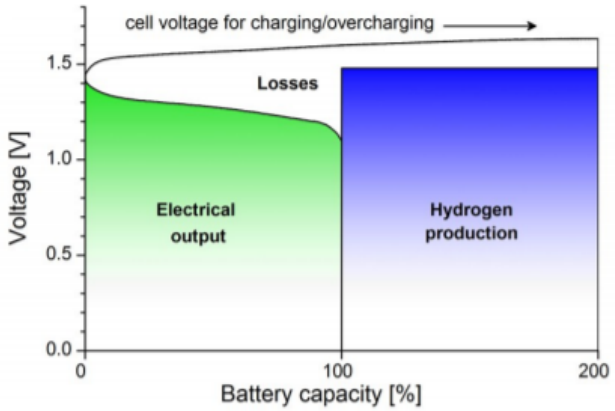

Figure 3.12: Overview of the cell voltage at a capacity usage of the Battolyser [7]

3.2.6 Comparison of Alkaline and PEM Electrolysers

The performance and availability of the AEC and the PEM electrolyser are previously discussed. There are however more criteria that could be compared between the two. In this subsection the AEC and the PEM electrolyser will be compared for the following discrete criteria: pressured operation, flexibility, sustainability and lifetime and maintenance costs.

Pressurised Operation
In most cases the standard pressure of commercial AEC is below 30 bar and for $PEMEC$ 40 bar or below. [3] Yet, very high pressure operation of around 345-448 bar for both electrolysers has been demonstrated used for filling of hydrogen-fuelled cars. For AEC it is challenging to operate at high pressure because of cross-permeation. However, for $PEMEC$ high pressure operation is promising as it shows low permeation across the membrane at higher pressure. It can be of value to operate the electrolyser at high pressure as hydrogen is usually stored and utilised at high pressure as well. Operating at high pressure can exclude the compressor, which reduces investment and maintenance costs and increases reliability. [3] An advantage of operation at atmospheric pressure, which can be done with the Alkaline electrolyser, is that cells can be easily replaced. This results in a higher up-time and higher operating cost of the electrolyser in comparison with PEM electrolyser, working under higher pressures. High pressure operation increases the reversible cell voltage and has a positive effect on the kinetics, hence, the efficiency. The kinetics are improved as a result of a reduction of the size of gaseous bubbles when operating at higher pressure. At the anode, this effect can stop the transport of liquid water up to the electrocatalytic layer through the current collectors and increase anodic overpotential and increase the ohmic overpotential. This, however, is counter-balanced by a negative effect on faradaic efficiency with pressure, because of higher cross-permeation of gasses. [33] Increased pressure also leads to higher degradation rate and a higher chance of gas leakages, which comes with safety risks. Especially for Alkaline electrolysers, this requires additional safety equipment which results in higher investment costs. Whether high pressure operation of electrolysis is potentially higher in efficiency and reduces investment and operation costs is debated controversially in literature. [34] [3] [35]

Flexibility
The flexibility of electrolysers can be divided in different factors: Load range, transient operation, cold and warm start-up and stand-by losses. The load range gives an indication of the minimum and maximum load with which an electrolyser can operate. Alkaline electrolysers are known to be limited with 20-25% of the nominal hydrogen production. If the load is lower, the cross-over of hydrogen to the oxygen side will increase too much, resulting in a flammable mixture. [3] Most commercial $PEMEC$ on the other hand, do not have a minimum load limit. Both $PEMEC$ and AEC are capable of reacting very rapidly with a power response signal less than 1 sec, which can be useful for stabilising power-grids. They both can be operated very dynamically. [3] $PEMEC$ have a shorter heat-up time (5-10 min) compared to AEC (1-2 hours). [3] Both can be kept on temperature in stand-by mode for a more flexible operation. The heating in stand-by mode contributes to the stand-by losses. Other stand-by losses can be caused by purging the gas compartments to avoid cross permeation, applying protective current to avoid degradation. These, however, do not show a significant difference or impact for both the $PEMEC$ and AEC. [3]

Sustainability
The catalysts are considered the main source of environmental impact in the manufacturing of electrolysers. Currently, the material that are most commonly used for catalysts for PEM electrolysers, are noble metals, such as iridium and platinum. Noble metals are scarce, contain a high toxicity and have a high environmental impact, in addition to being costly.[36] While, AEC usually contain non-noble catalysts made out of nickel. This shows potentially an environmental advantage for AEC and $SOEC$. However, when the hydrogen is produced by electrolysers, with electricity provided by renewable energy, GHG emissions are considered insignificant compared to alternative hydrogen production technologies (such as steam methane reformation). In addition, several experts believe that the potential of hydrogen to store renewable electricity, or to de-carbonise different energy sectors like heat or transport, outweighs any toxicity or emission impact associated with the manufacturing of electrolysers significantly. [6]

Lifetime, Investment and Maintenance costs
The balance of plant has a typical lifetime of 30-50 years for AEC and approximately 30 years for $PEMEC$. The cells of an Alkaline electrolyser have a lifetime in the range of 55.000-96.000 h and the $PEMEC$ cells report a lifetime in the range of 60.000-100.000 h. [3] The operating costs are small, hence reduction of capital costs

has priority for both the AEC and $PEMEC$ electrolysers. [6] $PEMEC$ are relatively newer in the commercial field and have potential of becoming more efficient in the future, thus cheaper. AEC is a mature technology and is currently lower in capital cost than then $PEMEC$. Cost estimates were compared in different literature studies for the 2 electrolysers. Capital costs, which are strongly dependent on size, lie approximately between 700 and 1200 €/kW for AEC. For $PEMEC$ the cost range is approximately 1000–1650 €/kW, representing a strong improvement over the years and a reduction of the gap to AEC system costs. [6][13][37][38][39][40][41] The main advantages and disadvantages of the Alkaline and PEM electrolyser are summarised in table 3.2:

	Alkaline	**PEM**
Advantages	+ Lower $CAPEX/OPEX$	+ High output pressure
	+ Proven long lifetime	+ High efficiency in partial operation
	+ High up-time	+ High purity level of hydrogen
		+ Operation under high range of power input
		+ High current density
		+ Very compact
		+ Short response time, fast heat-up and cool-off time
Disadvantages	- Need for purification	- Use of noble catalyst
	- Long time response	- Cells not easily replaceable
	- Long cold start-up time	
	- Lower range of power input	
	- Low current density	

Table 3.2: Advantages and disadvantages of Alkaline and PEM electrolysers

3.3 Storage of Hydrogen

For the storage of energy, hydrogen, is one of the most flexible energy storage methods available at the moment. [42] Hydrogen is capable of storing energy over longer periods of time (seasonal storage) more efficiently compared to storing energy in electricity. Batteries, for example, are only suitable for short-term storage (hours or days) as batteries deal with unwanted discharge when storing for a longer time and are very costly for large-scale applications.[43] This makes hydrogen an interesting solution to the problem of the occurring seasonal gap between demand and supply. As discussed previously, hydrogen has a very low volumetric energy density, which makes it challenging to store. It can be stated that the storage of hydrogen is one of the main barriers, if not the main barrier, to the widespread use of hydrogen. This makes the storage of hydrogen a key element in hydrogen energy systems. The Department of Energy proposed several standards and requirements for hydrogen storage on industrial scale. These requirements consist of not only a high volumetric and gravimetric energy density, but also fast kinetics, long cycle life and safety aspects. Most authors seem to use different categorisation systems for hydrogen storage. [44][45][46] A categorisation is applied for this research that covers and categorises all mature and still-under-development storage methods. Hydrogen storage can be classified as physical or chemical storage. Physical storage includes liquid hydrogen storage, compressed gaseous storage and cryogenic-compressed storage. In chemical storage, hydrogen is generated through a chemical reaction. Some materials which can store hydrogen through chemical storage are: Ammonia ($NH3$), metal hydrides, carbohydrates, synthetic hydrocarbons, formic acid and liquid organic hydrogen carriers ($LOHC$) = organic chemical hydride (hydrogen is stored in a molecule) Hydrogen and toluene are reacted to methylcyclohexane in which hydrogen is stored into a molecule. [47] A classification of hydrogen storage methods is shown in figure 3.13.

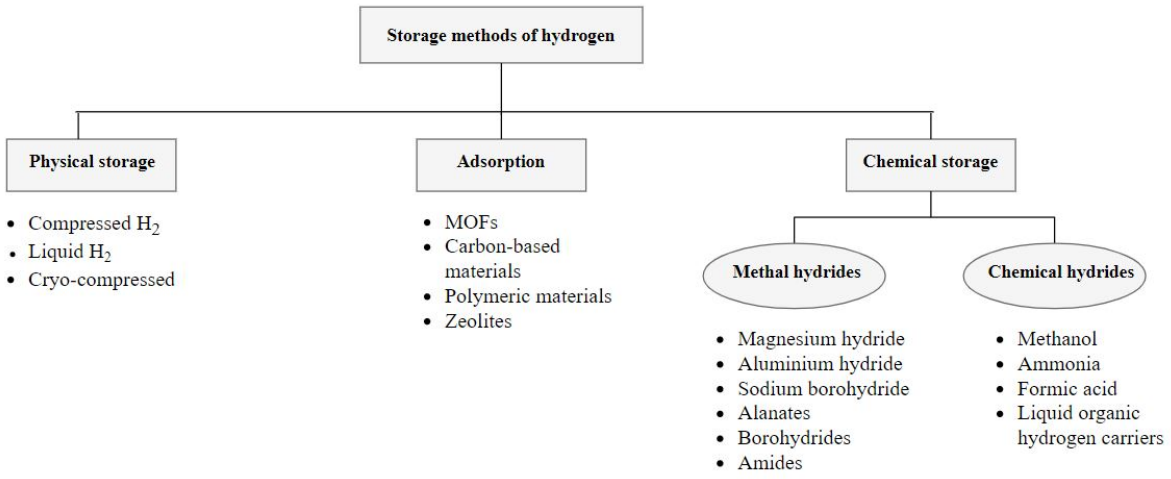

Figure 3.13: Classification of hydrogen storage methods

Currently, there are only a few technologies which are able to store hydrogen commercially used on a larger scale. Physical storage of hydrogen is the main form of storage used now a days. The characteristics of the physical storage technologies will be discussed in the following section.

3.3.1 Compressed Hydrogen Storage

Compressing hydrogen, increases the volumetric energy density of the gas thus allowing more energy to be stored in a given volume. The compression of hydrogen is a way to overcome the pressure difference between storage at lower pressures and refuelling, which requires up to a 1000 bar. Compressing hydrogen, is generally considered the most suitable technology and is widely used already for storing hydrogen used for hydrogen-fuelled cars. Hence, compression of hydrogen a mature technology. This is accomplished by step-wise compression by a series of compression's, up to the desired compression. A number of different compressors can be utilised to achieve the necessary compression. Compressors can roughly be divided in two types: Mechanical and non-mechanical compressors. The most widespread type of compressors used nowadays are mechanical compressors. There are several types of mechanical compressors, but for hydrogen compression, "positive displacement" compressors are mostly used. These make use of a piston, which squeezes the hydrogen in a smaller volume, which increases the pressure. Besides piston compression, more widely used mechanical compressors are: compressed air, diaphragm (or membrane) and ionic compressors. Widely used non-mechanical compressors that are used are: cryogenic compressors, metal hydride compressors, electrochemical compressors and adsorption compressors.The advantages of compressed storage of hydrogen include low energy consumption, high speed of inflation, low cost and hydrogen release, release is possible at room temperature and the release of hydrogen is very well adjustable. [45]

One of the negative effects of compressed hydrogen storage is that a lot of Work is required, to get the hydrogen up to very high pressures, which decreases the storage efficiency. For ideal gasses the specific Work can be calculated with the ideal gas law:

$$PV = nRT \tag{3.24}$$

Where P, V and T are the pressure in Pa, volume in m^3 and absolute temperature in K. n is the number of moles of gas and R is the ideal gas constant in $J/Kmol^{-}1$. The ideal gas law fits for hydrogen, unless pressures higher then 100 bar are used. At high pressures, hydrogen deviates from ideal gas behaviour significantly. At higher operating pressure, the real gas effects become important as shown in figure 3.14. It can be seen that the ideal gas law is suitable up to 100 bar and that, at higher pressures, when considering real gas effects, a higher Work demand is found.

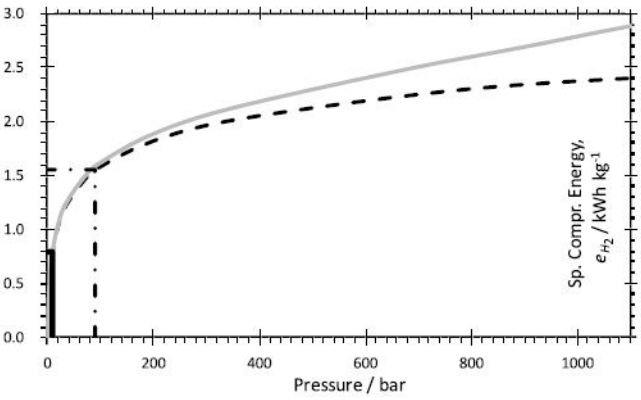

Calculated including real gas effects (in grey) and the ideal gas law (black dashed). The energy that is saved by starting the compression at higher pressures (10 and 90 bar) is indicated in the figure.

Figure 3.14: Specific Work needed for compressing hydrogen from 1 bar. [8]

3.3.2 Liquid Hydrogen Storage

Liquefaction is technically possible and requires cooling below the critical point of –253 °C to become liquid. Before liquefaction takes place, the hydrogen must be converted to para-hydrogen. Gases are called cryogenic when they can be liquefied only at extremely low temperatures, thus storing hydrogen in liquid form is as well referred to as cryogenic storage. The liquefying process of hydrogen involves a high energy consumption, which reduces the efficiency and increases costs. The boil-off phenomena is another aspect that reduces the efficiency and safety. 2-3% of evaporated hydrogen will be lost per day because of the necessary heat input into the storage vessel. [44] An advantage of liquid hydrogen ($LH2$) is the high volumetric energy density, compared to hydrogen in gaseous form. $LH2$ tanks can store 0.070 kg/L of liquid hydrogen and compressed gas tanks only 0.030 kg/L. [47] Nevertheless, liquefaction and high pressure storage could be combined. This storing method is called: cryogenic-compressed storage. Storing liquid hydrogen under high pressure is more efficient and reduces boil-off losses. Nowadays, liquid hydrogen is in demand for applications requiring high levels of purity, such as the chip industry, however, $LH2$ is primarily used in space applications.

Hydrogen comes in two different configurations: **Ortho** and **Para**. These configurations depend on the spin of the protons. When the spin of the proton in both hydrogen atoms is the same, then the term Ortho is used. When the spins have the opposite direction, then the term Para is used. Hydrogen at room temperature and higher temperatures, which is considered normal hydrogen, is in equilibrium when it consists of around 25% Para and 75% Ortho-hydrogen molecules. However, in liquid hydrogen, all hydrogen molecules are Para. Consequently, all Ortho-hydrogen molecules are converted into para-hydrogen molecules. This conversion requires energy. [42]

3.3.3 Other Storage Methods

Besides physical storage, two other methods can be classified: Storage through Adsorption and Chemical storage. Chemical storage can be divided into two sub categories: Metal hydrides and chemical hydrides.

Adsorption
Adsorption is the process of hydrogen molecules or atoms attaching to the surface of a material. Adsorption is also referred to as physisorption. There are many sorbents (materials used to adsorb liquid or gases) that have been suggested for the storage of hydrogen, a few prominent examples are: Carbon-based materials, metal-organic frameworks (MOF), Polymmeric materials and zeolites. [46] The most successful sorbents are certain carbon-based materials and MOF. Advantages of adsorption are the low operating pressure, the low-cost materials and the simply designed storage system. However, major drawbacks include the requirement of low temperature and high pressure to storage the hydrogen and the relatively low gravimetric and volumetric energy densities of the stored hydrogen [44]

- *Carbon materials for hydrogen storage*: A number of carbon materials can be used for adsorption, such as graphite, carbon nanotubes, zeolites, grapheme-based carbon, carbon nanofilters and so on. [44] Carbon materials show high storage capacities under relatively low temperature and pressure. The hydrogen storage capacity of carbon materials mainly depends upon surface area. Further research on modified carbon structures is needed to achieve the storage requirements set by the Department of Energy.
- *Metal-organic frameworks*: These light weighted solids, with a very large surface area are believed to be able to meet the storage requirements of the Department of Energy. The size, shape and volume of these materials can be tuned to improve the absorption properties. [45] Achieving the desirable volumetric hydrogen density is currently still a challenge though.

Metal Hydrides
Metal hydrides are considered as a promising storage method for hydrogen, as it makes storing large amounts of hydrogen possible within a relatively small volume. [44] Metal hydrides, as their name implies, contain metal atoms. Metal hydrides make us of chemisorption. Hydrogen molecules are split into hydrogen atoms and then integrated in the lattice of a metal like Li Na, alloy and so on, or in the lattice of an intermetallic compound to form metal hydrides. Chemisorption is also referred to as absorption. In general, metal hydrides have a large gravimetrical and volumetric density, are safe, high purity of hydrogen and good cycle performance. Metal hydrides cannot demonstrate satisfactory performance yet due to volume expansion issues, low thermal conductivity and slow hydrogen kinetics, however, metal hydrides are still considered very promising. [44] [45]

Hydrogen can be directly bonded to the metal atom, this is called a metal hydride. Hydrogen can also be part of a complex ion that is bonded to a metal atom, these are called complex metal hydrides.

- *Elemental metal hydrides*: Hydrogen can form binary compounds with metallic elements, these are called elemental hydrides. yet, because of thermodynamics and hydrogen storage capacity, most of these are not applicable for hydrogen storage. [46] Magnesium hydride and aluminium hydride are the elemental metal hydrides that are considered to be most promising for large-scale storage of hydrogen.
- *Intermetallic hydrides*: For intermetallic hydrides, an alloy is used. The alloy consist of one element, which is a strong binder of hydrogen, and another element, which binds hydrogen weakly. The gravemetrical hydrogen density of intermetallic hydrides is too low to be useful for vehicle applications, but they might be suitable for certain stationary applications. [46]
- *Complex metal hydrides*: This is another light weight hydrogen storage material. The biggest difference between the simple and the complex metal hydride is that during the absorption process of hydrogen, in complex metal hydrides, an ionic or covalent compound is formed. [44] Lighter metals are used and form solid state compounds with the hydrogen. Complex metal hydrides have a high gravimetric hydrogen density. Most complex hydrides unfortunately require high temperatures for their de-hydrogenation, and only a few can be reversibly dehydrogenated. Examples of complex metal hydrides are alantes, borohydrides and amides.

Chemical Hydrides

Chemical hydride storage is method of producing hydrogen via a chemical reaction. Although the composition of these materials seems to be similar to complex and simple metal hydrides, the chemical behaviour is entirely different. Contrary to metal hydrides, chemical hydrides only consist of non-metallic elements. Generally, chemical hydrides are liquids at normal conditions, therefor simplifying the storage and transport possibilities. [46] Metal hydrides can be decomposed at elevated temperatures and re-hydrogenation is possible under technically relevant conditions using catalysts. For chemical hydrides, the chemical reactions are not reversible, and the byproducts must be discarded. Chemical hydrides are lighter than reversible metal hydrides and release more hydrogen because the hydrogen is liberated from the water reactant. A few prominent examples of chemical hydrides include methanol, formic acid, ammonia and liquid organic hydrogen carriers such as: Methylcyclohexane and toluene. Ammonia, formic acid and methanol are bulk chemicals commonly synthesised from natural gas. Much of the necessary infrastructure required for their production, handling, and transport is already utilised as these chemicals are already widely produced.

The borohydride named sodium borohydride ($NaBH_4$) deserves a little more notice. In literature studies and conversations with multiple experts I noticed that a lot of attention is devoted to the subject of $NaBH_4$ as a clean fuel. It has fast kinetics, is highly exothermic and very well controllable. Another big advantage, is that sodium borohydride can be used directly as a fuel for a combustion engine in vehicles or ships. This takes a way the need for difficult and expensive storage applications. The widespread use of $NaBH_4$ is held back mainly by the bi-product ($NaB(OH)_4$) it leaves behind after the hydrolysis reaction: $NaBH_4 + 4H_2O \longrightarrow NaB(OH)_4 + 4H_2$. This makes regeneration of $NaBH_4$ challenging and the use of $NaBH_4$ more expensive. Today only a few companies offer $NaBH_4$ on the market, and for this study is decided that $NaBH_4$ is still too much in the developing phase and not usable for the energy system design at the Hemweg. However, it is definitely a very interesting option for the future.

3.3.4 Concluding Remarks

Many technologies for storing hydrogen exist, however compressed hydrogen is considered the most mature technology and is widely used already. Other storage methods are promising for the future but haven't been used currently on commercial scale. Below an overview of the advantages and disadvantages of the storage technologies that were discussed.

	Advantages	Disadvantages
Compressed hydrogen	+ Widely used & mature technology + High efficiency + High purity	- Despite high pressure, still low volumetric density - High cost of containers
Liquid hydrogen	+ High volumetric density + High purity + Lower storage pressure than compressed hydrogen	- High cost - Safety issues - Low efficiency liquefaction process - Requires low temperature
Adsorption	+ Low cost + Low pressure + Simple design	- Reversibility - Low temperature required
Metal hydrides	+ High volumetric density + High safety + High purity	- Low gravimetric density - Reversibility
Chemical hydrides	+ High volumetric density + Low pressure + Liquid, easily transportable	- Reversibility - Improvement needed for kinetics

Table 3.3: Advantages and disadvantages of hydrogen storage methods

3.4 Hydrogen as a Fuel

When hydrogen is burned in air, the hydrogen reacts with oxygen to form water and releases energy. There are two techniques to use hydrogen as a fuel in vehicles: A fuel cell and a hydrogen internal combustion engine ($HICE$).

3.4.1 Hydrogen Internal Combustion Engine

Hydrogen internal combustion engines are different from hydrogen fuel cells. The hydrogen internal combustion engine is similar to the traditional gasoline-powered internal combustion engine: Hydrogen is injected into a cylinder and based on the heat generated by the reaction, the motor is driven. The main difference is the exhaust product. $HICE$ emit NOx and small amounts of unburned hydrocarbons, CO2 and CO. The emissions of NOx in hydrogen engines are smaller than emissions from comparable gasoline engines. [48] Fuel cells and $HICE$ are two technologies that are intrinsically different and have very different efficiency-power characteristics. An $HICE$ has the maximum efficiency at or near its maximum power and the efficiency of a fuel cell system is highest at partial load. [49] A $HICE$ operates at thermodynamic efficiency level of around 20–25%, which is much lower than the efficiency of a fuel cell which is above 60% at partial load. [50]

3.4.2 Fuel Cell

A fuel cell is an electrochemical energy converter and can be used to convert the chemical energy of fuels such as hydrogen, natural gas, methanol, ethanol and hydrocarbons into electricity. It converts a fuel and an oxidant, for example oxygen, directly into electricity through an electrochemical process. [2] Fuel cells are more efficient than $HICE$. The efficiency rises when fuel cells are operated in partial load.

Fuel cells can be categorised in different types, all consisting of 2 electrodes (a cathode and an anode) and an electrolyte that allows positively charged hydrogen ions (protons) to move between the two electrodes of the fuel cell. The reaction between hydrogen and oxygen in the fuel cell produces an electric current. In figure 3.15 a basic cathode – electrolyte – anode construction of an acid electrolyte fuel cell is shown.

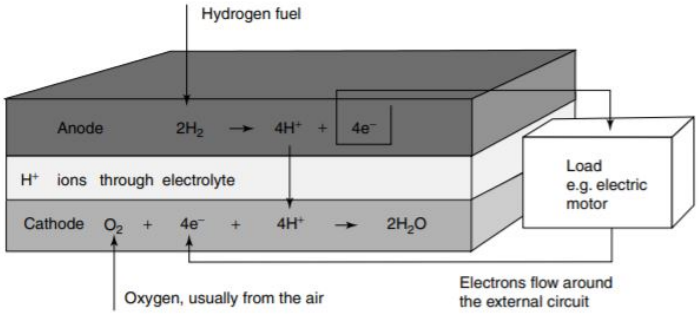

Figure 3.15: Fuel cell with acid electrolyte [2]

The components of the fuel cell differ for different types of fuel cells. A common criterion used for separating the different types, is the electrolyte that is used. At the anode of a fuel cell with an acid electrolyte, the hydrogen ionises into H^+ and electrons:

$$2\mathrm{H}_2 \longrightarrow 4\mathrm{H}^+ + 4\mathrm{e}^-$$

At the cathode, oxygen reacts with electrons and H^+ ions from the electrolyte to form water:

$$\mathrm{O}_2 + 4\mathrm{e}^- + 4\mathrm{H}^+ \longrightarrow 2\mathrm{H}_2\mathrm{O}$$

These reactions cause a flow of electrons from the anode to the cathode and an electric current is being produced. Note that although the negative electrons flow from anode to cathode, the current flows from cathode to anode. Thus, the cathode is the electrically positive electrode, since electrons flow from - to +.

Different Types of Fuel Cells

A selection of types of fuel cells that are in use [51]:

- PEM fuel cell
- Alkaline fuel cell
- Phosphoric acid fuel cell
- Direct methanol fuel cell
- Molten carbonate fuel cell
- Solid oxide fuel cell

PEM Fuel Cell
The PEM fuel cell makes use of an acid electrolyte that consists of a polymer matrix, which can transport $H+$ ions. The acid electrolyte has an operational temperature that ranges between $60°C$ and $130°C$. [51] The advantage of PEM fuel cells is that they are compact, have a high efficiency, fast start-up, low operation temperature and they don't need reservations of electrolyte or re-circulation. An advantage of the solid electrolyte, as opposed to those of liquid type, is that it allows the fuel cell to operate in any spatial position. The fuel use of the PEM fuel cell is restricted to almost exclusively pure hydrogen. If you want to make use of another fuel, a reforming phase to produce pure hydrogen is necessary. [51]

Alkaline Fuel Cell
In the alkaline fuel cell the electrolyte is an alkali, potassium hydroxide (KOH) solved in water is usually used. The operational temperature ranges between $60°C$ and $100°C$. [51] A disadvantage of the alkaline fuel cell is that the electrolyte reacts with CO_2, which is undesirable. If the oxygen or hydrogen used is not pure, but consists of CO_2 particles, the CO_2 can chemically react with the alkaline electrolyte. Hence, as air consists in a small measure out of CO_2 particles air cannot directly be used to provide O_2. [52] The alkaline fuel cell is restricted to exclusively pure hydrogen and additionally pure oxygen, similar as the PEM fuel cell.

Phosphoric Acid Fuel Cell
The electrolyte of this fuel cell is primarily composed of phosphoric acid (H_3PO_4). The operating temperature of the phosphoric acid fuel cell varies between the $150°C$ and $200°C$. [53] This type of fuel cell has an output between the 100 kW to 400 kW and they are also found in application in buses and other large vehicles. Most fuel cell units sold before 2001 were phosphoric acid fuel cell technology. [54]

Direct Methanol Fuel Cell
The direct methanol fuel cell is a variant of the PEM fuel cell, however methanol is used as the fuel. This fuel cell is until now utilised to replace batteries in mobiles, computers, other small portable devices and for military applications. [55] It is not certain whether the direct methanol fuel cell is applicable for vehicles, because of the low ability to deliver high power. [51] However, direct methanol fuel cells have high power density and quick start capability which makes them suitable for soldier and sensor power in military applications. [56]

Molten Carbonate Fuel Cell
This type of fuel cell operates with a molten electrolyte: a mixture of carbonates from alkaline metals. The carbonate ions (CO_3^-2) are transported from the cathode to the anode. The operating temperature is typically high: between the $600°C$ and $650°C$. [51] The high temperature allows the use of non-noble catalysts. These have the advantage of being insensitive to a certain degree of fuel contaminant which often damages other fuel cells. [57] The molten carbonate fuel cell had a high tolerance to air contamination and carbon monoxide. Hence, this fuel cell is able to consume fuels that contain monoxide and carbon dioxide, which makes reforming natural gas or coal is an option for obtaining gases as a fuel. [51] However, the fuel cell is sensitive to sulphur compounds in hydrocarbon fuels.

Solid Oxide Fuel Cell
The electrolyte in this fuel cell is made out of impermeable ceramics (solid oxides) that transports oxygen from the cathode to the anode. Advantages of high operation temperature of this type of fuel cells are that they do not require precious-metal electrocatalysts and the high operation temperature also makes it possible to use directly a wide range of fuels including natural gas, hydrocarbons and alcohol-based liquid fuels. Other advantage are: high efficiency, long-term stability, low emissions, fuel flexibility and relatively low cost. The largest disadvantage is the long start-up times and chemical and mechanical compatibility issues that come with the high operating temperature. The operating temperature is between the $800°C$ and $1000°C$. [51] The main applications of solid oxide fuel cells are: combined cycle power plant, co-generation/trigeneration and residential application. Solid oxide fuel cells are considered as promising for nautical applications. [58]

Fuel cells can be used for a wide range of applications e.g. trucks, cars, ships, powering buildings and backup power systems. As fuel cells can be grid-independent, they can also be an appealing option for critical load functions such as data centres, hospitals, emergency response systems and military applications. Which fuel cell is best to use for which application can be based on their characteristics. The advantages and disadvantages of each fuel cell are shown in table 3.4.

	Advantages	**Disadvantages**
PEM fuel cell	+ Compact	- Expensive catalyst
	+ High efficiency	- Sensitive to fuel impurities
	+ Solid electrolyte	
	+ Quick start-up time	
Alkaline fuel cell	+ Widely used	- Electrolyte management necessary
	+ Low in cost	- The electrolyte can react with CO_2
	+ High performance	
Phosphoric acid fuel cell	+ High efficiency	- Low current and power
	+ Tolerance for fuel impurities	- Long start-up time
		- Requires platinum catalysts
Direct methanol fuel cell	+ Quick start-up capacity	- Low power output
	+ Fuel flexibility	
Molten carbonate fuel cell	+ Fuel flexibility	- Long start-up
	+ High efficiency	- Low power density
	+ Non-noble catalyst	- High temperature enhances corrosion cells
Solid oxide fuel cell	+ High efficiency	- Long start-up times
	+ Fuel flexibility	- High temperature enhances corrosion of cells

Table 3.4: Advantages and disadvantages fuel cells

3.5 Concluding Remarks

Hydrogen can be utilised as a clean energy carrier. As of today, a broad variety of developed and operational technologies exist for the production, storage and usage of hydrogen as a fuel. For the production of green hydrogen the PEM and Alkaline electrolyser are the most suitable options, both with their advantages and disadvantages. The Alkaline electrolyser is a more mature technology, with lower cost. However the PEM electrolyser has a lot of other advantages such as good performance in partial operation, higher current density and flexible operation. For storing hydrogen many technologies exist, however compressed hydrogen is considered the most mature technology, widely used already. Other storage methods are promising for the future but haven't been used currently on commercial scale. Within mobility, hydrogen can be used as a fuel for vehicles and ships with fuel cells or internal combustion engines. Fuel cells, especially at partial loads, have a higher efficiency compared to hydrogen internal combustion engines. Also from a cost and complexity perspective the fuel cell could be considered as a promising technique.

Chapter 4

Case Study and System Design

4.1 Hemweg 8

The Hemweg plant consists of two units: Hemweg 8 and Hemweg 9. Power plant Hemweg 9 is a gas fired plant taken in operation in 2012 with a capacity of 440 MW. Power plant Hemweg 8 is a coal-fired installation with an electricity capacity of 650 MW. Hemweg 8 is dated from 1994 and was planned to stay in operation until 2024. However, in the beginning of 2019 the Dutch Parlement decided to close the power plant much earlier: the power plant will be shut down before 2020. This was decided in order to achieve a reduction of greenhouse gas emissions by the end of 2020 of 14 to 17% relative to 1990. The power plants (shown in figure 4.1) at the Hemweg, are located near the harbour of Amsterdam, easy accessible by ships and road transport. An overview of how Hemweg 8 is located on the map is displayed in Appendix A. Vattenfall is planning on starting renewable initiatives at the Hemweg 8 location. The location could be very valuable to Vattenfall. In this case study the available wind electricity at the location will be utilised to produce hydrogen.

Figure 4.1: Hemweg 8 and 9 [9]

4.1.1 Wind Speeds at the Location

The wind data, that is collected by Vattenfall, is used to simulate the possible supply of electricity by the wind turbines. The wind data was collected using a LiDAR (Light Detection and Ranging) instrument. LiDAR instruments use laser pulses to measure the wind characteristics at 94m. The exact location of the LiDAR has a latitude of 52.39650° and longitude of 4.82329° (Appendix A). The wind speed data obtained by Vattenfall ranges from 02-02-2018 until 25-09-2018. The monthly mean wind speeds of this period are calculated in MATLAB and shown in figure 4.2. Wind measurements show that there was relatively little wind in 2018 (as well as in 2016 and 2017), certainly compared to 2015, when the wind was above average. [59] Multiple studies indicate that the changes in the wind climate over the years are minor and not statistically significant. However,

there does seem to be an increase in the number of situations with extreme winds from western directions. There are also indications that in a warmer climate tropical cyclones reach the North Sea more often. [59] For this research the wind speeds of 2018 measured at the Hemweg location are considered representative, as the wind speeds are similar to the wind speeds in the years 2016 and 2017. However, this could possibly be a period of lower wind speeds of multiple years, which makes the utilising the wind speeds of the year 2018 a conservative choice.

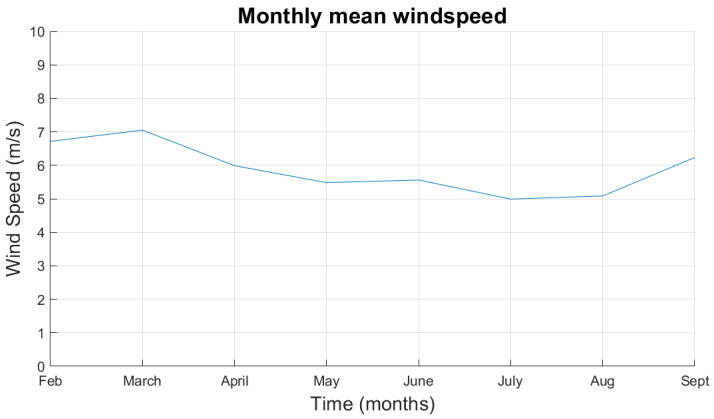

Figure 4.2: Measured monthly mean wind speed at the Hemweg site, at 94m in the year 2018

In figure 4.3, an example is shown of the horizontal wind speeds at 94m in a random week of the year 2018. As can be seen the wind speed varies between 5 and 7 m/s. 10 minute data is used from 03-02-2018 00:00 until 10-02-2018 00:00 and the data is modelled in MATLAB. As can be seen from figure 4.3, the wind speed is quite variable and low wind speeds occur occasionally.

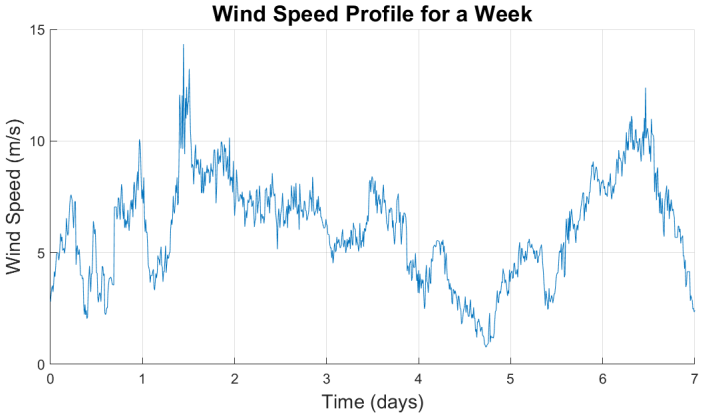

Figure 4.3: Wind speed profile for a week

Due to lack of wind data for the other months of the year, an estimation has been made for the months of January, October, November and December. The monthly/seasonal changes of wind speeds are estimated based on yearly wind data obtained by the KNMI. The average wind speeds per month for the year 2010-2014, measured at de Bilt, are plotted in graph 4.4. The wind speeds measured by the KNMI are lower in value, this can be caused by location and measure height. However the monthly/seasonal variation in the wind speeds is considered representative as it is the average over multiple years. In Matlab the difference in wind speed between the measured KNMI wind data and the measured wind data at the Hemweg is calculated for each month. The mean of this difference per month is taken and this is a value of 2.98 m/s. By adding the value of 2.98 m/s to all wind speeds measured over the years 2010-2014 by the KNMI, an new estimation, calculated in MATLAB, for the average wind speeds for all months has been made, including the months of January, October, November, December. [60] [61] The estimated average monthly wind speed over a year is shown in figure 4.5. To match the estimated average monthly wind speeds for the months January, October, November and December, the 10 minuted data of the wind speeds of February are manipulated with a factor and used for the missing months. The average wind speed over a year at a height of 94 meter is 6.2 m/s.

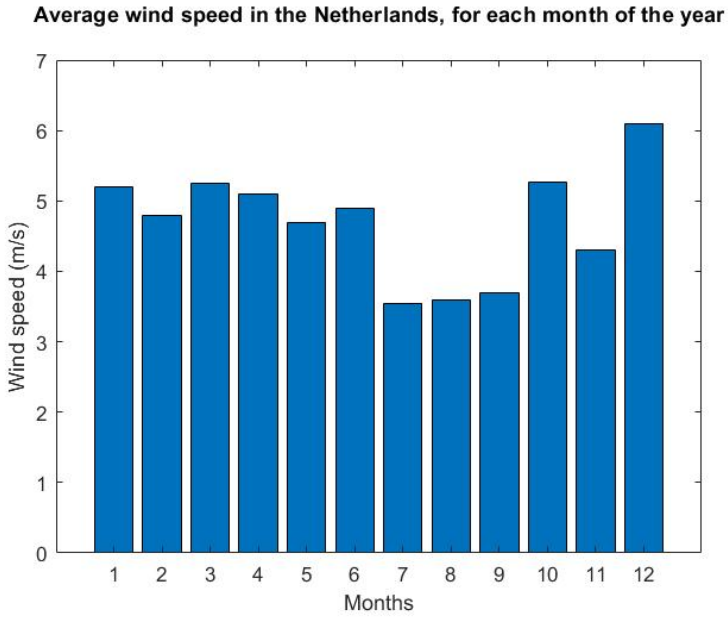

Figure 4.4: Average wind speed for each month of the year, for the year 2010-2014

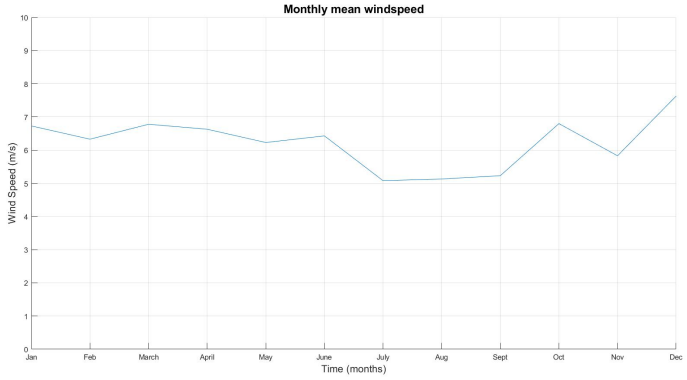

Figure 4.5: Average wind speed of estimated data for each month of the year at the Hemweg site, at 94m

4.2 Hydrogen Demand

At this moment, no direct demand for green hydrogen from the surrounding industries at the Hemweg 8 location was found. In many literature studies and conversations with experts the same problem arises for building large-scale electrolysers: building large-scale electrolysers is not economical during the initial phases of establishing a hydrogen economy as there is a low degree of market saturation of hydrogen fuelled transport and low-demand of green hydrogen in other industries. Companies will not invest before the infrastructure is in place. At the same time, offer creates demand: a hydrogen fuelling network and green hydrogen trading will only start to arise when hydrogen is offered at low cost, which requires large-scale electrolysers. There will be no demand for green hydrogen, as long as there is no low-cost production of green hydrogen. Producing a product creates demand according to Say's law, which has been a basic concept in economics for almost two centuries.[62] In this case, supply of hydrogen is required before demand arises. At the moment there is not a big demand, however if Vattenfall decides to produce green hydrogen, there is a good probability that demand will increase. Potential consumers of green hydrogen near the Hemweg 8 location are researched in this report with a main focus on hydrogen-powered ships.

4.2.1 Hydrogen-Powered Ships

A demand for hydrogen is expected as hydrogen-powered ships are being developed. The exhaust of diesel engines currently used for ships cause numerous negative environmental impacts and many of the organic carbon compounds in the exhaust are carcinogens. [63] The atmospheric emissions caused by the worlds transport with ships is around 1000 million tonnes of CO2 annually and is approximately 2.5% of global greenhouse gas emissions. [64] Fuel cell systems on board of a ship seem to be an attractive solution for renewable power generation. There has been a constant evolution of fuel cells in marine applications. [65] Fuel cells have the potential to be more efficient, lower in noise, faster in start-up and cleaner than the conventional internal engines used currently for ships. [66] The Hemweg location has an excellent position for providing ships with fuel, as it is positioned in the harbour of Amsterdam. Vattenfall could play a role in providing the ships with green hydrogen as a fuel. Hydrogen-powered ships are still at the investigation and demonstration stage but already some hydrogen-powered ships have been built for commercial use. There are 2 options for the fuels used by the fuel cells [67]:

- Pure hydrogen
- Gases with a high hydrogen content such as: methane and ammonia, metal hydrides such as: sodium borohydride or liquid hydrocarbons such as: methanol or diesel fuel

To evaluate if hydrogen-fuelled ships are a promising solution for maritime transport with less CO2 emissions, first marine applications that have already been developed were evaluated. Several research projects concerning hydrogen-powered maritime applications have been carried out in the last decades. In this section some of the most noticeable projects, that use hydrogen as a fuel will, be discussed briefly.

Class 212 Submarines
In 1998 the Class 212 Submarines were developed by Howaldtswerke-Deutsche Werft (HDW), using PEM fuel cells developed by Siemens. The system uses nine PEM fuel cells, each nominally rated at 34 kilowatts, yielding a total of approximately 300 kilowatts.[68] In a later stadium of the development also PEM fuel cells with a rated power of 120 kW were used. The efficiency of these fuel cells is very high; approximately 65%. [68] Many submarines with a similar fuel cell system have been commissioned so far. [69] The performance data of different PEM fuel cells from Siemens shown in figure 4.6. The highest generated power output is approximately 165 kW.

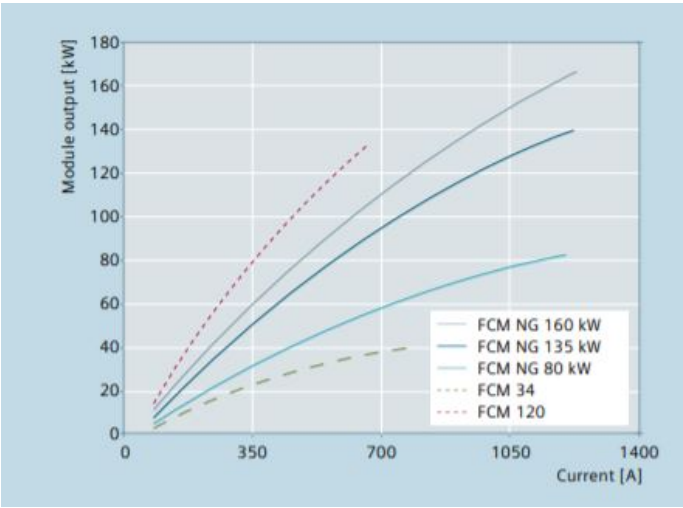

Figure 4.6: Performance data of PEM fuel cells Siemens [10]

ZEM-SHIP
In 2008 the zero-emission ship ($ZEM - SHIP$) project developed the first inland passenger ship: the FCS Alsterwasser. The FCS Altserwasser was build and operated in Hamburg. It combines two PEM fuel cell systems with a 560V lead gel battery pack. Both have a peak output of 48 kW This was the first time ever that an inland passenger ship has been driven - solely by fuel cells - at a power of over 5 kW and with hydrogen as its single source of energy. An amount of 50 kg of the hydrogen can be stored in 350 bar pressure tanks on board the ship, supplying it with enough energy for approximately three days in operation. The maximum cruising speed of the ship is 15 km/h. [70]

Nemo H2
The passenger vessel Nemo H_2 has been developed by Fuel Cell Boat BV to serve as a tourist boat in the canals of Amsterdam carrying approximately 100 persons. It has a PEM fuel cell system with an output of 60-7- kW, with a 55kW lead acid battery. The tourist vessel was a success, however, the costs for the fuel cell, safety and the fuel - hydrogen - was very high. Because of the absence of a permanent hydrogen fuelling station, chosen was to not proceed the project. [69]

METHAPU Project
An example of fuel cell systems in the merchant navy is the METHAPU (Methanol Auxiliary Power Unit) project. Methanol-powered $SOFC$ modules were used to supply electricity supply on board of the ship. The main objective in this project consisted on validating the use of methanol as a marine fuel.[71]

Hydrogen as a Fuel for Ships
These projects that already have been carried out show that is is possible to use hydrogen as a fuel for small ships, such as tourist boats, or as a fuel for submarines. Among the fuel cell technologies that have been used until this far for maritime applications, the PEM fuel cell is considered the most promising as described in section 3.4 in this report. The report, issued by Sandia National Laboratories [50] it states that neither power nor energy is a limiting factor by itself for fuel cell applications on ships. After examining the case studies it was found that in each case the first limit reached was the volume limit. The main disadvantages of using hydrogen as a fuel are [67]:

- Low volumetric energy density: storing hydrogen on the surface of a ship requires a high volume because of the low volumetric energy density.
- There is a lack of global infrastructure which limits the operational area for hydrogen fuelled ships. Fuelling stations are required at harbours.

Metal hydrides, such as sodium borohydride ($NaBH_4$), have the potential to overcome or mitigate some of the limitations that fuel cells bring. However, little is known yet about the implementation of a sodium borohydride system on a ship. More information on sodium borohydrides is provided in section 3.3.3. Another viable option for fuel cells on ships for commercial use are traditional marine fuels or higher-density liquid fuels such as methanol, natural gas, ethanol, liquefied petroleum gas and gasoline. These require a on-board fuel reformer to extract hydrogen from the fuel, using chemical processes. Also, ammonia is a technically feasible solution for de-carbonising international shipping. Ammonia is mostly known as a feedstock for agriculture or as a refrigerant, has been occasionally used as a fuel for internal combustion engines and fuel cells. Combustion of ammonia does not emit CO_2, because it is a carbon-free molecule. However, using ammonia for ships is still in research state. Storing hydrogen as a cryongenic liquid at -252°C is another possibility for the future. These storage methods result in a smaller and lighter overall system on the ship compared to a gaseous storage system. [67] However, in most hydrogen-fuelled ships, that are already developed and used, the hydrogen is stored at high-pressure (350 bar). In section 3.3 a detailed analysis is provided covering all storage methods. However, at this point there have not been a lot of experiments with the storage methods mentioned before and high pressure hydrogen gas is considered safer and easier to manufacture. The use of commercial ships with fuel cells will perhaps be limited to inland waterways and coastal waters in the future. [15] However, there are still many promising technologies in the research phase and hydrogen-fuelled ships of multiple megawatts are still being developed. Hence, for this case study hydrogen-powered ships will be considered as a valid option for future transport.

4.2.2 Fuel Cell Electric Vehicles

Fuel cell electric vehicles ($FCEV$s) make use of an on-board hydrogen storage tank of 600 bar with a capacity of approximately 5/6 kg of hydrogen, which is converted into electricity, heat and pure water with a fuel cell. $FCEV$s have an average range of 500 km. Currently, there are some $FCEV$ passenger cars available in the market and the Japanese company Toyota is leading the market on $FCEV$s. Electric vehicles based on batteries are currently more mature in the market, and the electric infrastructure including charging stations are well developed in most progressive markets. For $FCEV$s to develop as well, a large hydrogen fuelling station infrastructure is needed. The market is accelerating and there are approximately 125 hydrogen fuelling stations in Europe. [72] A road map created by McKinsey shows that in 2030, $FCEV$s are expected to cover 10% of the vehicle market. [73]

4.2.3 Heating with Hydrogen

In the future, hydrogen can be an alternative for sustainable heating of homes. Research by Kiwa shows that the current natural gas distribution network can be made suitable for hydrogen. The use of hydrogen in the existing gas network could be an alternative in the future, for example for the historic city centre of Amsterdam with many monumental buildings that are not easy to insulate. The use of hydrogen for domestic heating seems to have potential, but needs to be further investigated. Network operators in the Netherlands are therefore focusing on the development and use of hydrogen in industry and on a number of pilot projects by 2030 to gain more experience in the distribution of hydrogen through pipes. [74]

4.2.4 Demand Estimation

There are three options for starting a hydrogen supply at the Hemweg location. The first option would be to establish supply contracts with external consumers. Another option is to consume the hydrogen internal within Vattenfall. As a last option, investments could be made in a hydrogen production system and consumers will possibly arise, when the hydrogen production system is established. This last option has been conducted by EnergyStock and Gasunie New Energy. They have built a 1 MW electrolyser that converts electricity into hydrogen for possible consumers in the transport and industry sectors. Henk Abbing, managing director of EnergyStock, stated that this risk is not without consequences. The electrolyser of EnergyStock and Gasunie New Energy is not running in the first months of its existence, as problems did occur with the hydrogen consumers. However, Henk Abbing was very optimistic and he stated that potential clients did arise already.

As there is no hydrogen demand yet, part of the hydrogen demand could be created by Vattenfall itself. A hydrogen-powered crew transfer vessel (CTV) that will be used by Vattenfall for maintenance of the off-shore wind parks could offer a demand. A conventional Volvo Penta D13-1000 combustion engine is used in the ship. On board of the ship, one big tank of 90 kg and 2 smaller tanks of 40 kg will be used. For the CTV 12 hours of operation per day and average requirements regarding driving and thrust mode are assumed, according to Arne Jacobsen, hydrogen expert within Business Development BA Wind at Vattenfall. Operating the vessel will need approximately 750 L of diesel a day to maintain the wind park. Assuming the volumetric energy content of diesel is 9975 Wh/L [75], a total energy of 7,480 kWh is needed per day. The energy used in the combustion engine is a mixture of diesel and hydrogen. The hydrogen-part delivers approximately 80% of the energy needed, which is 5,990 kWh. The gravemetric energy density based on the HHV of hydrogen is 39.7 kWh/kg, thus 150 kg hydrogen at 350 bar per day is needed for the CTV.

If the hydrogen economy continues to grow, other demand opportunities will arise. An example of a possible client could be the Port of Amsterdam. The Port of Amsterdam owns 5 vessels. To estimate the emissions caused by the ships, data obtained from the Port of Amsterdam was used. First the consumption of fuel was estimated. The vessels owned by the Port of Amsterdam use in total 509,500 litre of diesel a year, and fuel every 14 days according to Henk van der Boom (Division Port Warden of the Port of Amsterdam). With a volumetric energy content of diesel being 9975 Wh/L [75], a total energy of 5100 MWh per year is needed by the vessels of the Port of Amsterdam. The gravemetric energy density based on the HHV of hydrogen is 39.7 kWh/kg is used to estimate the demand. If the Port of Amsterdam would use hydrogen-fuelled vessels, the demand for hydrogen could grow up to 127,500 kg per year. In what form the hydrogen could be supplied, is discussed in section 3.3

Another demand opportunity are $FCEV$s. The municipality of Amsterdam decided that as of the year 2030, no diesel or gasoline cars are accepted in the city anymore.[76] This will greatly impact the transport usage for the inhabitants of Amsterdam. At the moment only 50 $FCEV$s are registered in the Netherlands. [77] In 2020, four hydrogen fuelling stations will be built in Amsterdam. [77] The daily hydrogen demand of a hydrogen fuelling station varies. The average distance a car in the Netherlands drives is 13,000 km per year. [78] A $FCEV$ consumes 0.008 kg of hydrogen per kilometre. [79] The climate agreement assumes that 15,000 $FCEV$s are in operation by 2025, possibly increasing to 300,000 vehicles by 2030 in the Netherlands. The city of Amsterdam contains 5% of the inhabitants in the Netherlands. The amount of $FCEV$s in Amsterdam in the present scenario and in the 2030, is conservatively estimated to be 200 and 10,000, respectively. The average daily demand for hydrogen fuelling stations delivering to 200 and 10,000 $FCEV$s is estimated to be approximately 60 kg/day and 2,800 kg/day.

Sustainable heating of homes could offer a future demand for hydrogen. The forecast for the heat network in Amsterdam South and East in 2020 is 25,700 connections and 2.2 PJ of heat supply. [80] To produce a 2.2

PJ of heat a hydrogen supply of approximately 15 *kiloton* is needed. This is based on expanding the number of connections for new homes, existing construction and connecting the small-scale grids in existing buildings that now have a heat supply from co-generation. The amount of heat needed in the future will continue to grow. [80]

Lastly, an opportunity could be to trade the hydrogen to external demanding industries such as: transport, fertiliser production, cooling in power plant generators. There are many industries located closely to the Hemweg that currently use grey hydrogen such as: ICL Fertilisers, which is one of the world's largest fertiliser companies. It is uncertain if these industries will adjust to green hydrogen in the near future, but if so, it will contribute to the hydrogen economy and create a boost in the market for green hydrogen. The demand for hydrogen calculated per consumer for this case study are displayed in table 4.1:

	Demand for hydrogen
CTV Vattenfall	150 kg/day
Port of Amsterdam	127,500 $kg/year$
Hydrogen fuelling stations present scenario	60 kg/day
Hydrogen fuelling stations 2030 scenario	2,800 kg/day
Future sustainable heating	15,000,000 $kg/year$

Table 4.1: Hydrogen demand per consumer

As it is hard to predict how high the hydrogen demand currently is and how it will develop in 2030, three different scenarios have been created: low-, medium- and high-demand scenario. For now, the hydrogen demand for each scenario is chosen as follows: for the low-demand scenario a hydrogen demand of 500 kg/day is assumed, mainly based on the amount of hydrogen needed by the CTV and the hydrogen fuelling stations. For the high-demand scenario the demand is estimated as 1000 kg/day. For the amount of 1000 kg/day, hydrogen trade with external industries is assumed. The medium-demand scenario is estimated as 800 kg/day, an average of the high- and low-demand scenarios. For 2030, the low-demand scenario is estimated as 3,300 kg/day, based on the hydrogen needed for fuelling stations and the CTV. In the medium-demand scenario a hydrogen demand of 40,000 kg/day is considered, based on possible heating demand and trade with external industries. For the high-demand scenario, all hydrogen produced will be sold. The amount of hydrogen consumed for each scenario is shown in table 4.2:

Scenario	**Demand for hydrogen (kg/day)**	
	present	2030
Low	500	3,300
Medium	800	40,000
High	1,000	Unlimited

Table 4.2: Hydrogen demand scenarios

4.3 Overview of the System

The system to be evaluated is a hydrogen production system, using wind power as a source of electricity. The system is referred to as a wind-powered hydrogen energy system. The wind turbines produce power which is transformed from AC to DC with a rectifier, and the DC power is supplied to the electrolyser, which produces hydrogen. Excess wind power is exported to the grid. The grid capacity is considered to be sufficient to provide the electric load demand at times of low wind power generation. Hydrogen will be stored in a storage facility where the consumer can pick up its daily demand. A suitable system needs to be designed with a control strategy to fulfil the daily demand in addition to being economically feasible. in figure 4.7 an overview of the system is shown and in the following sections the system components are elaborated.

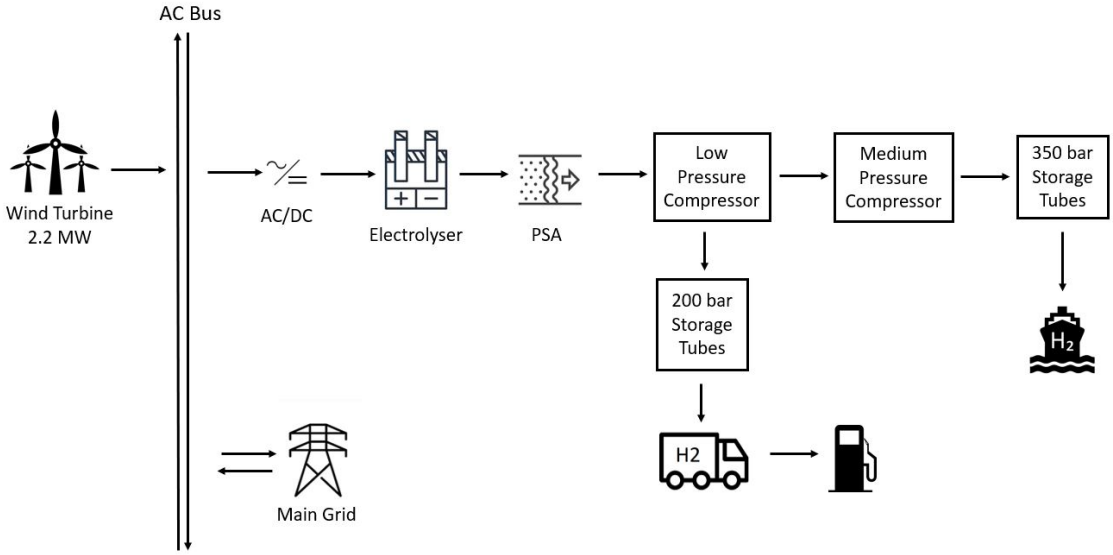

Figure 4.7: Hydrogen energy system with power supply from the wind turbines and the grid

4.3.1 Wind Turbines

In the end of 2019, Vattenfall starts building 6 new wind turbines at the Hemweg location. The wind turbine model that is selected is the Nordex N100/2200, with a rated output of 2.2 megawatts and a hub height of 99m. [81] The hub height of the wind turbines at the Hemweg is restricted at 100 meters by the government. A power curve was obtained from the wind turbine manufacturer and is shown in figure 4.8. The specifications of the wind turbine are shown in table 4.3.

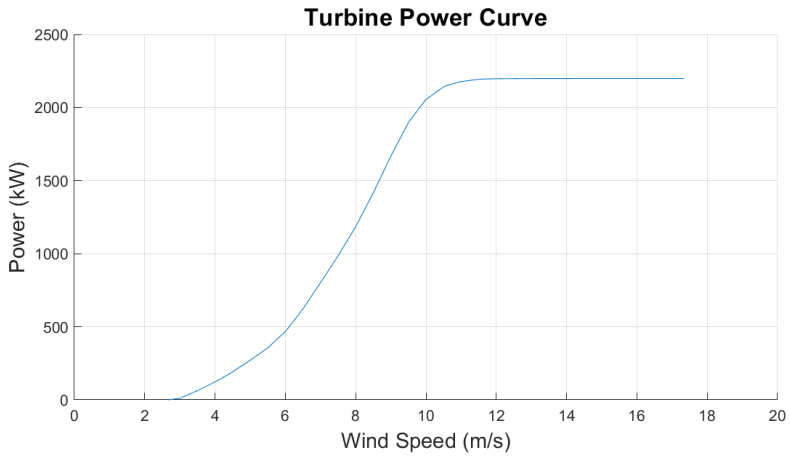

Figure 4.8: Power curve wind turbine N100/2200

Another possibility for the system could be the integration of the electrolyser inside the wind turbine. This is a very novel concept that has not been proven yet. In the Wieringermeer, in the Netherlands, HYGRO is building the first wind turbine with integrated electrolysis for the production of hydrogen, using a 4.8 MW wind turbine and a 2 MW integrated electrolysis system. There can potentially be fewer losses in the different system components: the rectifier can be more efficient, the lack of cables and heavier sizing of the wind turbine is possible. It its stated by HYGRO that the integrated electrolysis system is 40% more energy efficient than the wind turbines that are being developed today. There is no information on the exact effects on efficiency per component, neither on the $CAPEX$ or $OPEX$ of the system. If the $CAPEX$ and $OPEX$ are lower than they are in a regular system, this will positively impact the $LCoE_{H2}$. However, without any further information there cannot be made any assumptions on that aspect.
The website states that integrating the electrolysis in a wind turbine avoids electrical conversion and transport losses between the wind turbine generator and a nearby filling station. In literature it is found that for cable

	N100 / 2200 Turbine
Operation data	
Rated power	2.2 MW
Cut-in wind speed	3.5 m/s
Cut-out wind speed	25 m/s
Rotor	
Diameter	99.8 m
Swept area	7823 m^2
Operating range rotational speed	9.0-16.1 rpm
Rated rotational speed	14.3 rpm
Tip speed	75 m/s
Generator	
Voltage	660 V
Grid frequency	50/60 Hz
Dimensions	
Hub height	99 m

Table 4.3: Specifications Wind Turbine

losses an estimation of 1 % is sufficient and for the rectifier losses of 2 x 5% = 10% can be applied. [82] [13] In the best-case scenario an energy gain of 11% is assumed, which will positively impact the $LCOE_{H2}$. As mentioned, there is no information on the exact effects on the efficiency gain per component, thus unfortunately no calculations can be made here and a wind turbine with an integrated rectifier is not further evaluated in this research.

4.3.2 Electrolyser

Different types of electrolysers have been discussed in section 3.2, and concluded is that the Alkaline and PEM electrolyser are the most suitable options for this case study. In many conversations with experts at the Hydrogen days of Vattenfall and at the *Fueling the Future Congress* in Rotterdam, it was mentioned that the running time of the electrolyser is of great importance to recover investment cost. A very interesting aspect of the PEM electrolyser is the ability to work on small partial load. When working on 10% load, the efficiency can reach up to 95% according to Roberto Iriti, Director Business Development at Giner ELX. When there is low-demand for hydrogen, the electrolyser could work on small partial load, and especially the PEM electrolyser can produce hydrogen at a very high efficiency. This is an interesting aspect of PEM and Alkaline electrolysers to evaluate. Figure 4.9 shows a graph of the efficiency performance of a PEM electrolyser stack working at partial load. The lower the load, the lower the current density, which increases efficiency. The efficiency increase could be modelled using MATLAB and Simulink.

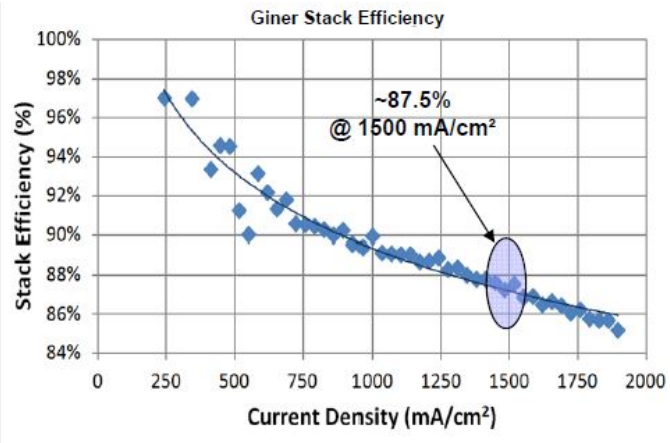

Figure 4.9: Effiency at partial operation of a Giner ELX PEM electrolyser [11]

In addition, PEM electrolysers are able of delivering a higher output pressure than Alkaline electrolyser. These two aspects could benefit the efficiency which therefor could benefit the levelised cost of hydrogen.

Both the PEM and the Alkaline electrolyser will be modelled for this case study. The main parameters and characteristics of the AEC and $PEMEC$ are summarised in table 4.4.

	AEC	$PEMEC$
Operation parameters		
Cell temperature (C)	60-80	50-80
Typical pressure (bar)	1-30	30-80
Current density (A/cm2)	0.25-0.75	1.0-2.0
Flexibility		
Load flexibility (% of nominal load)	10-110	0-160
Cold start-up time	1-2 h	5-10 min
Warm start-up time	1-5 min	$<$ 10 s
Efficiency		
Electrical efficiency (%)	63-70	56-60
Specific electricity consumption at nominal power (kWh/kg)	50	55
Specific electricity consumption at nominal power in 2030 (kWh/kg)	49	50
Available capacity		
Max. nominal power per stack (MW)	6	2
H_2 production per stack (Nm^3/h)	1400	400
Durability		
Lifetime (kh)	60-90	30-90

Table 4.4: Main parameters AEC and PEMEC electrolysers [6][15][3][16]

4.3.3 Purification

Pressure swing adsorption (PSA) processes are used for the production of hydrogen a high purity. The PSA technology is based on a physical binding of gas molecules to adsorbent material. The impurities on the adsorbent material are desorbed at high pressure, typically in the range of 10 to 40 bar, and the adsorbent material is regenerated. A specific electricity consumption of 1.3 and 1.1 kWh/kg for the present and 2030 scenario is assumed. [83] The cost of the PSA is included in the electrolyser cost.

4.3.4 Compressor

The hydrogen is stored in the stationary tank after production. These tanks have a capacity of 500 kg with a pressure of 200 bar, thus, the hydrogen needs to be compressed before entering the storage tubes. A part of the hydrogen needs to be compressed further to 350 bar and is stored in high pressure storage tubes that are placed directly on the CTV. Hence, the system requires a low- and a medium-pressure compressor for storing the hydrogen at 200 and 300 bar, respectively. The PEM electrolyser delivers hydrogen at a higher output pressure than the Alkaline electrolyser. The difference in output pressure has an effect on the specific electricity consumption. For all system configurations, the specific energy consumptions are modelled in the next chapter. For the year 2030, the same values for the specific electricity consumption are used. When part of the hydrogen is used for FCEVs, the hydrogen needs to be compressed at a very high-pressure before fuelling the vehicles. This compressor will not be modelled, but is included in the economic analysis to estimate a price for the fuelled hydrogen.

4.3.5 Storage Tubes

Stationary storage tubes on-site are necessary to store the hydrogen. Specifically, there are two kinds of storage tubes used in this system. One is for storing a large amount of hydrogen at a pressure of 200 bar, while the other one is for storing hydrogen at 350 bar pressure for the CTV. Storage tubes of 200 bar are used for on-site hydrogen storage. One additional tank of 200 bar is used as a backup, which can be assembled on a truck trailer for transport.

4.3.6 Hydrogen Fuelling Station

The energy system in this case study delivers hydrogen at 200 bar, which is transported in a trailer on a truck to consumers. As discussed in 4.2, hydrogen fuelling stations could offer a demand for the supplied hydrogen. The hydrogen is delivered, via the truck trailer, at 200 bar at the hydrogen fuelling stations. All fuelling stations consist of storage facilities for the hydrogen, compressors to bring the hydrogen to the desired gas pressure level, a cooling system and dispensers for delivering the fuel. A system overview is shown in figure 4.10. For this case study, the cost of hydrogen at 200 bar and the cost at the fuelling station is calculated. After the production and compression, the hydrogen needs to be stored at 200 bar. For the 1MW system, 2 compressors of 400 kg are assumed. For the 2MW system, 3 storage tanks of 400 kg are assumed. This is enough to store hydrogen at moments of low-demand and high production, to keep the electrolysers running.

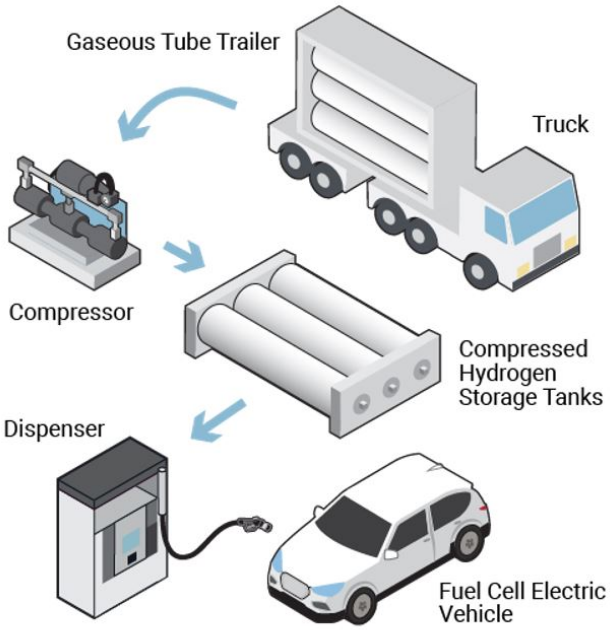

Figure 4.10: A hydrogen fuelling system [12]

4.3.7 CTV Vattenfall

The hydrogen-powered crew transfer vessel (CTV) that will be used by Vattenfall for maintenance of the offshore wind parks could offer a demand. On board of the ship, one big tank of 90 kg and 2 smaller tanks of 40 kg will be used. After compression to 200 bar, a medium-pressure (MP) compressor is used to compress the hydrogen to 350/400 bar. The compressed hydrogen is stored in the tanks of 90 kg and 40 kg, and the tanks are loaded into the CTV.

4.4 System Sizing

It is decided to model two different system sizes, which are referred to as the 1 MW system and the 2 MW system, based on the electrolyser size. The details of the scale of each component for the 1 MW and the 2 MW system are shown in table 4.5. Smaller sizes of system were excluded as they were not economically feasible. The sizing of all components of the system is based on literature and in accordance with Arne Jacobsen from Vattenfall BA Wind and Zeki Sarac from SEK Consulting.

	The scale of the system	
	1 MW electrolyser	2 MW electrolyser
Wind Turbines	2.2 MW	4.4 MW
LP Compressor	20 kg/h	40 kg/h
MP Compressor	6.3 kg/h	6.3 kg/h
Tube trailers 200 bar	800 kg	1200 kg

Table 4.5: System scale

Larger stations with 1000+ kg/day capacity will be economically favoured, however, smaller scale fuelling stations of 100-350 kg/day are more likely to be installed to accommodate early markets. [84] For this case study a hydrogen fuelling station (HFS) with a capacity of 350 kg/day is assumed. The sizes of all components of a hydrogen fuelling station with a 350 kg/day capacity are estimated as well. Based on the estimation that one car fuels 4 kg of hydrogen and that in peak hours approximately 30 cars will make use of the fuelling station, the high-pressure (HP) compressor is estimated to compress 35 kg/h and the storage tank is estimated to hold 100 kg of hydrogen, to provide enough when multiple cars are fuelling at once. [85] To be able to fuel 4 cars at once, 2 dispenser units are considered with both 2 fuel tank inlets each. The dispenser unit is estimated to provide cooling water at a rate of 9.2 kg/min according to [86]. One tube trailer truck is needed to deliver the hydrogen to the station.

	The scale of the HFS
HP Compressor	35 kg/h
Stationary Storage 875 bar	100 kg
Dispenser Units	2
Chiller Units	9.2 kg/min
Tube trailer Truck	1

Table 4.6: Sizing hydrogen fuelling station

For the hydrogen that is supplied to the CTV, one tube trailer truck is needed to deliver the hydrogen to the MP compressor and storage location. The MP compressor has a size of 6.5 kg/h. which is based on providing the demand of 150 kg/day. When the storage tubes of 150 kg are filled, the storage tubes are loaded onto the CTV. The other 150 kg of storage tubes are filled during a day. After that day, the empty storage tubes are switched with the full storage tubes. Hence the storage tubes have together have a total capacitiy of 300 kg, which is equal to 2 days of consumption.

	Sizing CTV
Tube trailer Truck	1
MP Compressor	6.5 kg/h
Storage Tubes 350 bar	300 kg

Table 4.7: The scale needed for hydrogen supply to the CTV

4.5 Concluding Remarks

In this chapter, the features of the location were discussed including wind speeds and hydrogen demand. The estimated hydrogen demand is divided into three scenarios with each a different demand, which are shown in table 4.2. The designed hydrogen energy system consists of an electrolyser, a purifacor and a low pressure compressor compressing the hydrogen to 200 bar. After the hydrogen is compressed to 200 bar, the hydrogen is supplied in tube trailers to industry, hydrogen fuelling stations and the CTV of hydrogen. An overview of the designed energy-system is shown in figure 4.7.

To evaluate how much effect the pressure output of an electrolyser and the type of electrolyser has on the costs, the wind-powered hydrogen energy system is modelled in the next chapter for two different electrolyser:

- An Alkaline electrolyser at 1 bar.
- A PEM electrolyser at 40 bar.

As well as two different system sizes:

- A 1 MW system
- A 2 MW system

All these different system configurations are modelled and economically compared in the next chapters.

Chapter 5

Modelling of Components

In this chapter, the modelling of each system component is discussed. The model of each component is defined based on commercial product specification from the present market. The wind-powered hydrogen energy system is modelled for two different electrolysers: a PEM electrolyser with an output pressure of 40 bar and an Alkaline electrolyser with an output pressure of 30 bar. These two electrolysers are modelled for 2 different sizes: 1 MW and 2 MW. Each simulation is executed for all demand scenarios as described in section 4.2.4. MATLAB and Simulink are used to model the wind-powered hydrogen energy system and then simulate the dynamic behaviour of the energy system. MATLAB is used for textual programming and Simulink (an extension of MATLAB) is used for the graphical programming. In figure 5.1 the programmed model of the energy system in Simulink is shown. It consists of a wind turbine model, an AC/DC converter, an electrolyser, a compressor and a storage tank.

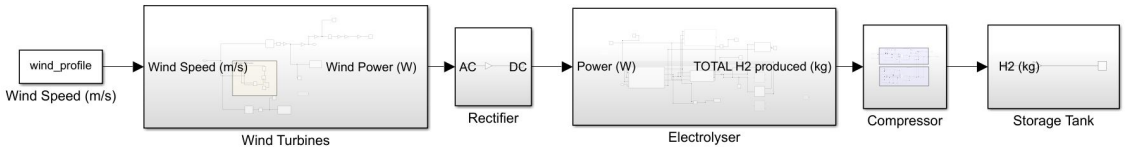

Figure 5.1: The model in Simulink

5.1 Modelling the Wind Speeds

To estimate the wind speed at the exact height of the hub the power law is utilised:

$$\frac{U(z)}{U(z_r)} = (\frac{z}{z_r})^{\alpha} \tag{5.1}$$

where $U(z)$ is the wind speed at height z in m, $U(z_r)$ is the reference wind speed at height z_r in m, and α is the power law exponent. The exponent *alpha* is a highly variable quantity. [87] An overall power law exponent of 0.295 was measured, conducted in MATLAB by using the wind profile measured by Vattenfall (section 4.1.1. With the power law equation the wind speeds are adjusted to the height of the hub of the wind turbine. The average wind speed with adjusted height is now 6.3 m/s.

The wind data is used to compute the probability of the occurrence of wind speed in MATLAB. The measured wind speed frequency distribution over the measured period is shown in the histogram in figure 5.2.

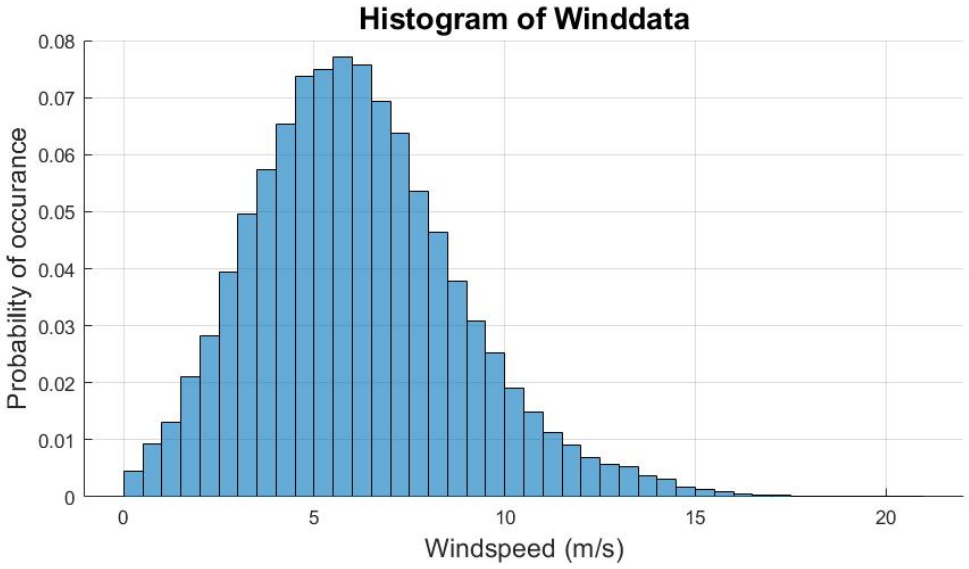

Figure 5.2: Wind speed histogram at 95m

5.2 Model Description Wind Turbines

5.2.1 Wind Power Model

The wind power model calculates the wind power generated based on the wind speed every ten minutes. A wind turbine does not respond in seconds to varying wind speeds, as the inertia of the wind turbine causes a delay time. The model uses wind speeds as the input and then applies a transfer function in order to simulate a delay in the response of the turbine output whenever the wind speed varies. The time constant for delay also varies with wind speed, making the model more realistic. The delayed wind speed output is then calculated by a lookup table in Simulink to find the power generated by the wind turbine corresponding to the wind speed at that moment in time. The Simulink model is shown in figure 5.3.

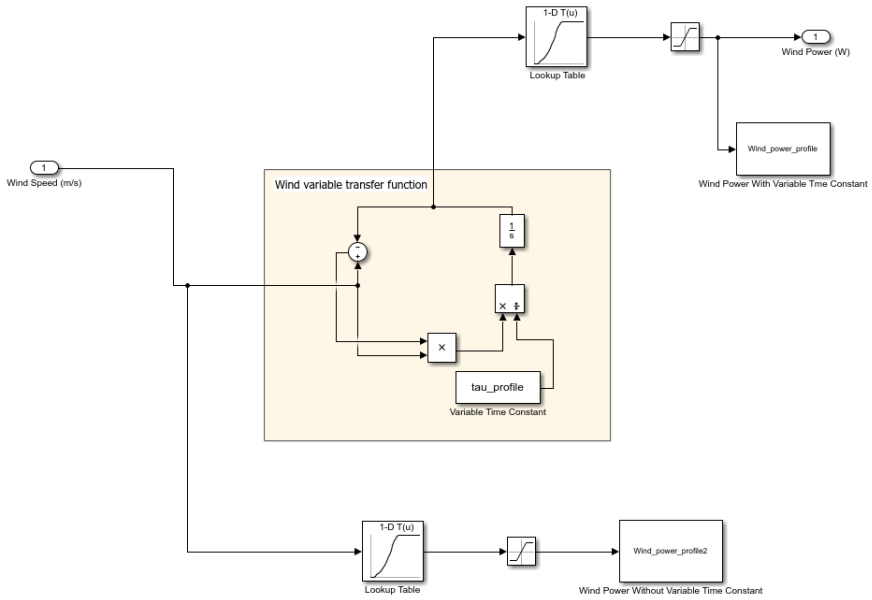

Figure 5.3: An overview of the wind power Simulink model

5.2.2 Wind Power Output

The mechanical power obtained from the wind turbines is defined with the equation:

$$P_m = \frac{1}{2} c_p \rho A v^3 \tag{5.2}$$

Where P_m the mechanical power is in Watt, c_p the power coefficient, A the area swept of the rotor blades in m^2, V the wind speed in m/s. c_p is a function of the pitch angle β, which is determined by the shape of the wind turbine blade and the tip speed ratio λ, which is dependent on the wind turbine rotation speed, but which is a controllable parameter. There are several equations that can be used to express c_p. Vattenfall makes use of a program called Windographer to determine the c_p, and with that the power. For this thesis the power curve obtained by Windographer was used in a look up table in Simulink. The power curve has been shown in figure 4.8.

The power extracted from the wind is strongly related to the inertia of the system. The natural time-constant (τ_0) is a measure of the time in which a wind turbine reaches the rated rotational speed from standstill under the rated torque. The actual time constant (τ) is defined as the time interval between two steady-state speeds when the shaft speed reaches to 63.3% of the total change. The time constant can be calculated with the natural time-constant. For the wind, a variable time constant is used and was calculated using the following equations [88] [89]:

$$Moment\ of\ Inertia, J = \frac{1}{6} \times m_{rotor} \times R^2 \tag{5.3}$$

$$Rated\ Torque, T_r = \frac{P_r}{\omega_r} \tag{5.4}$$

$$Natural\ Time\ Constant, \tau_0 = \frac{J}{T_r} \times \frac{\omega_r}{3} \tag{5.5}$$

$$Variable\ Time\ Constant, \tau = \tau_0 \times \frac{v_r}{v} \tag{5.6}$$

Where m_{rotor} is the mass of the turbine rotor in kg, R is the rotor radius in m, P_r is the rated power in W, ω_r is the rated angular speed in rad/s, v_r is the rated wind speed in m/s and v is the actual wind speed in m/s. The natural time constant τ_0 is found to be: 1069.8 s. The calculated variable time constant varies between: 606.05 and 130.41 $\times 10^7$ s. A transfer function is applied in order to simulate a delay in the response of the turbine output whenever the wind speed varies. The wind power profile for one week, with and without the variable time constant is shown in figure 5.4.

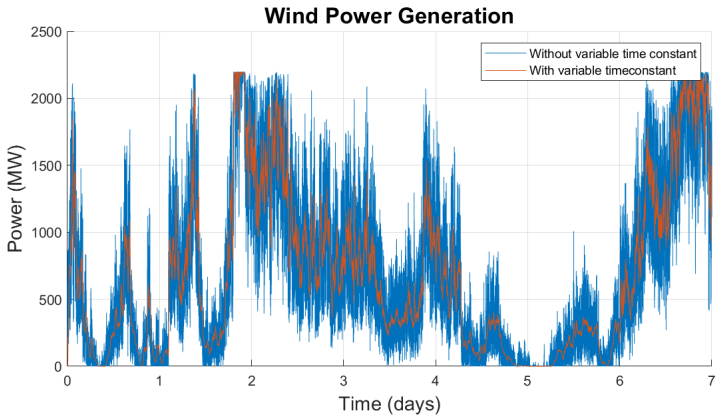

Figure 5.4: The wind power profile for one week, with and without variable time constant

The total power output of one wind turbine is 6500 MWh over a year, using the wind data as an input. The capacity factor (C_p) of the wind turbine is:

$$C_p = \frac{annual\ energy\ yield\ (MWh)}{hours\ in\ a\ year \times power\ capacity\ (MW)} = \frac{6500\ MWh}{8760\ hr \times 2.2\ MW} = 0.34 \tag{5.7}$$

The capacity factor is approximately 34% at the Hemweg location.

5.3 Modelling the AC/DC Converter

The efficiency of the AC/DC converter (or rectifier) is dependent on the load factor. The load factor is the ratio of the nominal capacity of the actual power demanded by the electrolyser. This relationship is shown in figure 5.5. As can be seen in the figure, for a load factor above 0.2, the efficiency of the rectifier is 0.95%. To simplify, an efficiency of 0.95% is assumed for the energy system in this research.

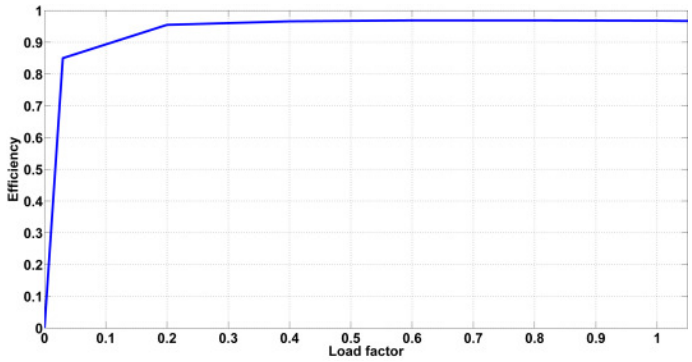

Figure 5.5: Rectifier efficiency as a function of the load factor as modelled in reference [13].

5.4 Model Description Electrolysers

As described earlier in section 4.3.2, electrolysers could work on small partial load and increase the efficiency. Especially the *PEM* electrolyser can produce hydrogen at a very high efficiency. The lower the load, the lower the current density, which increases efficiency, however, a lower current density lowers the hydrogen output. The efficiency increase at partial load could be modelled using MATLAB and Simulink.

The bipolar cell design of the electrolysers that are modelled, consist of several cells in series. A single cell is the basic unit making use of DC current to generate hydrogen. Therefore, a single electrolyser cell was modelled for both the *PEM* and Alkaline electrolyser. By multiplying several cell models, a stack can be modelled. An electrolyser cell can be divided into three submodels: the electrochemical submodel, the thermal submodel and the hydrogen production submodel. The general overview of the electrolyser cell model is shown in figure 5.6.

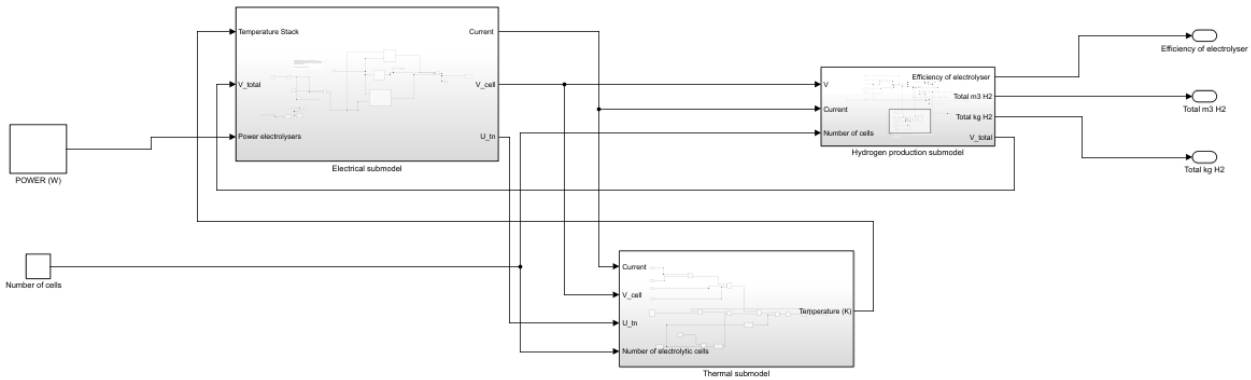

Figure 5.6: Model overview of the electrolysers, consisting of 3 submodels

5.4.1 Control System Electrolyser

Included in the model is the start-up time of each electrolyser. The start-up time is taken as 10 seconds and 5 minutes for the *PEM* and the Alkaline electrolyser, respectively, as stated in table 4.4. Every time the model of the output power of the electrolyser hits zero, a trigger is activated, which sends a pulse for the amount of seconds the start-up time lasts. Hence, the zero value is delayed with the start-up time for the modelled electrolyser. For each of the two modelled electrolysers, all present demand scenarios are modelled. The daily demand of hydrogen is subtracted from the hydrogen that is produced by the electrolyser. When this amount

reaches a value lower then the needed amount for the next day, a signal is send to the electrolyser and power is supplied by the grid to run the electrolyser on full load. When the amount needed for the next day is reached, the electrolyser runs on wind energy again until the storage tank is full. When the storage tank if full and the demand is met, a new storage tank is connected. This part of the control system of the electrolyser is displayed in figure 5.7:

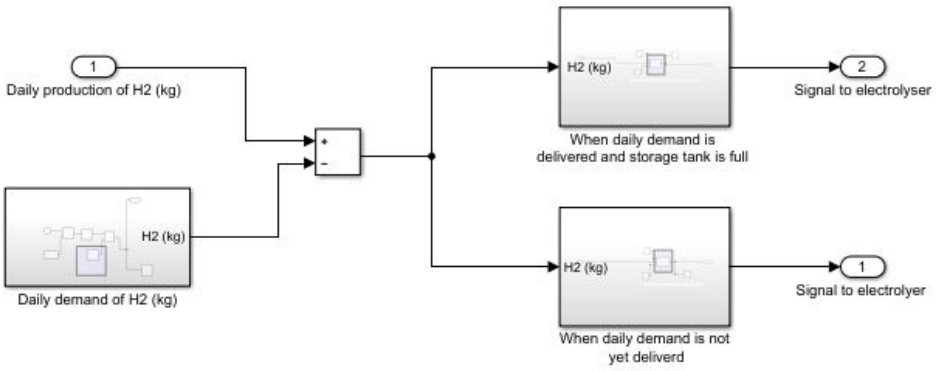

Figure 5.7: Control system electrolyser

5.4.2 Thermal Submodels

For the PEM and Alkaline electrolysers, the thermal submodel can be considered equal. The temperature in the electrolyser stack is supposed to be uniform, and in this model each cell is considered to have identical thermal behaviour. A lumped thermal capacitance model can be used for the thermal submodel according to Ulleberg [90]. The thermal energy balance can be expressed as:

$$C_{th}\frac{dT}{dt} = \dot{Q}_{gen} - \dot{Q}_{loss} - \dot{Q}_{cool} \tag{5.8}$$

Where $\dot{Q}_{gen}$ and $\dot{Q}_{loss}$ can be approximated with the equations:

$$\dot{Q}_{gen} = n_c(V_{cell} - U_{tn})I \tag{5.9}$$

$$\dot{Q}_{loss} = \frac{1}{R_{th}}(T - T_{amb}) \tag{5.10}$$

Cooling systems can differ significantly from each other and modelling the cooling system is beyond the scoop of this research. Thus $\dot{Q}_{cool}$ is taken as zero and a saturation block in Simulink is used to define a maximum temperature which is equal to the stack temperature as shown in figure 5.8. The lumped thermal capacitance (C_{th}) is estimated as 42.045 kJ/°C based on literature [91]. The thermal resistance R_{th} can be approximated based on the lumped thermal capacitance:

$$R_{th} = \frac{\tau_{th}}{C_{th}} \tag{5.11}$$

Where τ_{th} is the measured thermal time constant during natural cooling of the stack. Which in this model is also obtained from literature and is taken as 3435 s. [91]. The complete thermal submodel created in Simulink is shown in figure 5.8. The integrator block is used to integrate the temperature per second (in K/s) to the Temperature of the stack in K.

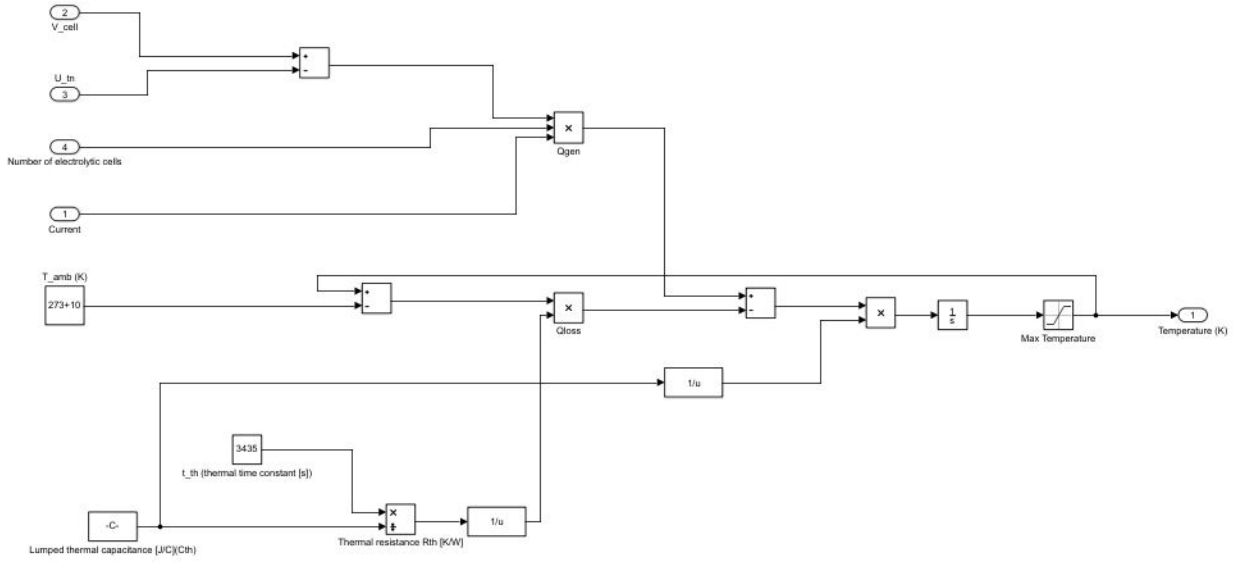

Figure 5.8: Thermal sub model

The effect of temperature on cell polarisation for various current densities in the model in Simulink is shown in figure 5.9. The increase in temperature of the cells results in a decrease in cell polarisation, which enhances the cell performance.

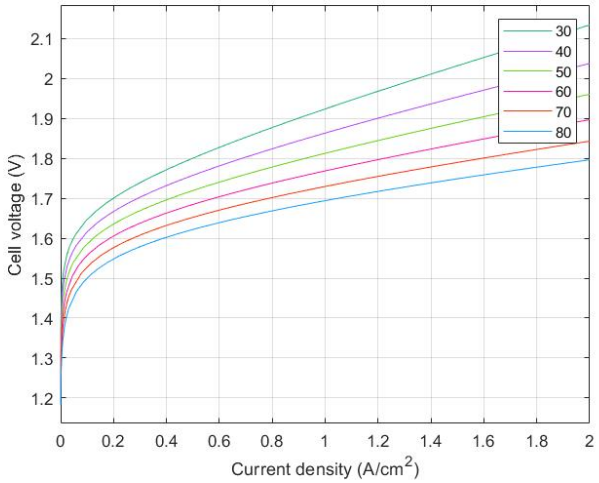

Figure 5.9: The cell polarisation at different temperatures (30°C, 40°C, 50°C, 60°C, 70°C, 80°C)

5.4.3 PEM Electrochemical Submodel

As discussed earlier in section 3.2.1, the minimum voltage to start water electrolysis is the reversible voltage. This is affected by pressure and temperature conditions. In non-ideal systems, the potential applied must be higher due to different losses. These losses are calculated in the electrochemical submodel shown in figure 5.10. The operating voltage of the cell is equal to the reversible voltage and the sum of the different overpotentials and modelled according to equation 3.7 as shown in the electrochemical submodel:

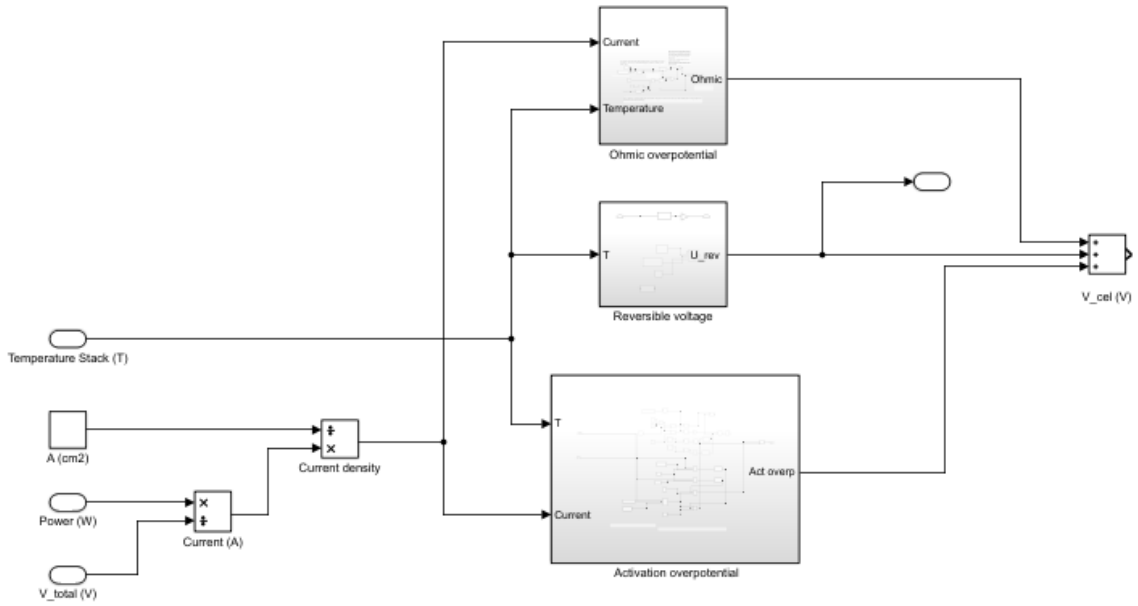

Figure 5.10: PEM electrochemical submodel

The reversible voltage for PEM electrolysis can be empirically expressed as [92] :

$$V_{rev} = 1.23 - 0.9 \times 10^{-3}(T - 298) + 2.3\frac{RT}{4F}log(P_{H_2}^2 P_{O_2}) \tag{5.12}$$

P_{H_2} and P_{O_2} are the partial pressures in Pa, F is the Faraday's constant, R is the gas constant equal to 8.3145 $J/Kmol^-1$, T is the temperature in K depending on different factors and calculated in the temperature submodel.

For commercial PEM electrolysers the concentration over-potential can be neglected. The gas transport limitations in thin electrodes are insignificant for PEM electrolysis under normal operation conditions. Hence, the concentration over-potential in this model is chosen to be zero.[91]

The activation overpotential is equal to the sum of the overpotential in the anode and the cathode and is expressed with the following equation:

$$\eta_{act} = \frac{RT}{\alpha_a nF} arcsinh(\frac{i}{2i_{0,a}}) + \frac{RT}{\alpha_{cat} F} arcsinh(\frac{i}{2i_{0,c}}) \tag{5.13}$$

$i_{0,a}$ and $i_{0,c}$ are the exchange current densities from the anode and the cathode, respectively, in A/cm^2. α_a and α_c are the charge transfer coefficients for the anode and the cathode, respectively. It is usually accepted to assume both charge transfer coefficients as 0.5 for the cathode and 2 for the anode. [91] The activation over-potential is highly effected by the exchange current densities, which are dependent on the electrocatalyst, electrode morphology, age, pressure and temperature. [91] A simplified expression for the exchange current density is described by equation:

$$i_0 = i_{0,ref} e^{[-\frac{E_{exc}}{R}(\frac{1}{T} - \frac{1}{T_{ref}})]} \tag{5.14}$$

Where the value for $i_{0,ref}$, the reference exchange current density, is selected according to literature studies and a value of $1 \times 10^{-6} A/cm^2$ is used for the anode and $1 \times 10^{-3} A/cm^2$ is used for the cathode. [91] [93] E_{exc} is the activation energy for the electrode reaction. A value for E_{exc} of 18 kJ/mol and 76 kJ/mol are assumed for the cathode and anode, respectively. [92] A reference temperature T_{ref} of $25°C$ is used. [24] The contribution to the activation over-potential from the anode and the electrode is not symmetric. The values for the exchange current density at the anode are much lower normally than for the cathode. [91]

The ohmic resistance can be expressed with the equation:

$$\eta_\Omega = (R_{ele} + R_{ion})i \tag{5.15}$$

With i the current in A, R_{ion} the ionic resistance in Ω and R_{ele} the electronic resistance in Ω, which is measured between the stack terminals at open circuit conditions. However R_{ele} is neglected in this model as

this will not lead to large errors in the estimation according to reference [91]. R_{ion} can be obtained with the equation:

$$R_{ion} = \frac{t_m}{\sigma} \tag{5.16}$$

With t_m the membrane thickness in m and σ the conductivity of the membrane in S/m. The membrane is considered to be fully saturated with water. For this reason, the conductivity is only a function of temperature. Usually the electrolyser has a water management system that assures the membrane is saturated. [91] The conductivity of the membrane can be modelled using the Arrhenius expression:

$$\sigma(T) = \sigma_{ref} e^{[\frac{E_{pro}}{R}(\frac{1}{T_{ref}} - \frac{1}{T})]} \tag{5.17}$$

With E_{pro}, which represents the activation energy for proton transport in the membrane and R the gas constant equal to 8.3145 $J/Kmol^{-}1$. In the model a value for E_{pro} of 10542 is used, T is the temperature in K and a reference temperature T_{ref} of 25°C is used. σ_{ref} is modelled according to reference [94].

To conduct the simulation of the PEM electrolyser, input data are required to determine the outputs of the system. Table 5.1 shows an overview of the input parameters that are used for the simulation of the PEM electrolyser:

Input parameters	
Cell area (cm^2)	100
Operating temperature (K)	300
Operating pressure (bar)	40
Membrane thickness (mm)	17.8
Operating pressure (bar)	40
E_{pro}	10542
T_{ref} (°C)	25
E_{exc} Cathode (kJ/mol)	18
E_{exc} Anode (kJ/mol)	76
α_a	0.5
α_c	2
$i_{0,ref}$ Cathode (A/cm^2)	1×10^{-3}
$i_{0,ref}$ Anode (A/cm^2)	1×10^{-6}

Table 5.1: Input parameters PEM electrolyser model

To validate the accuracy of the model that was created in Simulink, the PEM electrolyser model is compared with experimental data from literature. An electrolyser cell is characterised by its relationship between current density and voltage, which is represented by the polarisation overpotentials. All individual overpotentials are compared with the results obtained in [95], which corresponds well with the overpotentials of the modelled PEM electrolyser cell shown in figure 5.11, supporting the accuracy of all individual overpotentials in the model.

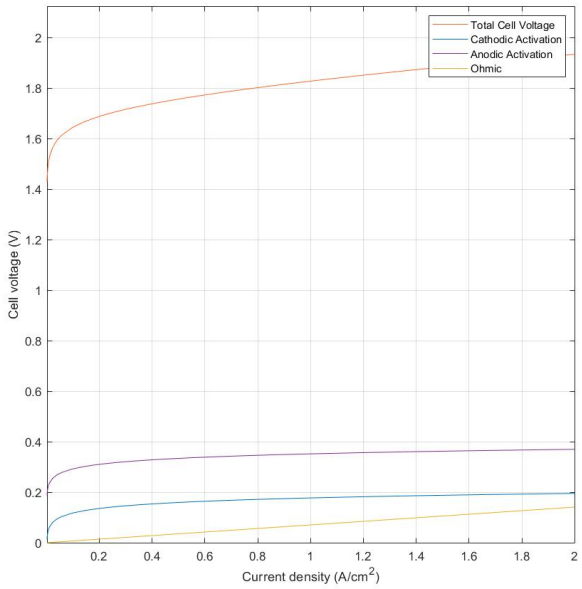

Figure 5.11: The modelled overpotentials of the PEM electrolyser

To validate the complete electrochemical submodel, the simulation results for the cell polarisation curve are compared with experimental data of literature [94] as shown in figure 5.12. This simulation is done for one cell, with a cell area of 100 cm^2 and a membrane thickness of 0.0178 cm. Other input parameters were adjusted such as the operating temperature of 80°C and operating pressure at 1 atm. The cell polarisation curve in figure 5.12 shows that the voltage current plot for an electrolyser of [94] (orange line) are well predicted by the model (blue line).

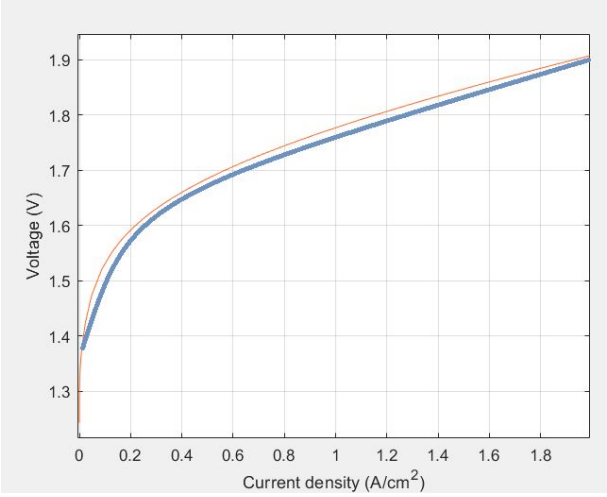

Figure 5.12: Comparison of the model and experimental data of PEM electrolyser J–V characteristics

5.4.4 Alkaline Electrochemical Submodel

For the alkaline electrochemical submodel an empirical model is used, proposed by Ulleberg et al in [90]. The cell voltage is expressed as in equation 3.7, with a value for V_{rev} of 1.229 V and with the following expression for the ohmic overpotential:

$$\eta_{\Omega} = \frac{r_1 + r_2 T}{A} I \tag{5.18}$$

With r_1 and r_2 parameters related to the ohmic resistance of the electrolyte. T is the operating temperature in K, A is the cell area in cm^3 and I is the current in A. The constant parameters r_1 and r_2 are used as in [96]

and are displayed in table 5.2. The activation overpotential is defined as:

$$\eta_{act} = slog(\frac{t_1 + \frac{t_2}{T} + \frac{t_3}{T^2}}{A} I + 1) \tag{5.19}$$

With s, t_1, t_2 and t_3 coefficients chosen according to reference [96], displayed in table 5.2.

Input parameters	
r_1 (Ωm^2)	8.05e-5
r_2 (Ωm^2 $^\circ C^{-1}$)	-2.5e-7
t_1 ($A^{-1}m^2$)	1.002
t_2 ($A^{-1}m^2$ $^\circ C$)	8.424
t_3 ($A^{-1}m^2$ $^\circ C$)	247.3

Table 5.2: Input parameters Alkaline electrolyser model

To validate the electrochemical submodel of the Alkaline electrolyser, the simulation results for the cell polarisation curve are compared with experimental data in literature [96] as shown in figure 5.13. This simulation is executed for one cell, with a cell area of 250 cm^2 and an operating temperature of 40$^\circ C$. The results for the cell polarisation curve of the model (in orange) agree well with the experimental data (in blue). This supports the accuracy of the developed model in MATLAB.

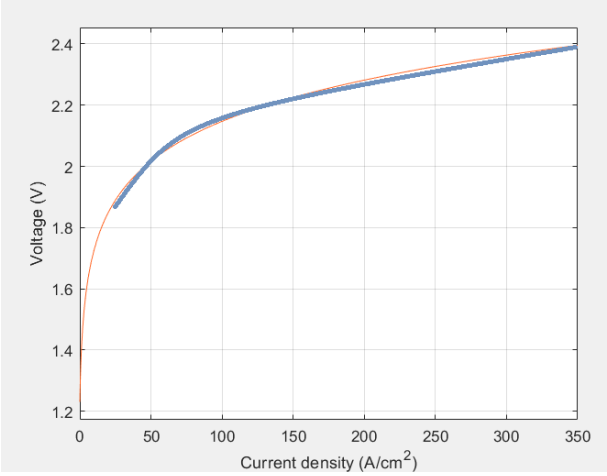

Figure 5.13: Comparison of the model and experimental data of Alkaline electrolyser J–V characteristics

5.4.5 Hydrogen Production Submodels

The hydrogen production submodel of the PEM and the Alkaline electrolyser can be modelled in the same manner. The molar flow rate of hydrogen that is produced can be described by the Faraday's law:

$$\dot{V}_{H2} = \eta_F \frac{n_c I}{2F} \tag{5.20}$$

With η_F the Faraday efficiency, n_c the number of electrolysis cells that are connected in series, I the current, F the Faraday constant and $\dot{V}_{H2}$ is given in mol/s. To model the hydrogen flow rate in kg/s, the hydrogen density needs to be calculated, which is dependent on pressure and temperature. The hydrogen density can be calculated through the ideal gas law (equation 3.24). This law is modelled in Simulink, in which different values for the desired temperature and pressures can be used. For higher pressures the ideal gas law does not fit anymore, as discussed in section 3.3.1. Instead of the ideal gas law, the real gas law is used:

$$PV = znRT \tag{5.21}$$

Where P is the pressure in atm, V is the volume in L, z is the compressibility factor, n is the number of moles in the gas, R is the ideal gas constant in L atm mol$^-$1 K$^-$1, T the temperature in K. z is a correction factor which describes the deviation of a real gas from ideal gas behaviour. As hydrogen acts as an ideal gas at low pressure,

but it starts deviating from ideal behaviour at higher pressure and transforms for different temperatures. z depends on both temperature and pressure and up to 1000 bar and at 300K, z can be expressed as [97]:

$$z = 1 + k_{z,300}(\frac{p}{p_{atm}}) \tag{5.22}$$

Where $k_{z,300} = 0.000631$ and p_{atm} is standard pressure. The used value for z can be verified in graph 5.14 [14].

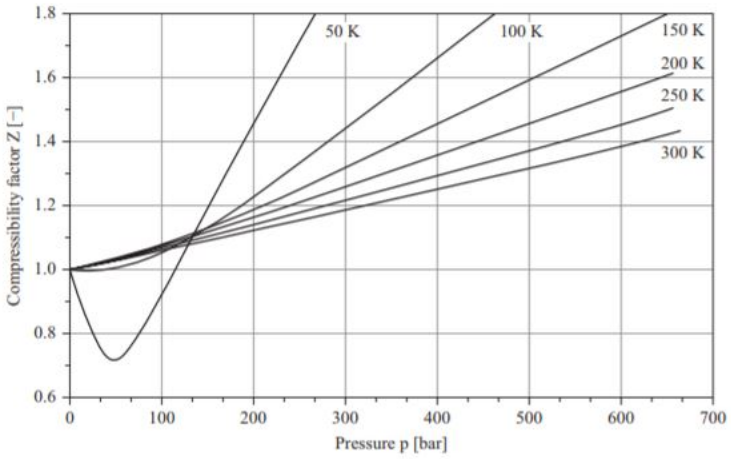

Figure 5.14: Compressibility factor of hydrogen [14]

The Faraday's law and the Ideal gas law are combined and the hydrogen flow rate is then modelled in kg/s as shown in figure 5.15.

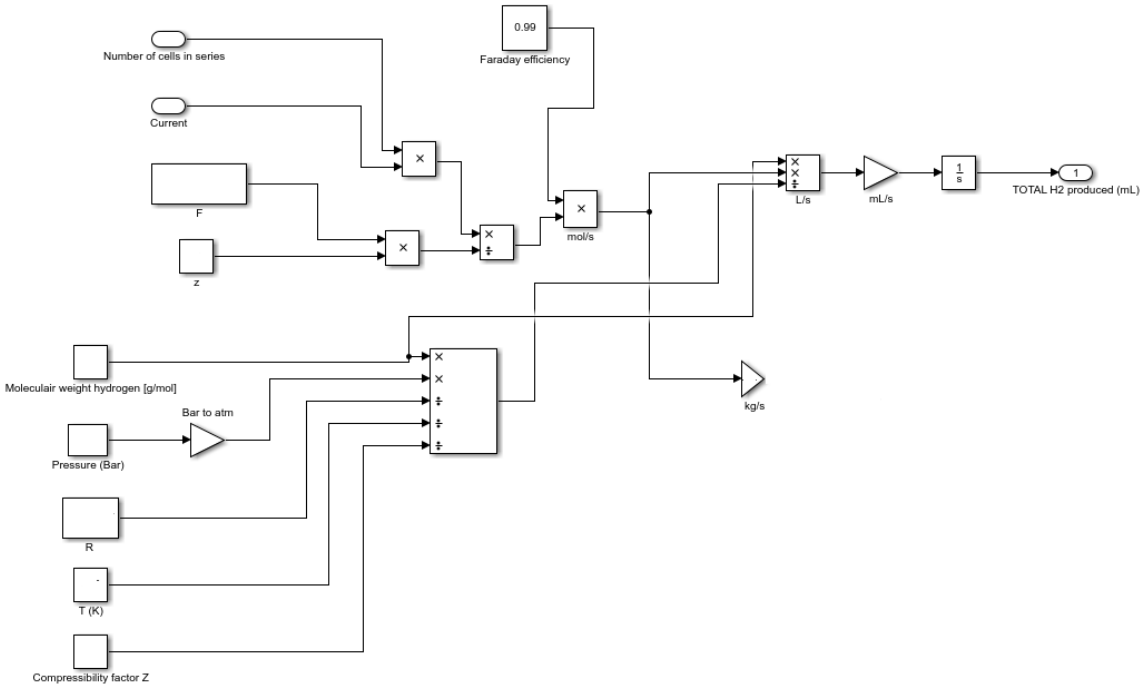

Figure 5.15: Hydrogen production submodel

The integrator block outputs the value of the integral of the hydrogen flow rate with respect to time to model the hydrogen output in kg. The hydrogen output is modelled as in figure 5.16.

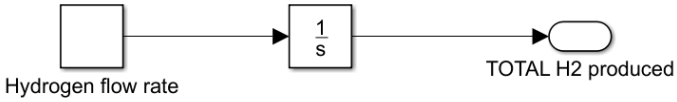

Figure 5.16: Hydrogen output

To validate the hydrogen production submodel, a comparison is made on a larger scale with multiple cells. The model is compared to a PEM electrolyser stack of 720 W consisting of 5 cells presented in literature [95] with a hydrogen output is 8.7 ml/min at 300K and 350 bar. Entering the same parameters in the model shows a similar hydrogen output of 8.77 ml/min as presented in figure 5.17.

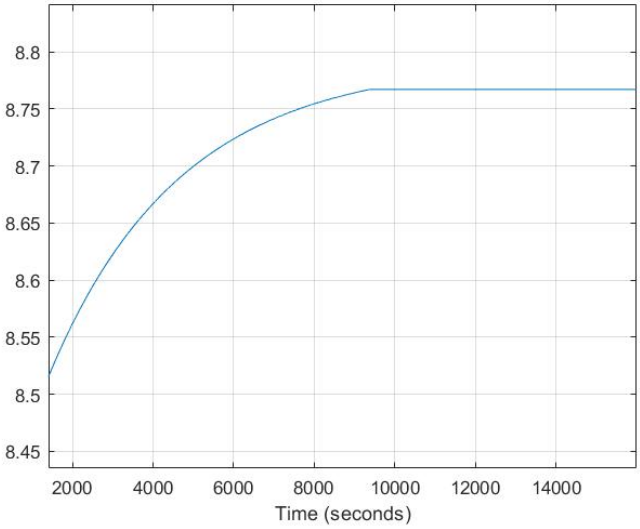

Figure 5.17: Hydrogen output model

5.5 Model Description Compressor

The energy consumed by the compressor is dependent on the hydrogen output pressure yielded by each considered electrolyser. The electrolysers compress the hydrogen to the delivery pressure, which is different for thePEM and Alkaline electrolyser. The lower the output pressure of the electrolyser, the more pressure needs to be added, the higher the energy consumption by the electrolyser, this leads to increased costs. As discussed, hydrogen pressures over 100 bar deviate from the ideal gas law and the compression factor, z, compensates for the non-ideality. Combining equation 5.22 with the real gas equation 3.24, the isothermal expression can be formed:

$$W = p_0 V[k_{z,300}\frac{(p_1 - p_0)}{p_{atm}} + ln(\frac{p_1}{p_0})] \tag{5.23}$$

According to equation 5.23,the Work required for every compressed kg of hydrogen is modelled in Simulink:

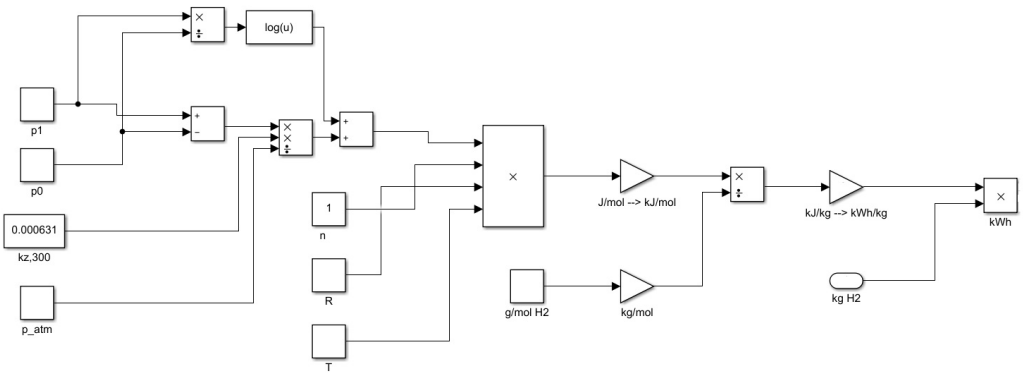

Figure 5.18: Isothermal compression model

However, the compression is never completely isothermal. In most compression systems, a significant amount of heat is formed during the process. When all heat produced is kept in the gas by ideal insulation, it is called adiabatic compression. The amount of Work (W) needed for adiabatic compression can be expressed as [97]:

$$W = \frac{y}{y-1} p_0 V [(\frac{p_1}{p_0})^{(y-1)/y} - 1] \tag{5.24}$$

Where y is the ratio of the specific heats (C_p/C_v). C_p is the heat capacity at constant pressure and C_v heat capacity at constant volume. According to equation 5.24, the Work required for adiabatic compression per kg of hydrogen is modelled in Simulink:

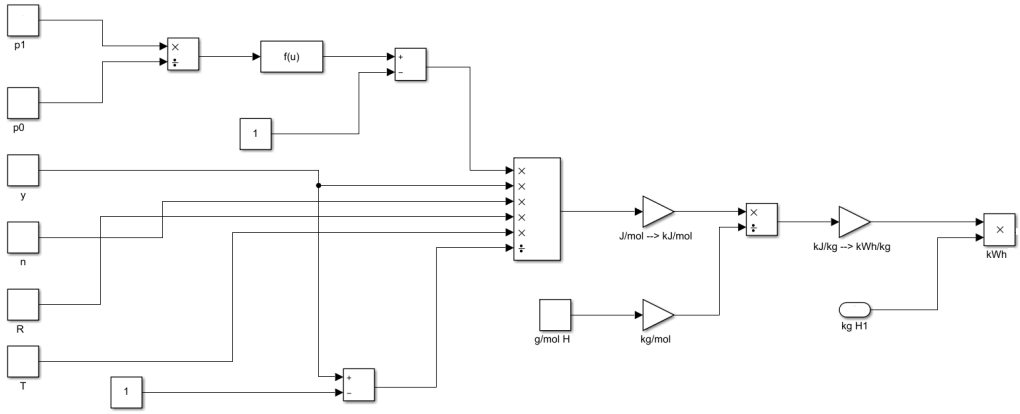

Figure 5.19: Adiabatic compression model

The Work for adiabatic compression is larger than the Work needed for isothermal compression, because the heat that is formed creates a higher pressure, which the compressor has to overcome. In reality, the Work of compression lies somewhere between the Work needed for isothermal compression and adiabatic compression. [97] In this model the compression for both isothermal and adiabatic is calculated and the average is used.

Chapter 6

Simulation Results

MATLAB and Simulink are used to model a system and then simulate the dynamic behaviour of that system. For each electrolyser, two different sizes have been considered. A 1 MW size and a 2 MW size, thus in total 4 different system-configurations have been modelled. For each system-configuration, the total hydrogen production is simulated when working on nominal load. In chapter 4, different demand scenarios for hydrogen have been discussed for the present and for 2030. For each system-configuration, it is calculated if the system can produce enough hydrogen to meet the hydrogen demand scenarios. When the electrolyser cannot meet the demand for hydrogen, it is assumed that the electrolyser works full-time on nominal load. When the electrolyser can meet the demand for hydrogen, the electrolyser will work for some time on partial load. As discussed previously, when electrolysers work on partial load, the efficiency is higher. Also a control system has been used (as described in chapter 5) that tries to increase the use of renewable wind electricity and lower the use of grid electricity. For each system configuration the results will be shown and discussed in this chapter. The system configurations are defined by three different parameters (moment in time, size and electrolyser), each consisting of two compared options, which results in the following comparison for the system-configurations:

- Two time scenarios: the present time scenario and the 2030 scenario
- Two different sizes: a 1 MW size and a 2 MW size
- Two different electrolysers: the PEM electrolyser and the Alkaline electrolyser

This is executed in the following steps:

- The amount of hydrogen that is produced at nominal load is calculated in the model for each system-configuration.
  - Is this amount of hydrogen enough to meet the demand for hydrogen?
    - If yes, the electrolyser is modelled to meet demand on partial load to higher the efficiency and include as much wind energy as possible.
    - If no, the electrolyser is modelled on nominal load to maximise the production of hydrogen.
- The total electricity usage for each system-configuration is calculated.
- The part of electricity that is supplied by the grid and by the wind turbine for each system-configuration is calculated.
- The specific efficiency is calculated for each system-configuration.
- An energy balance is visualised for a present and 2030 scenario for the systems with the highest efficiency.

6.1 Simulation Results for Hydrogen Production

To reach the maximum production rate, the electrolysers are connected to the grid and electricity is supplied when the power supplied by the wind turbines is lower than nominal power. The total hydrogen production for each electrolyser working at nominal power is displayed in table 6.4:

	Total hydrogen production working on nominal load (kg)			
	1 MW		2 MW	
	Present	2030	Present	2030
PEM Electrolyser	159,000	175,000	318,000	349,000
Alkaline Electrolyser	175,000	179,000	351,000	357,000

Table 6.1: The total hydrogen production in a year using wind energy combined with electricity from the grid

For all demand scenarios, the control system works as follows: when the storage tank is full, and demand is supplied, the electrolyser will stop running. When the Alkaline electrolyser works on a lower load than 10% of the nominal load, the electricity will be supplied by the grid. The present and 2030 demand scenarios, estimated in section 4.2, are displayed in table 6.2. The PEM and Alkaline electrolyser with the 1 MW size do not produce enough hydrogen to meet any of the demand scenarios. For the 1 MW systems, the electrolysers will work on nominal load all the time and produce their maximum capacity, which is 159,000 kg and 175,000 kg for the PEM and the Alkaline electrolyser respectively. The maximum amount of hydrogen production of the 2 MW PEM electrolyser and the Alkaline electrolyser is respectively 318,000 kg and 351,000 kg which are both enough to meet the low and medium-demand scenario but not enough to meet the high-demand scenario.

All the 2030 demand scenarios, as shown in table 6.2, are not in reach of the electrolyser systems. All system configurations will work on nominal load and produce as much hydrogen as possible in the 2030 scenario. The PEM and the Alkaline electrolyser are modelled at partial load for the low- and medium-demand scenario to maximise the utilisation of wind energy.

Scenario	**Demand for hydrogen** (kg/day)	
	Present Scenario	2030 Scenario
Low	182,500	1,204,500
Medium	292,000	14,600,000
High	365,000	Unlimited

Table 6.2: Hydrogen demand for present scenario

6.2 Simulation Results Electricity Usage Nominal Load

Electricity is used as an input for the model to calculate the amount of hydrogen production. The electricity usage for the 1 MW and the 2 MW systems, working on nominal load, is the same for the PEM and the Alkaline electrolyser, only the amount of hydrogen that is produced differs. The electricity that is used consist of electricity produced by the wind turbine and electricity supplied by the grid. The usage of electricity for the 1 MW and the 2 MW system is displayed in the table below.

Total electricity usage	
1 MW	2 MW
8,760	17,520

Table 6.3: The total electricity usage of the electrolysers in a year using wind energy combined with electricity from the grid

The amount of electricity used from the grid for each electrolyser, when working constantly on nominal load for a year, is displayed in table 6.4. The share of electricity from the grid is the same for each electrolyser and for the present and future scenario, when working at nominal load.

The amount of electricity supplied by the grid	
1 MW	2 MW
3,780	7,560

Table 6.4: The total amount of electricity from the grid

The share of electricity that is provided by the wind turbine is 53% for each system. As shown in figure 6.2a.

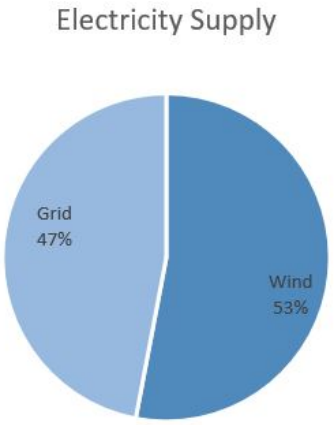

Figure 6.1: Distribution of electricity supply

6.3 Simulation Results Electricity Usage Partial Load

When the demand cannot be met, the electrolysers will work full-time on nominal load, and use all available electricity: 8,760 MWh and 17,520 MWh for the 1 MW and the 2 MW system, respectively. For the present low- and medium-demand scenario, the electrolysers are modelled at partial load, which highers the efficiency and maximises the utilisation of wind electricity. Only when the wind turbines will not produce enough power to meet the present low- and medium-demand scenario. The demand is met by keeping the electrolyser operational with electricity from the grid. The total electricity that is used per electrolyser for each demand scenario in a year is displayed in table 6.5.

	Electricity usage per demand scenario (MWh)
PEM Electrolyser 2 MW Low-Demand	9,820
PEM Electrolyser 2 MW Medium-Demand	16,020
Alkaline Electrolyser 2 MW Low-Demand	9,100
Alkaline Electrolyser 2 MW Medium-Demand	14,540

Table 6.5: The total electricity usage per demand scenario

For each demand scenario that can be met with the electrolyser, the total amount of electricity in MWh that is supplied by the grid for a year is calculated and displayed in table 6.6:

	Electricity supplied by the grid (MWh)
PEM Electrolyser 2 MW Low-Demand	2,080
PEM Electrolyser 2 MW Medium-Demand	6,770
Alkaline Electrolyser 2 MW Low-Demand	2,080
Alkaline Electrolyser 2 MW Medium-Demand	5,680

Table 6.6: The total electricity supplied by the grid per demand scenario

When the demand for hydrogen is low, the electrolyser can work at partial load when there is a lower supply of wind energy. This decreases the use of grid electricity, which is more expensive than electricity supplied by the wind turbine. The PEM electrolyser can use more electricity supplied by the wind turbine because of the wider range of operation in partial load as discussed in section 4.3.2. The share of wind electricity per electrolyser and demand scenario is shown in the graphs below. For the other demand scenarios, the electrolysers work at nominal load and the distribution of electricity is as in figure 6.1.

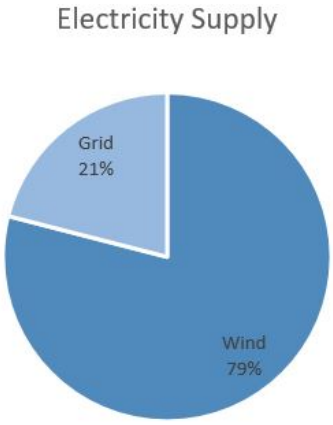

(a) Distribution of electricity supply for the 2MW PEM electrolyser at low-demand

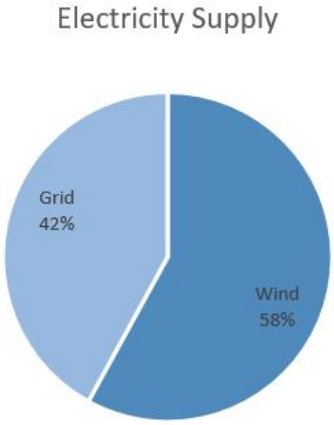

(b) Distribution of electricity supply for the 2MW PEM electrolyser at medium-demand

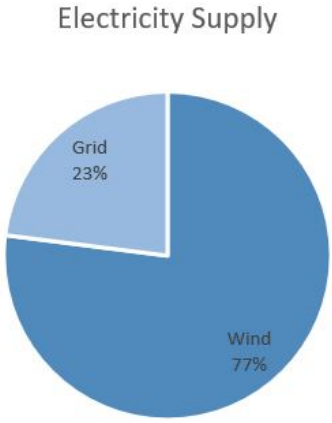

(c) Distribution of electricity supply for the 2MW Alkaline electrolyser at low-demand

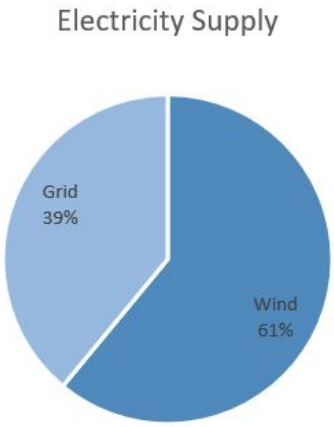

(d) Distribution of electricity supply for the 2MW Alkaline electrolyser at medium-demand

Figure 6.2: Distribution of electricity supply for each electrolyser working at partial load

6.4 Efficiency Simulation Results

The specific electricity consumption of an electrolyser varies per type of electrolyser (PEM and Alkaline) and with load. An electrolyser working at partial load has a lower specific electricity consumption, hence, higher efficiency, than an electrolyser working on nominal load. The model calculates the specific electricity consumption for each electrolyser on different loads and is described in the previous chapter. The specific electricity consumption for the PEM and the Alkaline electrolyser at nominal load and the specific electricity consumption of the compressors for different pressure inputs are calculated. In table 6.7 the specific electricity consumptions discussed in chapter 4 and the specific energy consumptions found in the model are combined:

	Specific electricity consumption	
	Current (kWh/kg H_2)	2030 (kWh/kg H_2)
PEM electrolyser at nominal power	55	50
Alkaline electrolyser at nominal power	50	49
PSA purificador	1.3	1.1
Compressor 1 to 200-250 bar	3.2	3.2
Compressor 40 to 200-250 bar	0.72	0.72
Compressor 200 to 350-400 bar	0.26	0.26
HP compressor 350 to 875-900 bar	1.8	1.1

Table 6.7: The specific electricity consumption per component

When the demand cannot be met, the electrolysers will work full-time on nominal load and use all available electricity. The overall efficiency for producing hydrogen at 200 bar for each system, working at nominal load, is displayed in table 6.8. As mentioned earlier in the report, all efficiencies are based on the HHV. The efficiency does not differ per size of the system. The efficiency is higher in the future, this is because of the expected lower specific electricity consumption for the electrolyser, compressor and purificador, as shown in table 6.7. The efficiency for the system using a PEM electrolyser is currently lower, however in 2030, the system efficiency for producing hydrogen at 200 bar is expected to be higher for the system using a PEM electrolyser. The efficiency of the PEM electrolyser rises, however is still lower than the efficiency of the Alkaline electrolyser. The higher system efficiency is explained by the specific electricity consumption of the MP compressor that compresses the hydrogen to 200 bar. The specific electricity consumption of the compressor used for the PEM electrolyser is 3.2 kWh/kg, which is higher than the specific electricity consumption for the compressor used for the Alkaline electrolyser, which is 0.72 kWh/kg. In the 2030 scenario, the efficiency of the PEM electrolyser becomes closer to that of the Alkaline electrolyser and the low compressor electricity consumption creates a higher overall system efficiency for producing hydrogen at 200 bar.

	System efficiency working on nominal load (%)			
	1 MW		2 MW	
	Present	2030	Present	2030
PEM Electrolyser	69	76	69	76
Alkaline Electrolyser	72	74	72	74

Table 6.8: The system efficiency for producing hydrogen at 200 bar, when working on nominal load

For the present low- and medium-demand scenarios, the efficiency becomes a little higher as shown in table 6.9. For the present low- and medium-demand scenario, the electrolysers are modelled at partial load, which highers the efficiency. However, in table 6.9, it is seen that the efficiency of the PEM electrolyser at medium demand scenario, is not higher than at partial load. This is because in the medium demand scenario, 292,000 kg per year is consumed and the 2 MW PEM electrolyser at nominal load can only produce 318,000 kg. Especially the daily hydrogen production is not high enough to work on partial load all the time. To supply enough hydrogen for the daily demand, the PEM electrolyser is still producing at nominal load part of the time. In the model it was found that the efficiency from the PEM electrolyser increases faster at partial load than the efficiency from the Alkaline electrolyser. Hence, the PEM electrolyser has a better partial load performance.

	System efficiency per demand scenario (%)
PEM Electrolyser 2 MW Low-Demand	71
PEM Electrolyser 2 MW Medium-Demand	69
Alkaline Electrolyser 2 MW Low-Demand	73
Alkaline Electrolyser 2 MW Medium-Demand	73

Table 6.9: The system efficiency for producing hydrogen at 200 bar per demand scenario, working at partial load

When comparing table 6.8 and table 6.9, it can be concluded that working in partial load increases the efficiency of the electrolyser, hence, the system. When designing a hydrogen production system, a trade-off needs to be made between the quantity of hydrogen that is produced and the efficiency of the electrolyser. This decision can be based on the demand for hydrogen in the market. When there is low demand, is it useful to produce a lower amount of hydrogen on partial load at a high efficiency. When demand for hydrogen is high, the production of hydrogen can be maximised by producing at nominal load. Working at partial load can reduce the system cost. However, working at a very low partial load increases the cost share of the capital cost of the electrolyser, which could increase the cost of hydrogen. This production trade-off is discussed in the economic analysis and discussion.

6.5 Energy Balance

A Sankey diagram is made to visualise the energy balance for the present scenario, shown in figure 6.3. The produced hydrogen is supplied to three different consumers: the CTV from Vattenfall for maintenance of offshore wind parks, $FCEV$s and supply to external industries at 200 bar. The 2 MW Alkaline electrolyser with a low-demand scenario is visualised as this system configuarion has the highest efficiency (73%, see table 6.9). The Alkaline electrolyser and the PEM electrolyser do not differ a lot. The PEM eletrolyser has a little more electrolyser losses. however less LP compressor losses. The 1 MW sizes only differs in the consumption, the efficiencies are the same as for the 1 MW size (see table 6.8). Less hydrogen is produced, thus almost all produced hydrogen is consumed by the CTV of Vattenfall. Consequently a lower amount of the hydrogen is supplied to external industries and HFS. For higher demand scenarios, more hydrogen is produced, using more grid electricity and more hydrogen is supplied to external industries. As can be seen in the Sankey diagram, the largest part of the energy provided is supplied by the wind turbine and the largest loss is from the electrolyser. An overall system efficiency of 63% is displayed in the Sankey diagram. The system efficiency is however greatly dependent on the type of consumption. When the hydrogen is transported to external industries at 200 bar, less energy is lost and a higher efficiency of 73% is obtained than when the efficiency is calculated for when the hydrogen is transported to a fuel station and used as a fuel for $FCEV$s. To efficiencies for each system are discussed in section 6.4.

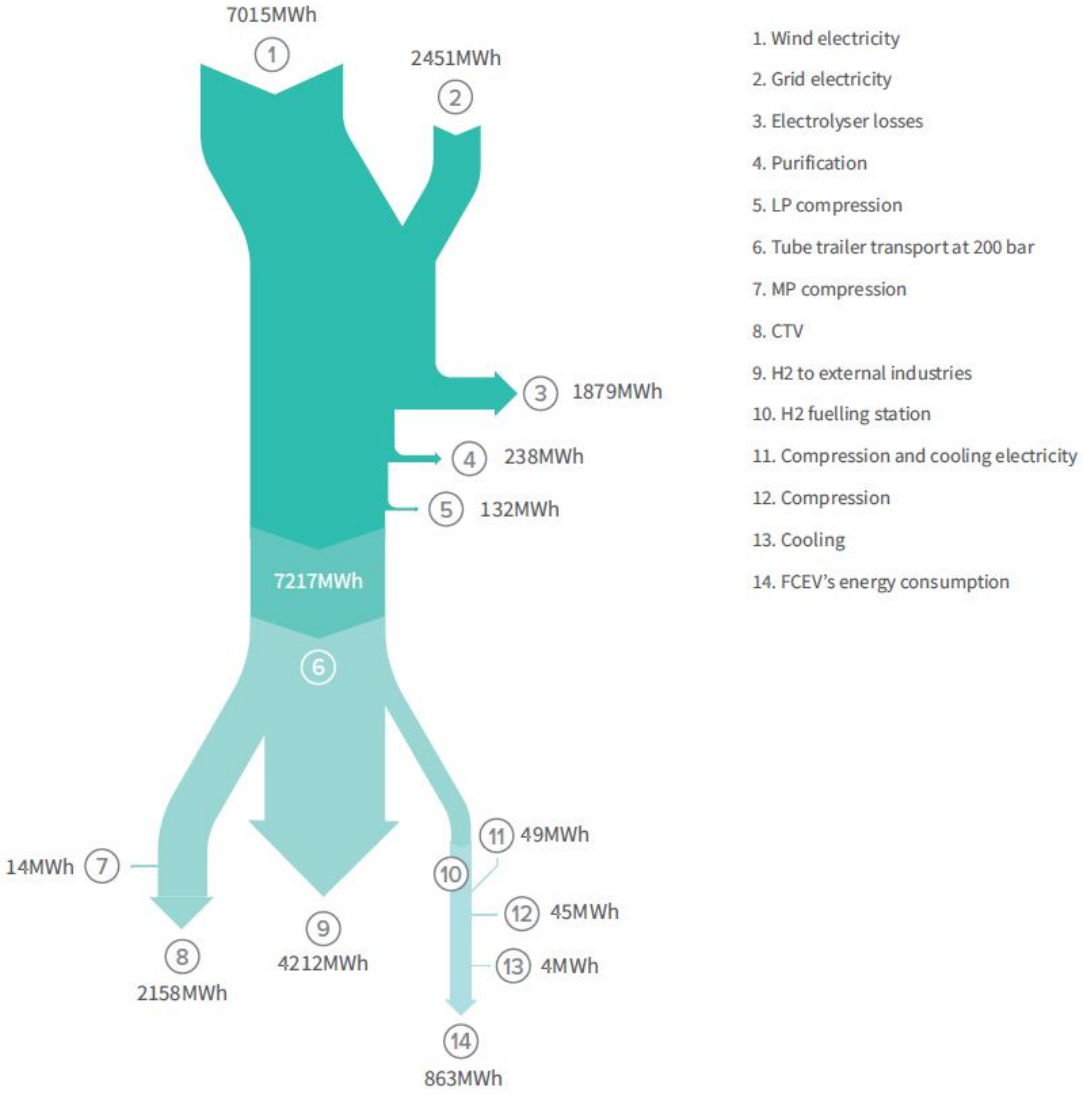

Figure 6.3: The energy balance for the present scenario

The energy balance for the 2030 scenario is shown in a Sankey diagram as well. The PEM 2 MW electrolyser is shown, as this system has the highest system efficiency in the 2030 scenario (table 6.8) and can can produce 34,910 kg of hydrogen in a year. All the hydrogen is transported at 200 bar to consumers such as $FCEV$s, hydrogen fuelled ships and other industries. Producing hydrogen at 200 bar has a total system efficiency of 76% . The system efficiency in the current scenario is higher than for the present scenario because of the increased efficiency of the electrolysers, compressor and purificador.

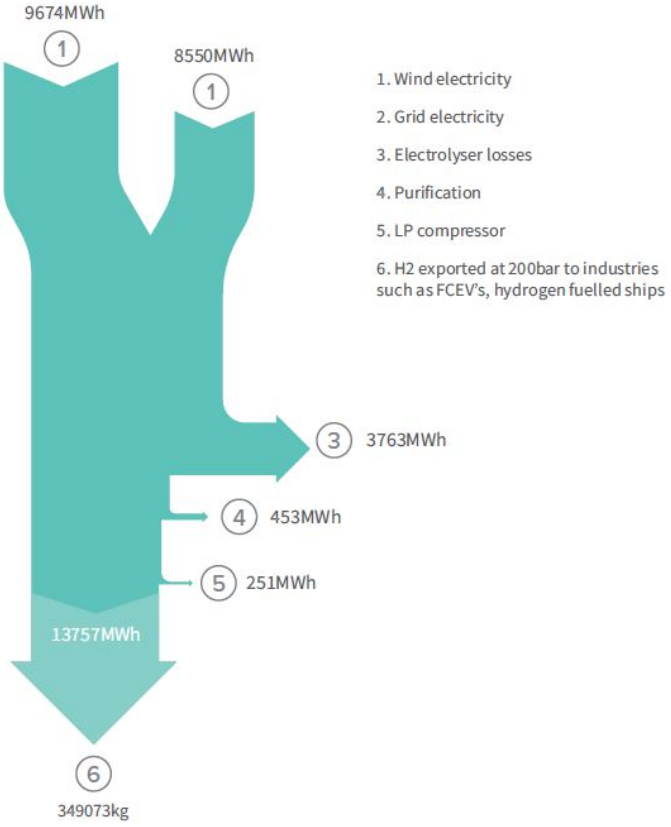

Figure 6.4: The energy balance for the future scenario

6.6 Concluding Remarks

When working at nominal load, 53% of the electricity used is supplied by the wind turbines for each system. The electrolysers can work at partial load when there is a low-demand for hydrogen, increasing the system efficiency and decreasing the use of grid electricity. The system configurations are compared for two time scenarios, in size and for two different electrolysers.

The system configurations are compared for two scenarios: the present scenario and the 2030 scenario. The efficiency of the system-configurations increases with 7% for the PEM electrolyser system and with 2% for the Alkaline electrolyser. This is because of the expected decrease in specific electricity consumption of 5 kWh/kg for the PEM electrolyser, in comparison to a decrease of 1 kWh/kg for the Alkaline electrolyser (see table 6.7). In the 2030 scenario, the PEM electrolyser system-configuration is more efficient than the Alkaline electrolyser, however the difference is only 2%.

When comparing the system size, it is found that the size of the system does not have any influence on the efficiency, only on the amount of hydrogen that is produced. However, lowering the hydrogen production, by working on partial load does increase the efficiency of the electrolyser and increases the utilisation of wind energy. When considering the expected demand scenarios for hydrogen consumption, it is more efficient to build a system at a larger scale of 2 MW than of 1 MW. The 2 MW system-configuration can work at partial load, which increases the efficiency and can increase the usage of wind energy. The efficiency of the 2 MW Alkaline system can increase to 73% when working in partial load. The share of wind energy can increase to 79% for the 2MW PEM electrolyser system working at partial load. Using a larger system size of multiple MW could increase the efficiency and wind share even more.

When comparing the PEM and Alkaline electrolyser, it is seen that the Alkaline electrolyser has a higher hydrogen production rate than the PEM electrolyser when working at nominal load. The share of wind energy can increase to 79% for the 2 MW PEM electrolyser system working at partial load for the low-demand scenario. The total electricity share supplied by the grid is larger for the Alkaline electrolyser than for the PEM electrolyser for two reasons:

1. In general, the Alkaline electrolyser uses a higher share of grid electricity when working at partial load than the PEM electrolyser because of the lower load range. An Alkaline electrolyser has a load range of 10-100% and a PEM electrolyser can use a load range of 0-100%.

2. The Alkaline electrolyser produces hydrogen at atmospheric pressure. Compression of the hydrogen to 200 bar requires a higher amount of electricity than the PEM electrolyser, as the calculated specific electricity consumption is higher for the Alkaline electrolyser.

The total electricity usage per system-configuration and demand scenario and the share that is supplied by the grid are displayed in table 6.3, 6.4, 6.5 and table 6.6. In the present scenario, the Alkaline electrolyser has a higher efficiency than the PEM electrolyser. However, in the 2030 scenario, the PEM electrolyser system-configuration is 2% more efficient than the Alkaline electrolyser.

Chapter 7

Economic Analysis

Two scenarios are presented in this section based on present state and the future 2030 scenario. The costs of the present scenario are based on present prices and the costs of the 2030 scenario are based on predictions found in different literature studies.

The aim is to carry out a techno-economic analysis that takes into account every aspect of the economics for the system as a whole, for both the present as the 2030 scenario. The two scenarios can be characterised as follows:

- The present scenario uses current state of the art technology that is used for hydrogen production, compression and transport. Only commercially available hydrogen technologies are used. For all components of the system, technology characteristics that are currently available and the present costs are used. The present scenario describes a system that could be implemented right now.
- In the 2030 scenario, hydrogen technology has become more mature and the costs and efficiencies have improved. The potential specific energy consumptions are displayed in table 6.7 and the technology cost are elaborated in this chapter.

7.1 Levelised Cost Calculation

A common economic measure to compare different energy sources is the levelised cost of energy ($LCoE$). $LCoE$ is used as an indication factor on whether a project will provide financial gain. $LCoE$ takes into account fixed and variable costs as well as total energy production throughout the system's lifetime. By estimating these costs and the total energy produced, the $LCoE$ will provide a simple estimate of the amount of money that must be made per unit of energy produced in order to break even. This value is obtained by utilising equation:

$$LCoE = \frac{Total\ Annual\ Cost}{Total\ Annual\ Output\ Energy} \tag{7.1}$$

The total annual cost consists of the costs of each individual component, (TC_i) in €/year and the cost of electricity utilised by each component, TCE_i. TCE_i is elaborated in section 7.4. The total cost of each individual component is calculated with the annual capital cost, ACC_i, and the annual operation and maintenance cost, $AOMC_i$, per component:

$$TC_i = ACC_i + AOMC_i \tag{7.2}$$

With TC_i, ACC_i and $AOMC_i$ in €/year. The annual capital cost (ACC_i) is defined for every component using the $CAPEX$ and the annuity factor per component.

$$ACC_i = \frac{CAPEX_i}{Annuity\ factor} \tag{7.3}$$

The annuity factor (AF) is used to calculate present values. The annuity factor for every component can be calculated with:

$$AF = \frac{WACC \times (1 + WACC)^n}{(1 + WACC)^n - 1} \tag{7.4}$$

With n the lifetime of the component (table 7.11) and $WACC$ presents the weighted average cost of capital. A $WACC$ of 3% is used. In the cost analysis an exchange rate is used of 0.91 USD to €. Two type of costs can be identified: $CAPEX$ and $OPEX$. An operating expense ($OPEX$) is an expense required for the day-to-day functioning of the system. In contrast, a capital expense ($CAPEX$) is an expense to create a benefit in the future for the system, an investment. The $CAPEX$ and $OPEX$ are estimated for all parts of the whole system. This includes all components: the wind turbines, the selected electrolyser, compressor and storage tubes and additional costs are included, such as: cable, installation, side preparation, engineering and design costs. The $CAPEX$ per component can be expressed as:

$$CAPEX_i = Q_i \times IC_i \tag{7.5}$$

With Q_i the installed capacity per component and IC_i the investment cost in € per specific capacity. The installed capacity per component is shown in table 4.5 and the IC per component is shown in table 7.1. The $OPEX$ per component is also referred to as $O\&M_i$ and is expressed as a percentage of the capital cost of that component, displayed in table 7.11. The annual operation and maintenance costs $AOMC_i$ are expressed with an $O\&M$ percentage of the ACC_i.

$$AOMC_i = O\&M_i \times ACC_i \tag{7.6}$$

7.2 System Costs

The investment costs (IC) of all components in the energy system for the present scenario and the 2030 scenario are estimated based on multiple references. The estimations used in this research are shown in table 7.1:

Component	**IC**		**References**
	Present	2030	
Wind Turbines (€/kW)	1,600	1,500	[86][98][99][37][100]
PEM Electrolyser 1 MW (€/kW)	1,500	1,000	[37][38][6][13][39][40]
PEM Electrolyser 2 MW (€/kW)	1,000	900	[37][38][6][13][39][40][41]
Alkaline Electrolyser 1 MW (€/kW)	1,000	800	[38][6][13][39][40]
Alkaline Electrolyser 2 MW (€/kW)	800	750	[38][6][13][39][40]
LP Compressor (€/kg/h) [a]	5,000	3,600	[101][86][102] [40][103][104]
Tube Trailers 200 bar (€/kg)	640	500	[105][105][86]
MP Compressor (€/kg/h) [b]	5,500	4,200	[101][86][102][106][40][107]
Tube Trailers 350 bar (€/kg)	710	550	[108][109]

[a] Low pressure (LP) compressor compresses the hydrogen to 200-250 bar.
[b] Medium pressure (MP) compressor compresses the hydrogen to 350-400 bar.

Table 7.1: The installed investment costs for the present scenario and the 2030 scenario

For all components the engineering and planning cost are included in the installed cost. The installed cost for the wind turbines includes cables, infrastructure, converter and the grid connection costs (which is on average 11.5% for onshore wind turbines [86]). The rectifier and the purification costs of water and hydrogen are included in the installed cost for the electrolysers. The $O\&M$ cost and lifetime expectation for each component are shown in table 7.11. The $O\&M$ cost of the wind turbine include land rent, costs for repair and related spare parts. The cost of the PSA is included in the electrolyser IC.

Component	**O&M (%/year)**		**Lifetime (years)**		**References**
	Present	2030	Present	2030	
Wind Turbines	5.4%	5.4%	20	20	[86][98][110]
PEM Electrolyser	2%	2%	30	30	[86][39]
Alkaline Electrolyser	1%	1%	30	30	[86][39]
Compressor to 200-250 bar	4%	2%	10	10	[86][111]
Tube Trailers	1%	1%	30	30	[86][112]
Compressor 200 to 350-400 bar	4%	2%	10	10	[86][111]

Table 7.2: The O&M costs and lifetime for the present scenario and the 2030 scenario

7.3 Levelised Cost of Electricity

The electrolyser will consume electricity from the grid if its minimum capacity cannot be fulfilled by electricity produced by the wind turbine. The APX electricity market is chosen for the trade of electricity, since this market has vast volumes of wind power that are being traded at favourable prices. The APX prices are given in €/MWh for each hour slot. A minimum volume of 0.1 MWh is necessary for trades and the trades can be made until thirty minutes before delivery begins. The data received from Vattenfall for the APX market prices are taken for the same year as the wind data and the data is modelled in MATLAB to synchronise the values over time. To discover if there is a correlation between low wind power output and higher grid prices, the correlation coefficient ρ is calculated in MATLAB using the equation:

$$\rho(X,Y) = \frac{cov(X,Y)}{\sigma(X)\sigma(Y)} \tag{7.7}$$

With X and Y the two data sets, cov the covariance, the measure of the joint variability of two random variables and σ the standard deviation, a measure of the variation of a set of values. A value of $\rho(X,Y)$ of -0.0947 was found. A negative value was expected as with larger amounts of wind power, the electricity price from the grid is expected to decrease, which results in a negative correlation factor. However, the data sets are only considered as correlating when the value for the correlation coefficient of $|\rho(X,Y)| > 0.3$. Hence, no correlation was found. In the future, when there is a higher contribution of wind energy to the grid, a correlation could possibly be found. The contribution of wind energy to the grid electricity in the Netherlands at the moment is less than 2%. [113] For this reason, the electricity price from the grid is estimated to be 0.080 €/kWh, which is the average price over the year 2018. [114] Electricity prices in the year 2030 are hard to predict. Based on a study in reference [115] a grid electricity price for 2030 of 0.053 €/kWh was chosen.

The levelised cost of electricity from the wind turbines, $LCoE_{e,Wind}$ in €/kWh, is calculated with equation 7.1, adjusted for electricity from the wind turbines:

$$LCoE_{e,Wind} = \frac{TC_{Wind}}{EP_e, Wind} \tag{7.8}$$

Where TC_{Wind} is the total installed investment cost for the wind turbines in €/year and $EP_{e,Wind}$ is the annual electricity production by the wind turbine in kWh/year. $LCoE_{e,Wind}$ is equal to 0.054 €/kWh for the present scenario and 0.051 €/kWh for the 2030 scenario.

The levelised cost of electricity from the grid and from the wind turbine are displayed in table 7.3:

	Levelised Cost of Electricity	
	Present (€/kWh)	2030 (€/kWh)
$LCoE_{e,Wind}$	0.054	0.051
$LCoE_{e,Grid}$	0.080	0.053

Table 7.3: The levelised cost of electricity for the present scenario and the 2030 scenario

Multiple components of the system utilise electricity. The electricity utilised for hydrogen production consists mostly of electricity from the wind turbine and when there is no wind the necessary electricity is compensated with electricity from the grid. To constantly produce the demand of hydrogen per day, the total amount of electricity that has to be supplied by the grid is roughly calculated with the MATLAB model and shown in table 6.6. In Excel the $LCoE_{e,Wind+Grid}$ for each system and demand scenario is calculated (table 7.4 and 7.5), combining the amount of electricity used from the grid per scenario and $LCoE_{e,Wind}$ and $LCoE_{e,Grid}$.

$LCoE_{e,Wind+Grid}$ (€/kWh)	
Present	2030
0.07	0.05

Table 7.4: The levelised cost of electricity for the present and future scenario, working on nominal load

	$LCoE_{e,Wind+Grid}$
PEM Electrolyser 2 MW Low-Demand	0.06
PEM Electrolyser 2 MW Medium-Demand	0.07
Alkaline Electrolyser 2 MW Low-Demand	0.06
Alkaline Electrolyser 2 MW Medium-Demand	0.06

Table 7.5: The levelised cost of electricity when working on partial load for low-demand scenarios

7.4 Levelised Cost of Hydrogen

In this section the levelised cost of hydrogen production at a pessure of 200 bar is calculated. To calculate the levelised cost of hydrogen, $LCoE_{H2}$, the general equation for calculating levelised cost of energy (7.1) is adjusted for hydrogen:

$$LCoE_{H2} = \frac{\sum_1^n TC_i + TCoF}{EP_{H2}} \tag{7.9}$$

$TCoF$ is the total cost of fuel. EP_{H2} is total production of hydrogen in kg. The TC_i per component is calculated and is shown in table 7.6.

	Present			**2030**		
	ACC (€/year)	AOMC (€/year)	TC (€/year)	ACC (€/year)	AOMC (€/year)	TC (€/year)
1 MW System						
Wind Turbine	236,600	12,780	249,380	221,810	11,980	233790
PEM Electrolyser	76,530	1,530	78,060	51,020	1,020	52,040
Alkaline Electrolyser	51,020	510	51,530	40,820	408	41,220
LP Compressor	11,720	470	12,190	8,440	170	8,610
Tube Trailers 200 bar	26,120	260	26,380	20,410	200	20610
2 MW System						
Wind Turbine	473,200	25,550	498,750	443,620	23,960	467580
PEM Electrolyser	102,040	2,040	104,080	91,830	1,840	93,670
Alkaline Electrolyser	81,630	820	82,450	76,530	770	77,290
LP Compressor	23,450	940	24,380	16,880	340	17,220
Tube Trailers 200 bar	39,180	390	39,570	30,610	310	30920

Table 7.6: The installed investment for the present scenario and the 2030 scenario

The total cost of fuel is the sum of the total cost of electricity and the total cost of water.

$$TCoF = TCoE + TCoW \tag{7.10}$$

The total cost of water ($TCoW$) is is expressed with the levelised cost of tap water and the total production of hydrogen.

$$TCoW = LCoW \times EP_{H2} \tag{7.11}$$

An electrolyser consumes water to produce hydrogen and in this case study, tap water is used. The tap water consumption of the electrolysers is assumed to be 15 L/kg H_2. [40] The cost for tap water in the Netherlands is approximately 1.14 €/m^3. [116] The cost for tap water are assumed to be equal for the present scenario and the 2030 scenario and is displayed in table 7.7. The cost of tap water is very small in comparing to other costs.

	Levelised Cost of Tap Water (€/kg)
$LCoW$	0.02

Table 7.7: The levelised cost of tap water

The total electricity cost per demand scenario, $TCoE$, is expressed with the levelised cost of electricity, $LCoE_{Wind+Grid}$ for each demand scenario and the total electricity consumption per demand scenario, TEC:

$$TCoE = LCoE_{Wind+Grid} \times TEC \tag{7.12}$$

The $LCoE_{Wind+Grid}$ for each demand scenario and system are displayed in table 7.4 and table 7.5. The total electricity consumption per electrolyser for producing hydrogen (TEC) at 200 bar for each scenario is displayed in table 6.3 and 6.5.

The levelised cost of hydrogen for each system working at nominal and partial load, $LCoE_{H2}$, is calculated according to equation 7.9. The levelised cost of hydrogen is displayed in table 7.8 and 7.9. The levelised cost of hydrogen is calculated including the compression to 200 bar. The compression has been included to evenly compare the Alkaline and PEM electrolyser as they have different output pressures, which influences the cost of compression to 200 bar.

	$LCoE_{H2}$	
	Present	2030
PEM Electrolyser 1 MW (€/kg)	4.6	3.3
PEM Electrolyser 2 MW (€/kg)	4.4	3.2
Alkaline Electrolyser 1 MW (€/kg)	4.2	3.4
Alkaline Electrolyser 2 MW (€/kg)	3.9	3.4

Table 7.8: The levelised cost of hydrogen that is produced at 200 bar for each system working at nominal load

	$LCoE_{H2}$
PEM Electrolyser 2 MW Low-Demand (€/kg)	4.3
PEM Electrolyser 2 MW Medium-Demand (€/kg)	4.3
Alkaline Electrolyser 2 MW Low-Demand (€/kg)	3.8
Alkaline Electrolyser 2 MW Medium-Demand (€/kg)	3.9

Table 7.9: The levelised cost of hydrogen that is produced at 200 bar for the electrolysers per demand scenario

Currently the production cost for hydrogen that is produced with SMR is 1-1.5 €/kg. [15][117] Producing green hydrogen is more expensive. The production cost of green hydrogen (at 1 bar pressure) ranges at the moment between 1.8 €/kg to 5.31 €/kg, varying per region. [15][118][119] The $LCoE_{H2}$ calculated in this research is for production of hydrogen at 200 bar, thus includes extra compression costs. The extra compression cost ($CAPEX$, $OPEX$ and electricity cost) vary for the PEM and Alkaline electrolyser and producing hydrogen at 1 bar causes a maximum cost reduction of 8%. When lowering the $LCoE_{H2}$ with 8%, the $LCoE_{H2}$ is comparable with the production cost of green hydrogen (ranging between 1.8 €/kg to 5.31 €/kg) found in literature.

It is difficult to predict the price of green hydrogen in the future. The prices are strongly dependent on system $CAPEX$ and $OPEX$ and electricity prices. [115] At the *Hydrogen Days of Vattenfall*, Oliver Weinmann (Managing Director at Vattenfall Europe Innovation) expected that the price of green hydrogen in 2030 will be 2.6 €/kg H2. Likewise, according to reference [86], 2030 hydrogen production cost using electrolysis is expected to be 2.6 €/kg H2. Reference [120] states that the cost of green hydrogen will vary between 2.27 €/kg to 3.20 €/kg. Applying a cost reduction of 8% for the compression cost on the $LCoE_{H2}$ found in this case study for the year 2030, results in a $LCoE_{H2}$ of approximately 3 €/kg, which is comparable with the before mentioned expected production cost price of hydrogen.

7.5 System Levelised Cost of Dispensed Hydrogen at a HFS

Part of the hydrogen that is produced is transported in tube trailers at 200 bar. The levelised cost of the hydrogen in the tube trailers is displayed in table 7.8 and 7.9. As discussed earlier, the produced hydrogen could be used for $FCEV$s, which involves some additional steps. After the transportation in the tube trailers, the hydrogen is compressed to 875 bar and stored at the hydrogen fuelling stations. [86] At the fuelling station, the hydrogen is cooled and dispensed. The extra components that are involved with these additional steps are included and therefore, the term "system" is added to the "levelised cost" term. The system levelised cost of hydrogen ($SLCoE_{H2,HFS}$) is expressed as in equation 7.13. The energy consumption of the compressor and chiller at the hydrogen fuelling station and the total cost of the fuelling station are all included in the $SLCoE_{H2}$. The energy consumption of the tube trailer transportation is included in the $AOMC$ of the tube trailer transport.

$$SLCoE_{H2,HFS} = LCoE_{H2,HFS} + LCoE_{H2} \tag{7.13}$$

With $LCoE_{H2,HFS}$, the levelised cost of hydrogen for the hydrogen fuelling station:

$$LCoE_{H2,HFS} = \frac{TC_{HFS} + CoE_{HFS}}{EP_{H2}} \tag{7.14}$$

The TC_{HFS} is the sum of the total cost (TC) per component. The IC and $O\&M$ cost and lifetime expectation for each component are shown in table 7.10 and 7.11.

Component	**IC**		**References**
	Present	2030	
HP Compressor (€/kg H2/h)	16,100	8,000	[86][101]
Stationary Storage 875 bar (€/kg H2)	1,100	800	[108][121][86]
Dispenser Units (€/unit)	112,800	102,900	[86][101][105]
Chiller Units (€/kg H2/min)	143,900	130,000	[86][101][105]
Tube Trailer Tractor (€/unit)	160,000	160,000	[86][122][123]

Table 7.10: The installed investment costs of the HFS components for the present scenario and the 2030 scenario

Component	**O&M (%/year)**		**Lifetime (years)**		**References**
	Present	2030	Present	2030	
HP Compressor	4%	2%	10	10	[86][101]
Stationary Storage 875 bar	1%	1%	30	30	[86][108][121]
Dispenser Units	1%	1%	10	10	[105][86]
Chiller Units	2%	2%	15	15	[101][105][86]
Tube Trailer Tractor	109%	91%	8	8	[86][122][123]

Table 7.11: The O&M costs and lifetime of the HFS components for the present scenario and the 2030 scenario

The TC per component is calculated according to equation 7.1 and is shown in table 7.12.

	Present			**2030**		
	ACC (€/year)	AOMC (€/year)	TC (€/year)	ACC (€/year)	AOMC (€/year)	TC (€/year)
Hydrogen Fuelling Station						
HP Compressor	66,060	2,640	68,700	32,820	660	33,480
Stationary Storage 875 bar	5,610	60	5670	4,080	40	4,120
Dispenser Units	26,450	260	26,710	24,130	240	24,370
Chiller Units	110,900	2,220	113,110	100,180	2,000	102,190
Tube Trailer Tractor	22,790	24,840	47,640	22,790	47,640	102,190
Additional Cost HFS	80,000		33,000		80,000	33,000

Table 7.12: The installed investment of the HFS components for the present scenario and the 2030 scenario

The TC_{HFS} for the present and future scenario are respectively: €346,190 and €243,960 per year. For the cost of energy of the hydrogen fuelling station the electricity price of the grid is assumed as in section 7.3. The fuelling station cost of energy, $TCoE_{HFS}$, is expressed as:

$$TCoE_{HFS} = EC_{HFS} \times LCoE_{grid} \tag{7.15}$$

The energy consumption of the hydrogen fuelling station (EC_{HFS}) is calculated with the specific electricity consumption of the high pressure compressor and the cooling equipment (EC_{HFS}) and the total hydrogen consumption of the hydrogen fuelling station ($EP_{H2,HFS}$):

$$EC_{HFS} = SEC_{HFS} \times EP_{H2,HFS} \tag{7.16}$$

The total hydrogen consumption of the hydrogen fuelling station ($EP_{H2,HFS}$) is estimated to be 350 kg/day = 127,750 kg/year. As discussed in section 4.3.6. The total energy consumption of the hydrogen fuelling station

is 255 MWh and 160 MWh for the present and future scenario, respectively. The fuelling station cost of energy, $TCoE_{HFS}$ is, respectively, €23100 and €10220 for per year the present and future scenario. The $LCoE_{H2,HFS}$ for the present and future scenario is displayed in table 7.13:

	Levelised Cost of hydrogen for the fuelling station	
	Present (€/kg)	2030 (€/kg)
$LCoE_{H2,HFS}$	2.9	2.0

Table 7.13: The levelised cost of hydrogen for the fuelling station

	$SLCoE_{H2,HFS}$	
	Present	2030
PEM Electrolyser 1 MW (€/kg)	7.5	5.2
PEM Electrolyser 2 MW (€/kg)	7.3	5.1
Alkaline Electrolyser 1 MW (€/kg)	7.1	5.2
Alkaline Electrolyser 2 MW (€/kg)	6.8	5.2

Table 7.14: The system levelised cost of hydrogen

	$SLCoE_{H2,HFS}$
PEM Electrolyser 2 MW Low-Demand	7.2
PEM Electrolyser 2 MW Medium-Demand	7.2
Alkaline Electrolyser 2 MW Low-Demand	6.7
Alkaline Electrolyser 2 MW Medium-Demand	6.8

Table 7.15: The levelised cost of hydrogen per demand scenario

As displayed in equation 7.13, the $LCoE_{H2,HFS}$ and the $LCoE_{H2}$ are added together to calculate the system levelised cost of hydrogen. For the present scenario, the Alkaline 2 MW for in combination with a low-demand scenario is the lowest in cost and can produce a $LCoE_{H2,HFS}$ of 6.7 €/kg. For the 2030 scenario, the PEM 2 MW electrolyser is the lowest in cost and can produce a $LCoE_{H2,HFS}$ of 5.2 €/kg for a low-demand scenario. The price for fuelling green hydrogen for public transport busses is expected to be in the range of 6-7 €/kg of hydrogen, according to Jacco Rijerkerk (Commercial director Ekinetix B.V.). $LCoE_{H2,HFS}$ includes the compression, storage and dispensing (CSD) at the hydrogen fuelling station. How large each of the levelised cost contribute to the system levelised cost is displayed in Appendix C. As can be seen in Appendix C, the production cost of hydrogen (to store the hydrogen at 200 bar) is higher for each scenario. In 2030, a larger decrease in $LCoE_{H2,HFS}$ is seen because of expected lower cost of high pressure compressors and storage. A $FCEV$ consumes 0.8-1 kg of hydrogen per 100 kilometres. [79] A car driving on gasoline consumes approximately 5 L per 100 kilometres. [124] The present price for gasoline is approximately 1.6 €/L. [125], which corresponds to €8 per 100 kilometres. A $LCoE_{H2,HFS}$ of 6.7 €/kg is approximately €6.7 per 100 kilometres, which is cost competitive with gasoline.

7.6 System Levelised Cost of Hydrogen supplied to the CTV

Part of the hydrogen is supplied to the CTV. After compression to 200 bar, a medium-pressure (MP) compressor is used to compress the hydrogen to 350/400 bar. The compressed hydrogen is stored in the storage tubes of 90 kg and 40 kg, and the storage tubes are loaded into the CTV. The system levelised cost of hydrogen for the CTV consists of the levelised cost of production at 200 bar and the levelised cost of transporting the hydrogen at 200 bar, compressing it to 350 bar and storing it at that pressure. The system levelised cost of hydrogen ($SLCoE_{H2,CTV}$) is expressed as in equation 7.17. The energy consumption of the compressor and chiller at the hydrogen fuelling station and the total cost of the fuelling station are all included in the $SLCoE_{H2}$. The energy consumption of the tube trailer transportation is included in the $AOMC$ of the tube trailer transport.

$$SLCoE_{H2,CTV} = LCoE_{H2,CTV} + LCoE_{H2} \tag{7.17}$$

With $LCoE_{H2,CTV}$, the levelised cost of hydrogen for the CTV:

$$LCoE_{H2,CTV} = \frac{TC_{CTV} + CoE_{CTV}}{EP_{H2}} \tag{7.18}$$

The TC_{CTV} is the sum of the total cost (TC) per component (in table 7.18). The IC and $O\&M$ cost and lifetime expectation for each component are shown in table 7.16 and 7.17.

Component	**IC**		**References**
	Present	2030	
Tube Trailer Tractor (€/unit)	160,000	160,000	[86][122][123]
MP Compressor (€/kg H2/h)	5,500	4,200	[86][101]
Storage Tubes 350 bar (€/kg H2)	710	550	[108][121][86]

Table 7.16: The installed investment costs of the CTV components for the present scenario and the 2030 scenario

Component	**O&M (%/year)**		**Lifetime (years)**		**References**
	Present	2030	Present	2030	
Tube Trailer Tractor	109%	91%	8	8	[86][122][123]
MP Compressor	4%	2%	10	10	[86][101]
Storage Tubes 350 bar	1%	1%	30	30	[86][108][121]

Table 7.17: The O&M costs and lifetime of the HFS components for the present scenario and the 2030 scenario

	Present			**2030**		
	ACC (€/year)	AOMC (€/year)	TC (€/year)	ACC (€/year)	AOMC (€/year)	TC (€/year)
CTV						
MP Compressor	4,190	170	4,360	3,200	60	3,260
Tube Trailers 350 bar	10,870	110	10,980	8,420	80	8,500

Table 7.18: The installed investment of the CTV components for the present scenario and the 2030 scenario

The $LCoE_{H2,CTV}$ is calculated according to equation 7.18 and is displayed in table 7.19 and the system levelised cost for the hydrogen supplied to the CTV is calculated according to equation 7.17 and displayed in table 7.20 and 7.21.

	Levelised Cost of hydrogen for the CTV	
	Present (€/kg)	2030 (€/kg)
$LCoE_{H2,CTV}$	1.2	1.0

Table 7.19: The levelised cost of hydrogen for the CTV

	$SLCoE_{H2,CTV}$	
	Present	2030
PEM Electrolyser 1 MW (€/kg)	5.8	4.2
PEM Electrolyser 2 MW (€/kg)	5.5	4.2
Alkaline Electrolyser 1 MW (€/kg)	5.4	5.2
Alkaline Electrolyser 2 MW (€/kg)	5.1	4.2

Table 7.20: The system levelised cost of hydrogen for the CTV

	$SLCoE_{H2,CTV}$
PEM Electrolyser 2 MW Low-Demand (€/kg)	5.4
PEM Electrolyser 2 MW Medium-Demand (€/kg)	5.4
Alkaline Electrolyser 2 MW Low-Demand (€/kg)	5.0
Alkaline Electrolyser 2 MW Medium-Demand (€/kg)	5.1

Table 7.21: The levelised cost of hydrogen per demand scenario for the CTV

7.7 Cost Distribution for Hydrogen Production at 200 bar

The annual total cost of energy of the system ($TCoE$) for the present and future scenario for the 4 system-configurations working at nominal load and producing hydrogen at 200 bar are calculated according to equation 7.19 and displayed in table 7.22. As can be seen in the table, a cost reduction for each system is found in 2030. In the levelised cost of hydrogen calculations in section 7.4, it is found that hydrogen is lower in cost for the 2 MW system. The breakdown of the annual cost for each system-configuration is displayed in figure 7.1.

$$TCoE = \sum_{1}^{n} TC_i + TCoF \tag{7.19}$$

	$TCoE$	
	Present	2030
PEM Electrolyser 1 MW (€/year)	730,800	520,440
PEM Electrolyser 2 MW (€/year)	1,387,780	1,023,860
Alkaline Electrolyser 1 MW (€/year)	737,710	597,320
Alkaline Electrolyser 2 MW (€/year)	1,377,680	1,179,430

Table 7.22: The total annual cost of energy for producing hydrogen at 200 bar at nominal load

As can be seen in the cost breakdown of all system configurations, the share of electrolyser cost is lower for the 2 MW systems, which explains the lower levelised cost for the 2 MW systems. As the 2 MW system is lowest in levelised cost for all demand scenarios, the annual cost distribution for the production of hydrogen at 200 bar, for the CTV and the dispensed hydrogen at the HFS is only shown for the 2 MW system-configurations in figure 7.1. The share of grid electricity is lower in the 2030 scenarios, because the price per MWh for grid electricity is assumed significantly lower in the 2030 scenario. In the cost distribution, it can be seen that in the 2030 scenario the share of wind electricity cost reduces. This is mainly because of the lower electricity consumption of the electrolysers and partly because of the assumed lower electricity prices for the electricity supplied by the wind turbine. This can be explained by the fact that the specific electricity consumption of the electrolysers reduces in the 2030 scenario, which makes the necessary amount of electricity lower (of which 53% is wind electricity). However, the specific electricity consumption of the LP compressor and the purification are not assumed to reduce (see table 6.7). These devices work on grid electricity only, which explains the overall higher share of grid electricity cost in the 2030 scenario. The tap water costs are very low in comparison to other costs. In the PEM electrolyser system-configurations, the cost for the electrolyser have a higher share than in the Alkaline system-configurations. This is explained by the higher $CAPEX$ and $OPEX$ of the PEM electrolyser.

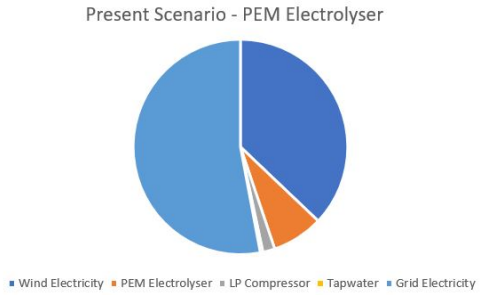

(a) Distribution of annual cost for the 2MW PEM electrolyser system-configuration at nominal load

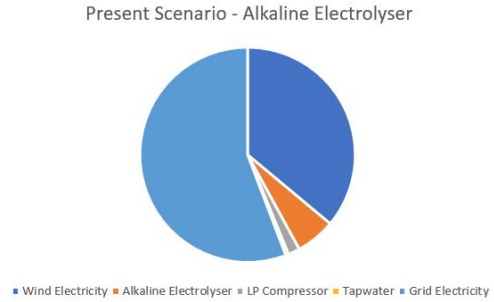

(b) Distribution of annual cost for the 2MW Alkaline electrolyser system-configuration at nominal load

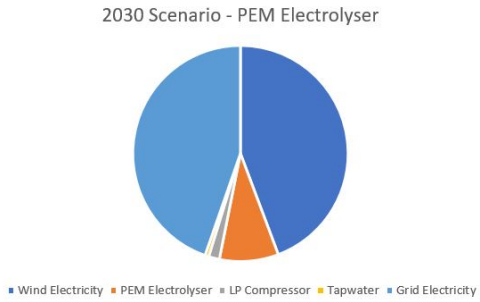

(c) Distribution of annual total cost for the 2MW Alkaline electrolyser system-configuration at nominal load

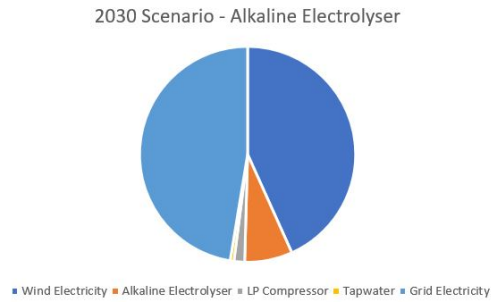

(d) Distribution of annual total cost for the 2MW Alkaline electrolyser system-configuration at nominal

Figure 7.1: Distribution of annual total cost for each electrolyser in the present and 2030 scenario for producing hydrogen at 200 bar at nominal load

For the present low- and medium-demand scenario, the electrolysers are modelled at partial load, which highers the efficiency and maximises the utilisation of wind electricity. Only when the wind turbines will not produce enough power to meet the present low- and medium-demand scenario. The demand is met by keeping the electrolyser operational with electricity from the grid. The distribution of annual cost per system-configuration for each demand scenario is shown in figure 7.2. In section 7.4, it is shown that the levelised cost of hydrogen is lowest when the electrolysers work on partial load in the present low- and medium-demand scenario. As can be seen in the pie graphs, the share of wind electricity increases a lot for the low demand scenario. This is because the electrolysers can easily deliver enough hydrogen for the daily demand and can use more wind electricity and less grid electricity. This explains why the levelised cost of hydrogen is lowest when producing for the low-demand scenarios: The share of wind electricity increases, which is lower in cost than grid electricity.

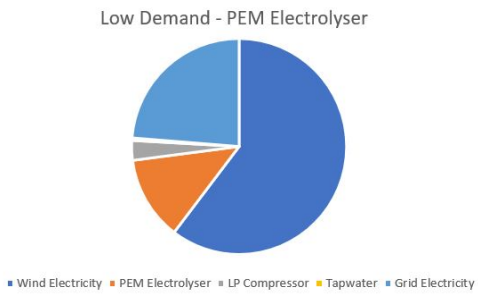

(a) Distribution of annual cost for the 2 MW PEM electrolyser system-configuration at low demand

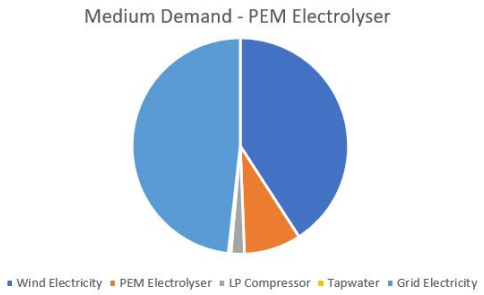

(b) Distribution of annual cost for the 2 MW PEM electrolyser system-configuration at medium demand

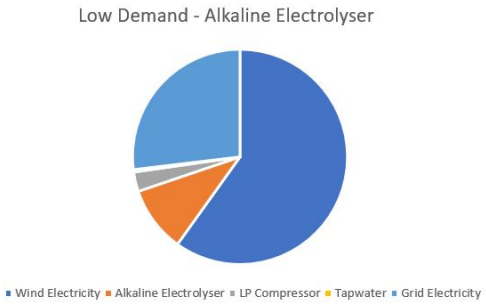

(c) Distribution of annual cost for the 2 MW Alkaline electrolyser system-configuration at low demand

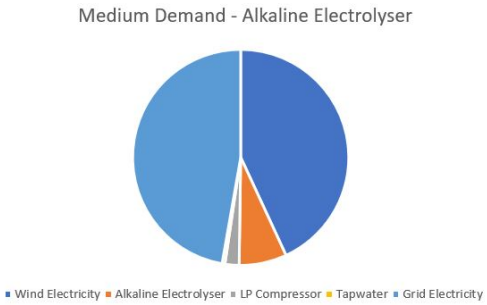

(d) Distribution of annual cost for the 2 MW Alkaline electrolyser system-configuration at medium demand

Figure 7.2: Distribution of annual total cost for each electrolyser, working at partial load, in the low- and medium-demand scenario for producing hydrogen at 200 bar

7.8 Cost Distribution for Dispensed Hydrogen HFS

In the annual cost distribution for producing dispensed hydrogen for a HFS, the largest contributors to the total annual cost are again the wind and the grid electricity. The electrolyser, the dispenser and cooling system at the HFS and the additional cost for the HFS have a much lower contribution to the annual cost. The annual cost distribution for the Alkaline electrolyser is shown in a pie chart in figure 7.3. The other pie charts with the annual cost distribution for the 2 MW systems are displayed Appendix B. Only the cost distribution are shown for the electrolysers working on nominal load is shown. This has been done because it has been made clear already in section 7.7 and section 7.9 that when working on nominal load the share of wind electricity will increase and the share of grid electricity decreases. As can be seen in the charts, the PEM electrolyser has a little higher contribution to the annual cost than the Alkaline electrolyser, because of higher $OPEX$ and $CAPEX$. Furthermore, the cost distribution for the PEM and Alkaline do not differ a lot in the present scenario. In the future scenario, the PEM and Alkaline system, still do not differentiate a lot. For both systems, the grid electricity contribution lowers because of the expected lower grid prices in 2030.

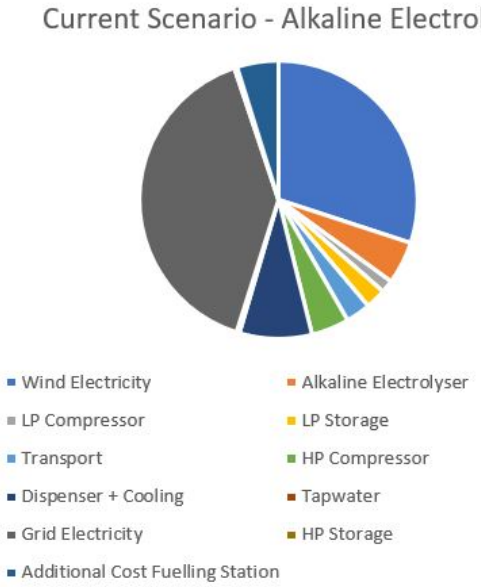

Figure 7.3: Distribution of annual cost for dispensed hydrogen at a HFS for the 2 MW Alkaline electrolyser system-configuration at nominal load in the present scenario

7.9 Cost Distribution for Supply to CTV

As discussed in section 7.4, is the levelised cost of hydrogen supplied to the CTV (at 350 bar), in the present scenario, lowest for the 2 MW Alkaline electrolyser system-configuration. In the future scenario, the 2 MW PEM electrolyser system-configuration is lowest in levelised cost. The distribution of the annual cost for these two system-configurations is shown in figure 7.4. In the present scenario the largest part of the annual cost is the cost of electricity from the wind turbine, followed by the cost from grid electricity. The high share of wind electricity cost is caused by the partial load operation of the electrolyser as discussed in section 7.7. It is shown that low and medium pressure storage and compression have minor impact on the cost. In the 2030 scenario, the share of grid electricity us higher, as the electrolyser is assumed to work full-time on nominal load. However, electricity costs of the grid and of the wind turbine are lowered and the medium pressure compressor takes up a higher share of the annual cost.

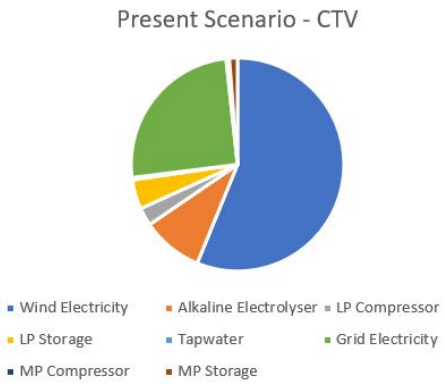

(a) Distribution of annual cost for producing hydrogen at 350 bar for the CTV in the present scenario

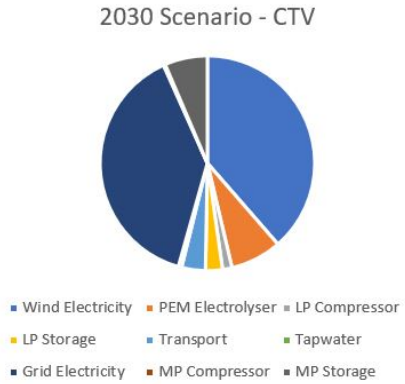

(b) Distribution of annual cost for producing hydrogen at 350 bar for the CTV in the 2030 scenario

Figure 7.4: Distribution of annual total cost for producing hydrogen at 350 bar for the CTV

7.10 Sensitivity Analysis

The difference in levelised cost of hydrogen is already calculated for different demand scenarios. A sensitivity analysis for the cost of energy in the 2030 scenario for three other parameters is performed as well. The sensitivity parameters are based on 'pessimistic' and 'optimistic' deviations from the baseline. The optimistic values result in lower costs and the pessimistic values in higher costs. A higher or lower $WACC$ has a direct impact on the cost of energy. The assumed range of the $WACC$ used for the sensitivity analysis is based on [86]. The cost of the electrolyser could create a difference in cost as well. The future cost of electrolysers could vary from estimations that have been made in the economic analysis. A cost variation of 30% is used, according to reference [86]. In the cost distribution graphs, in the previous chapter, is was shown that the electricity has a major share in the cost distribution. That is why the cost of wind electricity is chosen as a parameter as well. A cost variation of 30% is assumed. The sensitivity parameters are shown in table 7.23.

	Sensitivity parameters	
	Optimistic scenario	Pessimistic scenario
WACC	-30%	+30%
Electrolyser Cost	-30%	+30%
Wind Electricity Cost	-30%	+30%

Table 7.23: Sensitivity parameters for an optimistic and a pessimistic scenario

The relative change in system levelised cost of hydrogen for each system is shown in the figures below. The change in electrolyser cost and $WACC$ have relatively a larger impact on the system levelised cost for the PEM electrolyser than for the Alkaline electrolyser, however the difference is only less than 0.1%. It is clear from this graph that the relative change in electrolyser cost does not have a large impact on the levelised cost of hydrogen. The $WACC$ has a larger impact on the levelised cost of hydrogen. However, the price of electricity supplied by the wind turbine has the largest effect on the levelised cost, a relative change of 8%. When working on partial load, and the share of wind electricity is increased, the impact will be even larger.

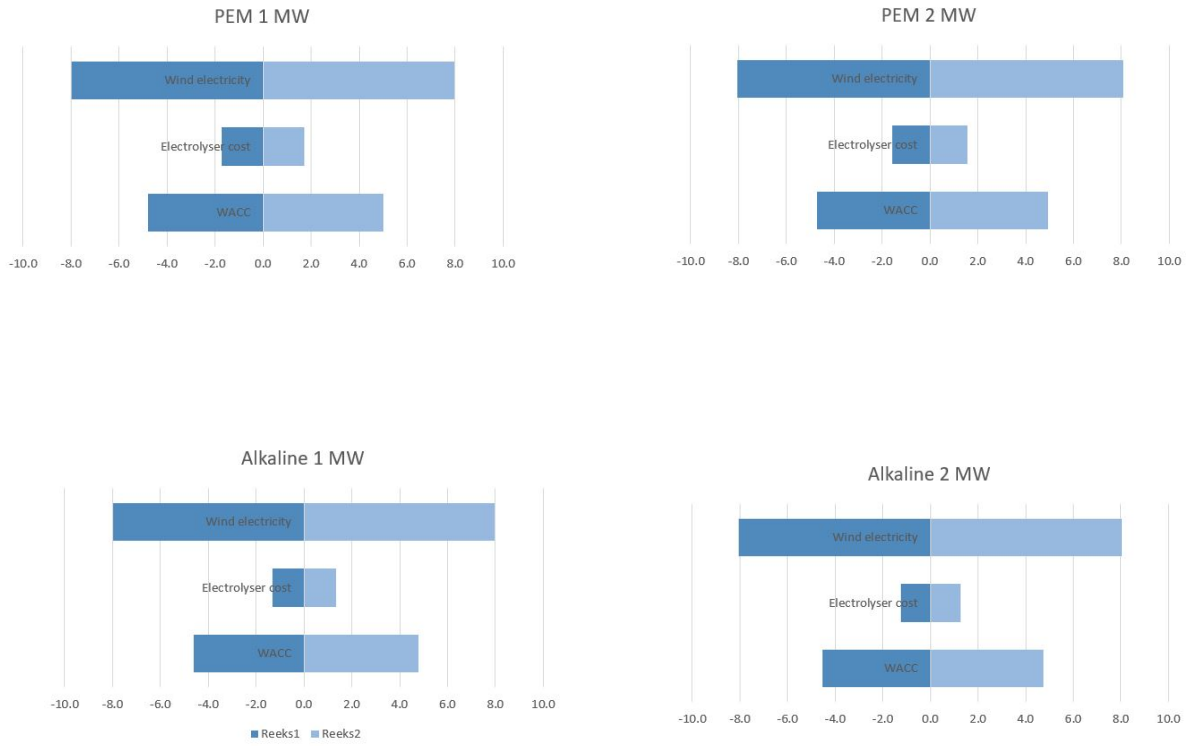

Figure 7.5: Relative change in system levelised cost of hydrogen compared to base scenario.

7.11 Concluding Remarks

With increasing operating hours, the higher utilisation of the electrolyser leads to a decline in the cost of production. As electrolyser operating hours increase, the impact of $CAPEX$ and $OPEX$ costs on the system levelised cost of hydrogen declines and the impact of electricity costs rises. Low utilisation of the electrolyser leads to high hydrogen costs that reflect the $CAPEX$ costs. However, in the economic analysis, it was found that working at partial load decreases the levelised cost of hydrogen as the share of wind electricity can be increased. Running the electrolyser at full load, without relying on surplus electricity from the wind turbine and buying electricity at high prices, can increase the cost of hydrogen.

In this research it is found that the price of the electricity has a large impact on the system levelised cost of hydrogen in comparison with the $CAPEX$ of the system-components as shown in figure 7.2. Electricity has a major share in cost. this can be seen in the graphs showing annual cost distribution for hydrogen supply to the HFS and the CTV.

In the sensitivity analysis the impact of the $WACC$, the electrolyser cost and the wind electricity cost were analysed. It was found that the $WACC$ and the cost of electricity supplied by the wind turbine have a large impact and the $CAPEX$ of the electrolyser has a minor impact on the levelised cost of hydrogen.

In conclusion, the electricity cost is the largest contributor to the levelised cost of hydrogen. For the production of hydrogen, it should be key priority to lower the usage of electricity and lower the cost of electricity. This can for example be achieved by increasing efficiency of components and by increasing the share of low-cost electricity supplied by wind turbines.

Chapter 8

Discussion and Conclusion

8.1 Discussion

This section discusses the research conducted as part of this thesis and uncovers the main uncertainties. As Hemweg 8 is forced to close by the end of 2019, this valuable location could be used for renewable alternatives. In this research it was analysed how hydrogen could be produced at the Hemweg 8 location and if a wind-powered energy system could be cost competitive. The results for this case study confirm that a wind-powered energy system at the Hemweg location could be cost competitive compared to other green hydrogen energy systems and that the system can ensure reliability of hydrogen supply. However, before providing the results, several uncertainties and opportunities have to be considered.

8.2 System Design

In this research, only two sizes of system have been compared: a 1 MW and 2 MW system. The size of every component in the system has been discussed in chapter 4.4. The 2 MW system produces hydrogen at a lower levelised cost, with a difference of €0.4 per kg of hydrogen in comparison with the 1 MW system, which is a 10% decrease in levelised cost. It is expected that the levelised cost of hydrogen will decrease further when production is executed at larger scale. This phenomena is called economies of scale and is described as the cost advantages that companies obtain due to their scale of operation, typically measured by amount of output produced: the cost per unit of hydrogen decreases with increasing scale. The lower levelised cost of hydrogen for the 2 MW indicates that the economies of scale principle is applicable for hydrogen production. It would be interesting to evaluate larger system sizes at the Hemweg location.

In this research the calculated levelised cost of hydrogen production at 200 bar and dispensed hydrogen at a HFS are quite low in comparison with findings in literature. This can be explained by the very low price for wind electricity that is used for the calculations. In reality the cost of electricity could be higher. A 30% higher cost for wind electricity results in a cost increase of 8% as calculated in section 7.10. The low $SLCoE_{H2,HFS}$ in comparison with findings in literature can be explained by the recent reduce in cost of components that belong to a HFS station. Recent estimations of costs for the HFS can be found in the paper of Oldenbroek, V. et. al [86].

In the system design it is assumed that the hydrogen is compressed and transported at 200 bar. Pipelines have not been considered, however, pipelines could reduce the cost of transportation of hydrogen as the compression step could be left out. Using tube trailers for hydrogen transport is very flexible, however very expensive. A very promising solution could be using pipelines which exist in many European countries already, currently for the natural gas grid. With adjustments, such as insulation of the pipelines, the natural gas grid could be used for the transportation of hydrogen. When using pipelines another interesting option could be the offshore production of hydrogen. Offshore wind turbines could generate electricity that can be converted to hydrogen via the electrolysis of seawater and the hydrogen could be transported via the existing gas pipelines. These are all options that were outside the scope of this research.

One of the main findings in this research is the large amount of influence of the electricity price on the levelised cost price of hydrogen. Using electricity that is produced at low cost would be a great benefit for the system. A key focus for the system design should be lowering the electricity cost or lowering the electricity usage. This can be done by reducing the electricity consumption. It was found in this research that when the electrolysers work on partial load, especially the PEM electrolyser, the specific electricity consumption reduces and the efficiency of the system increases. To achieve this, an oversized system design could be beneficial for the

levelised cost price of hydrogen. The electrolyser producer Giner ELX is currently selling PEM electrolysers that have an oversized design and consequently work on partial load all the time at very high efficiencies. When working on 10% load, the efficiency can reach up to 95%, according to Roberto Iriti, Director Business Development at Giner ELX. A recommendation for future research would be to model the PEM and Alkaline electrolyser to find the optimal working load, which results in the lowest levelised cost of hydrogen.

Another possibility to reduce the electricity usage could be by supplying the compressors and purificador with electricity from the wind turbines, which is lower in cost. In the designed system-configurations, only the electrolyser is running on wind electricity. Another option could be to lay more focus on lower electricity cost, by using innovative wind turbine designs i.e. an integrated electrolyser inside the wind turbine, as discussed in section 4.3.1.

8.2.1 Simulink Model

For this research, the electrolysers were modelled on a macro level. This has been helpful for understanding of how electrolysers work and for modelling the electrolysers at partial load. In addition, the Simulink model enables flexibility in gathering insights on how adjustments on temperature and pressure influence the hydrogen output. The electrolyser model uses a variable specific electricity consumption which is dependent on the load, which is an advancement in comparing to many static models used in literature or case studies. In further research this variable electricity consumption could also be applied by other elements of the model such as the rectifier. Modelling the dependency on load would deliver a more precise efficiency, hence specific electricity consumption.

The wind data obtained by Vattenfall ranges from 02-02-2018 until 25-09-2018. The wind generation for the coming years can vary from the data obtained in 2018. Furthermore, the missing data is estimated according to literature and data provided by the KNMI. These assumptions could decrease the accuracy of the Simulink model results compared to reality. The demand of consumers which was included in the scope for three scenarios (low, medium and high) has also been estimated based on expert interviews, as there is not a market for green hydrogen yet. The data for consumption does not include seasonal or daily variation. Neither demand response management is included in the model.

The electrolyser model works with a control system that sends a signal to the electrolyser model when the storage tank cannot meet the demand anymore. When the signal is sent, the electrolyser starts extracting electricity from the grid, and starts running on full power. As an improvement of the control system, the duration of time to produce the hydrogen demand on full power could be calculated and could be included in the control system. If it would take, for example, three hours to produce enough hydrogen to meet demand, the control system could only starts working at that exact moment in time. This adjustment in the control system would create a higher usage of electricity supply by the wind turbines, which is more cost effective than using electricity from the grid.

8.2.2 Economic Analysis

In this model, electricity cost from the grid remains constant, while in reality electricity cost from the grid do vary. However, no correlation was found between low wind power output and high grid prices (section 7.3). Hence, the average grid operator tariff of 2018 is assumed.

Also, subsidies are not included in the cost calculation for this model. A similar system conducted by EnergyStock and Gasunie New Energy, received a subsidy from the European Commission. If this would be the case for conducting this wind to hydrogen energy system, this would be beneficial for the system cost, hence, the levelised cost of hydrogen.

Implementing energy market dynamics for grid prices would be a valuable addition for the system. When grid prices are low, more hydrogen could be produced. Below a certain price value per MWh for grid electricity, the electrolyser could start running on nominal load on electricity from the grid. Not only fluctuating grid tariffs but also demand response management could benefit the system, to make use of the intermittent wind energy and to reduce the necessity of large storage capacities.

Also, grid services towards grid operators were not included in this thesis, however grid services in order to counteract grid congestions could be of value by providing an extra revenue stream. At the moment, transmission grid operators resolve congestions by applying remedial network and marked related measures. [126] When more renewable energy is used, with high fluctuating energy production, these congestions will occur more often. When all these measures are exhausted, grid operators currently issue an instruction to limit the power output of specific generators. [126] Instead of curtailing renewable energy sources, electrolysers could be used to increase the load at the same grid location in critical situations. Increasing the load, decreases the total power feed-in of the grid at that location and helps resolve the congestions.

The numbers provide clear indications which technology options are favourable and could serve as reference. The calculated values for the levelised cost of hydrogen in this research can be used as a reference in decision-making for the development of a wind-to-hydrogen energy system at the Hemweg.

8.2.3 Future Scenario

A sensitivity analysis has been performed for the 2030 scenario for the electrolyser cost and the $WACC$. A variation in electrolyser cost of 30% leads to a levelised cost variation of less than 2% and a variation in $WACC$ of 30% leads to a relative change in levelised cost less than 5%. However, there is a high level of uncertainty in the economic analysis for the 2030 scenario, as predictions are made concerning future cost of technologies and design improvements. Price estimations from literature were used to estimate prices of all components in the system. The efficiency of some components increases as well, which results in a more cost-effective system. As renewable energy production is growing and producing electricity at low cost, the costs for electricity are expected to decrease as well. However it is difficult to estimate how fast the contribution of renewable energy supply to the grid will grow. Furthermore, the assumptions made for electricity prices greatly affect the prices for hydrogen. Prices for hydrogen production are expected to decrease rapidly in the coming years. This rapid decrease in the price of hydrogen production, combined with uncertain electricity prices, increases the uncertainty of the actual future price of hydrogen.

8.3 Conclusion

This research aimed to provide Vattenfall with an technical and economical analysis to support decision making about the potential of a hydrogen plant at the Hemweg 8 location for hydrogen supply to the industry and mobility. The main research question was formulated as: *How can a cost competitive hydrogen energy system be designed at the Hemweg location, using available wind power, ensuring reliability of hydrogen supply at all times?* To answer the main question, four sub questions were formulated and approached during the research, the results are concluded below:

8.3.1 Sub Questions

1. Which characteristics of technologies for production, storage and usage of hydrogen are relevant?

The electrolyser is an integral part in the production of green hydrogen, therefore the different types of electrolysers were evaluated. The PEM and the Alkaline electrolyser are considered the most suitable electrolysers. This is mainly based on pressure of operation, flexibility, cost price of the system and the level of development on large scale. The Alkaline and the PEM electrolyser produce hydrogen at pressures of 1 bar and 40 bar, respectively. The running time of an electrolyser is very important for being cost effective. As the electrolyser operating hours of an electrolyser increase, the impact of the $CAPEX$ of the system declines and the impact of electricity cost increases. Low utilisation of the electrolyser leads to high hydrogen costs that reflect the $CAPEX$ costs. However, in the economic analysis, it was found that working at partial load decreases the levelised cost of hydrogen as the share of wind electricity can be increased. For electrolysers, it is necessary to make a trade-off between current density and voltage. Working at nominal load results in a higher current density and a larger hydrogen production. However, running on high current densities, lowers the voltage, hence decreases the efficiency of the electrolyser. This is why electrolysers running on partial load, at low current densities (resulting in a higher voltage) can run at high efficiencies. When running on partial load, the share of low-cost electricity supplied by the wind turbine can be increased. In this research it is found that the price of the electricity has a large impact on the system levelised cost of hydrogen in comparison with the $CAPEX$ of the system-components, which has a minor impact on the levelised cost of hydrogen.

There is a large variety of different forms of hydrogen storage technologies. The technologies still differ greatly in energetic efficiency, gravimetric energy density, volumetric energy density and cost-efficiency. Hydrogen has a very low volumetric energy density, which makes it hard to store. It can be stated that the storage of hydrogen is one of the main barriers to the widespread use of hydrogen. This makes the storage of hydrogen a key element in hydrogen energy systems. A variety of storage technologies have been analysed in the report, however, for now the compressed storage of hydrogen is accessed as the most suitable technology for this case study. Compressed storage of hydrogen is a mature and widely used technology and therefore considered as most reliable.

Within mobility, hydrogen can be used as a fuel for vehicles and ships with fuel cells or internal combustion engines. Fuel cells have a higher efficiency and seem to be the most promising technique. When using hydrogen as a fuel for ships, the low volumetric energy density of hydrogen is again one of the main barriers. Compressed hydrogen on a ship requires a large volume to meet the fuel demand of ships, especially for long distances. In most hydrogen-fuelled ships, that are already developed and used, the hydrogen is stored at a pressure of 350 bar. To facilitate the widespread use of hydrogen, more fuelling stations are required at harbours. In the future, the chemical hydride named sodium borohydride could possibly be used as a storage technology and fuel for ships. However, the technology is currently too immature to include expectations on this in the 2030 scenario.

2. Which electrolyser is the best option for this case study: A PEM electrolyser or an Alkaline electrolyser?

When comparing the PEM and Alkaline electrolyser, it is seen that in the present scenario, the Alkaline electrolyser system-configuration has a higher efficiency than the PEM electrolyser. However, in the 2030 scenario, the PEM electrolyser system-configuration is 2% more efficient than the Alkaline electrolyser. The system efficiencies for each electrolyser for producing hydrogen at 200 bar are displayed in table 8.1. The high increase in efficiency for the PEM electrolyser is mainly caused by the good partial-load performance of the PEM electrolyser and the expected decrease in specific electricity consumption of 5 kWh/kg for the PEM electrolyser, in comparison to a decrease of 1 kWh/kg for the Alkaline electrolyser. In addition, the higher outlet pressure of the PEM electrolyser causes a lower electricity consumption of the 200 bar compressor.

	Present	2030
Alkaline electrolyser	73%	74%
PEM electrolyser	71%	76%

Table 8.1: System efficiency for producing hydrogen at 200 bar

In the economic analysis it is concluded that, in the present scenario, the Alkaline electrolyser results in the lowest $LCoE_{H2}$, with a difference of 0.5 €/kg with the $LCoE_{H2}$ of a PEM electrolyser. When there is a low-demand for hydrogen, the electrolyser can work on partial-load, which not only increases the efficiency but also helps increase the share of wind electricity and consequently lowers the share of grid electricity, which is more expensive. When comparing the results, the low $LCoE_{H2}$ of the Alkaline electrolyser in the present scenario is mainly caused by the low $CAPEX$ and $OPEX$ of the electrolyser. In the 2030 scenario, the PEM electrolyser has the lowest $LCoE_{H2}$, as shown in table 8.2. The expected reduce in $CAPEX$ and the increase in efficiency causes the low $LCoE_{H2}$ for the PEM electrolyser.

		$LCoE_{H2}$
Present scenario	2 MW Alkaline	3.9 €/kg
2030 scenario	2 MW PEM	3.2 €/kg

Table 8.2: Electrolyser selection

According to the economic analysis, it can be concluded that in the present scenario, the Alkaline electrolyser is the lowest in cost and for the 2030 scenario, the PEM electrolyser is lowest in cost. The difference between the Alkaline and PEM electrolyser in levelised cost is calculated as 0.5 €/kg and 0.2 €/kg for the present and 2030 scenario, respectively. It can be concluded that for the 2030 scenario, the selection of electrolyser will not have a major impact on the levelised cost of hydrogen.

3. How much hydrogen can be produced and is that amount sufficient to meet the demand of consumers?

The hydrogen consumption is hard to predict. Several demand scenarios have been determined based on potential hydrogen consumption near the Hemweg (section 4.2). For each demand scenario 4 system configurations were modelled. None of the daily demand scenarios for hydrogen were met when being solely dependant on wind power. This is why electricity is extracted from the grid when necessary. When including electricity from the grid, it is concluded that there will be sufficient hydrogen production to meet the demand only for the low and medium-demand scenario in the present time scenario, only for the 2 MW systems. The daily amount needed for the low- and medium-demand scenario is displayed in table 8.3:

Scenario	**Demand for hydrogen (kg/day)**
Low	500
Medium	800

Table 8.3: Present low- and medium-demand scenarios for hydrogen

The other demand scenarios exceed the total production of hydrogen for each system. For all other demand scenarios, the electrolysers do not produce enough hydrogen to meet the demand and the systems are assumed to work on nominal load with electricity supplied by the grid. The low- and medium-demand scenario are only met by the 2 MW size configurations. The maximum hydrogen production for the 2 MW PEM and Alkaline electrolyser is presented in table 8.4. In the 2030 scenario, there is an increase in efficiency for both electrolysers assumed, which explains the higher amount of hydrogen that is produced.

	Total hydrogen production working on nominal load (kg)	
	Present	2030
PEM Electrolyser	318,000	349,000
Alkaline Electrolyser	351,000	357,000

Table 8.4: The total hydrogen production for the 2 MW electrolysers in a year using wind energy combined with electricity from the grid

4. Can a wind to hydrogen energy system on the Hemweg location be cost competitive compared to alternative hydrogen energy systems?

The research results indicate that a wind powered hydrogen energy system at the Hemweg location could be cost competitive. However, this comes with constraints and is dependent on the applied load. It is only cost competitive with other green hydrogen production facilities, as it is still more cost effective to produce hydrogen with SMR (discussed in section 7.4). The $LCoE_{H2,HFS}$ and $SLCoE_{H2,HFS}$ that were found in this research are displayed in table 8.5. The levelised cost are dependent on the electrolyser that is used and are strongly dependent on the load that is applied as discussed in section 7.4.

	Present	**2030**
$LCoE_{H2}$ (€/kg)	3.9	3.2
$SLCoE_{H2,HFS}$ (€/kg)	6.8	5.1

Table 8.5: The levelised cost of hydrogen production at 200 bar and system levelised cost for dispensed hydrogen

The levelised cost price of hydrogen at 200 bar for this system is cost competitive with green hydrogen production prices found on the market. [15] In the 2030 scenario the levelised cost price is lower, mainly caused by lower electricity prices, more efficient equipment and a reduce in $CAPEX$. The present price for gasoline is approximately 1.6 €/L. [125], which corresponds to €8 per 100 kilometres (calculations are performed in section 7.5). The $LCoE_{H2,HFS}$ of 6.8 €/kg results in approximately €6.8 per 100 kilometres. Hence, using hydrogen as a fuel for $FCEV$s is cost competitive with gasoline.

8.3.2 Main Research Question

The conclusions of the sub questions leads us to the answer of the main research question:

How can a cost competitive hydrogen energy system be designed at the Hemweg location, using available wind power, ensuring reliability of hydrogen supply at all times?

The closure of Hemweg 8 brings new opportunities for Vattenfall for the land use of the Hemweg by creating a fossil free hub for sustainable energy production. Therefore a technical assessment and economical assessment was conducted. From the research findings, a PEM and Alkaline electrolyser, powered by wind and grid electricity, were accessed as cost competitive hydrogen energy systems. The running time, partial load performance, scale of system, output pressure, the $WACC$ and the share of renewable energy used for electricity were identified as important factors that influence either the amount of hydrogen output or the levelised cost of the hydrogen directly. A cost compatible way of transporting hydrogen to different industries and to fuelling stations for $FCEV$s and hydrogen-powered ships, is in compressed form and transported at 200 bar. The 2 MW Alkaline and 2 WM PEM systems can produce enough hydrogen for a low and medium-demand scenario. In this research it was found that a wind-powered hydrogen energy system at the Hemweg is competitive with green hydrogen production prices found on the market and the $LCoE_{H2,HFS}$ is cost competitive with gasoline. Using hydrogen as an energy carrier opens the opportunity to reduce GHG emissions and combat climate change.

Appendix A

Hemweg 8 and LiDAR Location

Figure A.1: Location Hemweg 8 [9]

Figure A.2: Location of LiDAR instrument

Appendix B

Annual Cost Distribution

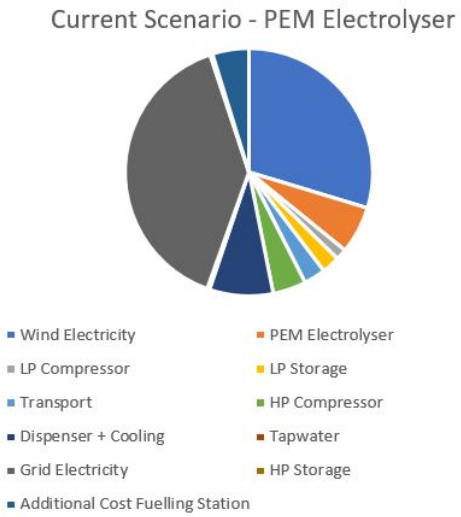

Figure B.1: Annual cost distribution PEM electrolyser - Current Scenario

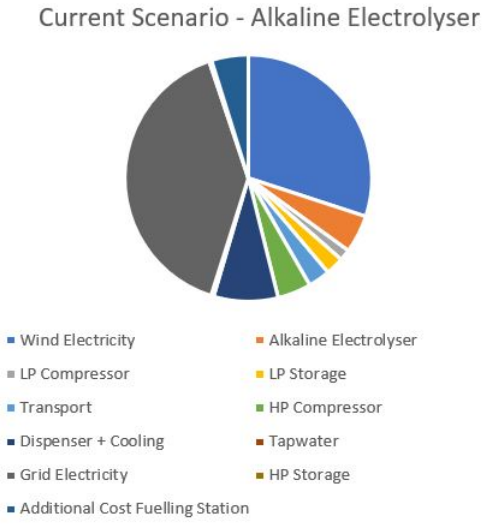

Figure B.2: Annual cost distribution Alkaline electrolyser - Current Scenario

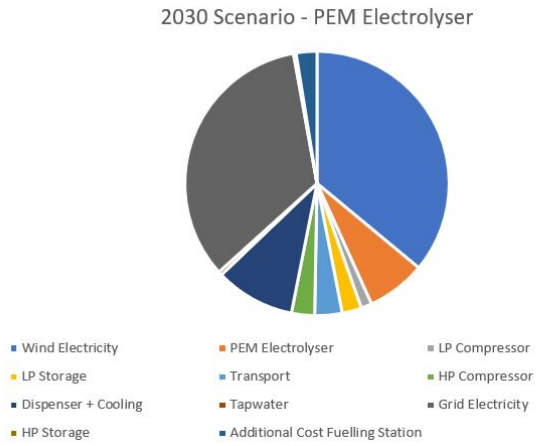

Figure B.3: Annual cost distribution PEM electrolyser - 2030 Scenario

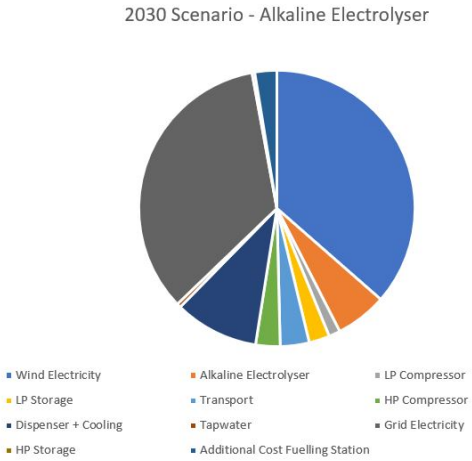

Figure B.4: Annual cost distribution Alkaline electrolyser - 2030 Scenario

Appendix C

Levelised Cost Distribution

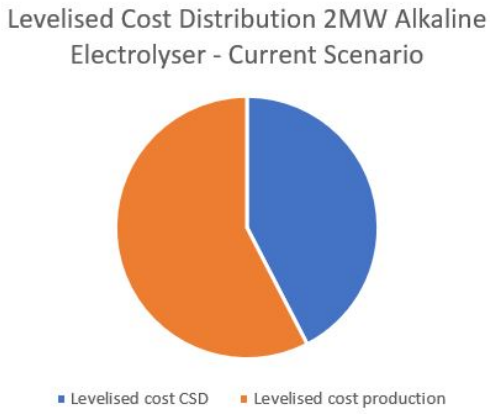

Figure C.1: Levelised cost distribution Alkaline electrolyser - current Scenario

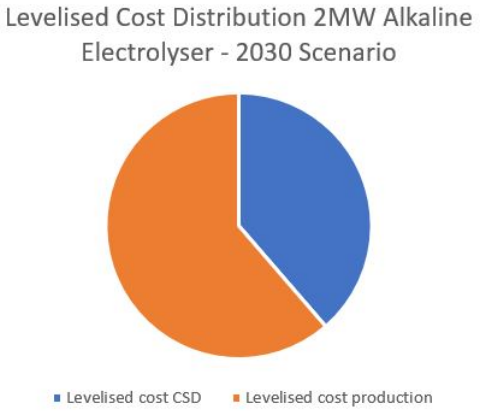

Figure C.2: Levelised cost distribution Alkaline electrolyser - 2030 Scenario

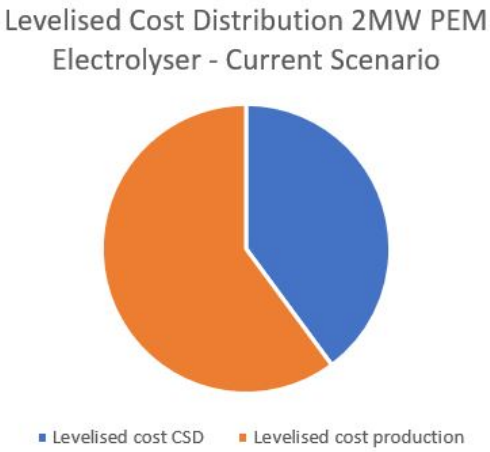

Figure C.3: Levelised cost distribution PEM electrolyser - current Scenario

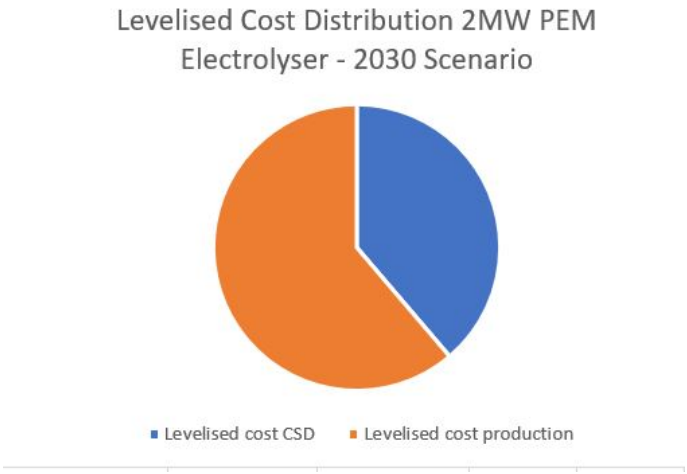

Figure C.4: Levelised cost distribution PEM electrolyser - 2030 Scenario

Bibliography

[1] A. Ozbilen, I. Dincer, and M. A. Rosen, "Comparative environmental impact and efficiency assessment of selected hydrogen production methods," *Environmental Impact Assessment Review*, vol. 42, pp. 1–9, 9 2013.

[2] J. Larminie, A. Dicks, and M. S. McDonald, *Fuel cell systems explained*, vol. 2. J. Wiley Chichester, UK, 2003.

[3] A. Buttler and H. Spliethoff, "Current status of water electrolysis for energy storage, grid balancing and sector coupling via power-to-gas and power-to-liquids: A review," *Renewable and Sustainable Energy Reviews*, vol. 82, pp. 2440–2454, 2018.

[4] M. Mori, T. Mrzljak, B. Drobnic, and M. Sekavcnik, "Integral characteristics of hydrogen production in alkaline electrolysers/karakteristike delovanja in proizvodnje vodika v elektrolizerju za elektrolizo alkalne vodne raztopine," *strojniski vestnik-Journal of Mechanical Engineering*, vol. 59, no. 10, pp. 585–596, 2013.

[5] I. Papagiannakis, "Studying and improving the efficiency of water electrolysis using a proton exchange membrane electrolyser," *Mechanical Engineering Thesis, Strathclyde University*, 2005.

[6] O. Schmidt, A. Gambhir, I. Staffell, A. Hawkes, J. Nelson, and S. Few, "Future cost and performance of water electrolysis: An expert elicitation study," *International journal of hydrogen energy*, vol. 42, no. 52, pp. 30470–30492, 2017.

[7] F. Mulder, B. Weninger, J. Middelkoop, F. Ooms, and H. Schreuders, "Efficient electricity storage with a battolyser, an integrated ni–fe battery and electrolyser," *Energy & Environmental Science*, vol. 10, no. 3, pp. 756–764, 2017.

[8] O. S. Burheim, "Chapter 8 - hydrogen for energy storage," in *Engineering Energy Storage* (O. S. Burheim, ed.), pp. 147 – 192, Academic Press, 2017.

[9] "Coal plant hemweg 8, https://powerplants.vattenfall.com/en/hemweg-8." Accessed: 2019-09-30.

[10] "Sinavy pem fuel cell for submarines, https://www.industry.siemens.com." Accessed: 2019-05-30.

[11] M. Hamdan, "Pem electrolyzer incorporating an advanced low-cost membrane," tech. rep., Giner, Inc./Giner Electrochemical Systems, LLC, Newton, MA, 2013.

[12] "Costs and financing." https://h2stationmaps.com/costs-and-financing, Accessed: 12-11-2019.

[13] D. Parra and M. K. Patel, "Techno-economic implications of the electrolyser technology and size for power-to-gas systems," *International Journal of Hydrogen Energy*, vol. 41, no. 6, pp. 3748 – 3761, 2016.

[14] S. Makridis, "Hydrogen storage and compression," *arXiv preprint arXiv:1702.06015*, 2017.

[15] *The future of hydrogen: seizing today's opportunities: report prepared by the IEA for the G20, Japan*. IEA Publications, 2019.

[16] J. Gigler, M. Weeda, and N. G. TKI, "Outlines of a hydrogen roadmap," *TKI Nieuw Gas*, 2018.

[17] J. Rogelj, M. Den Elzen, N. Höhne, T. Fransen, H. Fekete, H. Winkler, R. Schaeffer, F. Sha, K. Riahi, and M. Meinshausen, "Paris agreement climate proposals need a boost to keep warming well below 2 c," *Nature*, vol. 534, no. 7609, p. 631, 2016.

[18] R. FALKNER, "The Paris Agreement and the new logic of international climate politics," *International Affairs*, vol. 92, pp. 1107–1125, 08 2016.

[19] "Eerste battolyser voor elektriciteitsopslag en waterstofproductie in groningen dankzij waddenfonds," Jun 2018. https://group.vattenfall.com/nl/newsroom/actueel/persbericht, Accessed: 2019-06-14.

[20] "Ns en vattenfall gaan nieuw windpark bouwen in amsterdam," Jan 2019. Windenergie Courant.

[21] O. Ellabban, H. Abu-Rub, and F. Blaabjerg, "Renewable energy resources: Current status, future prospects and their enabling technology," *Renewable and Sustainable Energy Reviews*, vol. 39, pp. 748–764, 2014.

[22] K. Sainath, Y. Krishna, M. Salahuddin, M. S. Ahmed, M. Ismail, S. Rahman, M. Noman, M. K. Ullah, F. U. R. Azhar, M. Moizuddin, *et al.*, "Comparative study and design of solar water heater," *International Journal of Engineering Research*, vol. 3, no. 10, pp. 559–563, 2014.

[23] C. Neagu, H. Jansen, H. Gardeniers, and M. Elwenspoek, "The electrolysis of water: an actuation principle for mems with a big opportunity," *Mechatronics*, vol. 10, no. 4-5, pp. 571–581, 2000.

[24] P. Basu and P. Basu, "Biomass Characteristics," *Biomass Gasification and Pyrolysis*, pp. 27–63, 1 2010.

[25] K. Gluesenkamp and R. Radermacher, "Heat-activated cooling technologies for small and micro combined heat and power (CHP) applications," *Small and Micro Combined Heat and Power (CHP) Systems*, pp. 262–306, 1 2011.

[26] A. Ursua, L. M. Gandia, and P. Sanchis, "Hydrogen production from water electrolysis: current status and future trends," *Proceedings of the IEEE*, vol. 100, no. 2, pp. 410–426, 2012.

[27] K. E. Ayers, E. B. Anderson, C. Capuano, B. Carter, L. Dalton, G. Hanlon, J. Manco, and M. Niedzwiecki, "Research advances towards low cost, high efficiency pem electrolysis," *ECS transactions*, vol. 33, no. 1, pp. 3–15, 2010.

[28] M. Hamdan, "Advanced electrochemical hydrogen compressor," in *Meeting Abstracts*, no. 26, pp. 885–885, The Electrochemical Society, 2018.

[29] M. Hamdan and K. Harrison, "Doe hydrogen and fuel cells program," Apr 2019.

[30] L. Wang, M. Chen, R. Küngas, T.-E. Lin, S. Diethelm, F. Maréchal, and J. V. herle, "Power-to-fuels via solid-oxide electrolyzer: Operating window and techno-economics," *Renewable and Sustainable Energy Reviews*, vol. 110, pp. 174 – 187, 2019.

[31] F. Mulder, B. Weninger, J. Middelkoop, F. Ooms, and H. Schreuders, "Efficient electricity storage with a battolyser, an integrated ni–fe battery and electrolyser," *Energy & Environmental Science*, vol. 10, no. 3, pp. 756–764, 2017.

[32] "Kolen - nuon," 09 2018. https://www.nuon.com/activiteiten/kolen/, Accessed: 2019-07-03.

[33] S. Grigoriev, P. Millet, S. Korobtsev, V. Porembskiy, M. Pepic, C. Etievant, C. Puyenchet, and V. Fateev, "Hydrogen safety aspects related to high-pressure polymer electrolyte membrane water electrolysis," *International Journal of Hydrogen Energy*, vol. 34, no. 14, pp. 5986 – 5991, 2009. 2nd International Conference on Hydrogen Safety.

[34] A. Roy, S. Watson, and D. Infield, "Comparison of electrical energy efficiency of atmospheric and high-pressure electrolysers," *International Journal of Hydrogen Energy*, vol. 31, pp. 1964–1979, 11 2006.

[35] K. Onda, T. Kyakuno, K. Hattori, and K. Ito, "Prediction of production power for high-pressure hydrogen by high-pressure water electrolysis," *Journal of Power Sources*, vol. 132, pp. 64–70, 5 2004.

[36] B. K. Gebbink, M. Costas, X. Hu, H. Junge, M. Albrecht, J. Harvey, F. Neese, P. Schollhammer, and M.-E. Moret, "Non-noble metal catalysis–nonomecat," *Impact*, vol. 2016, no. 2, pp. 20–22, 2016.

[37] A. Hassan, M. K. Patel, and D. Parra, "An assessment of the impacts of renewable and conventional electricity supply on the cost and value of power-to-gas," *International Journal of Hydrogen Energy*, vol. 44, no. 19, pp. 9577–9593, 2019.

[38] J. Proost, "State-of-the art capex data for water electrolysers, and their impact on renewable hydrogen price settings," *International Journal of Hydrogen Energy*, vol. 44, no. 9, pp. 4406–4413, 2019.

[39] J. De Bucy, O. Lacroix, and L. Jammes, "The potential of power-to-gas," *ENEA Consulting, Paris, France*, 2016.

[40] G. Matute, J. Yusta, and L. Correas, "Techno-economic modelling of water electrolysers in the range of several mw to provide grid services while generating hydrogen for different applications: A case study in spain applied to mobility with fcevs," *International Journal of Hydrogen Energy*, 2019.

[41] L. Allidieres, A. Brisse, P. Millet, S. Valentin, and M. Zeller, "On the ability of pem water electrolysers to provide power grid services," *International Journal of Hydrogen Energy*, vol. 44, no. 20, pp. 9690–9700, 2019.

[42] O. S. Burheim, *Engineering energy storage*. Academic Press, 2017.

[43] S. G. Chalk and J. F. Miller, "Key challenges and recent progress in batteries, fuel cells, and hydrogen storage for clean energy systems," *Journal of Power Sources*, vol. 159, no. 1, pp. 73–80, 2006.

[44] F. Zhang, P. Zhao, M. Niu, and J. Maddy, "The survey of key technologies in hydrogen energy storage," *International Journal of Hydrogen Energy*, vol. 41, no. 33, pp. 14535 – 14552, 2016.

[45] Y. huan ZHANG, Z. chao JIA, Z. ming YUAN, T. YANG, Y. QI, and D. liang ZHAO, "Development and application of hydrogen storage," *Journal of Iron and Steel Research, International*, vol. 22, no. 9, pp. 757 – 770, 2015.

[46] J. Andersson and S. Grönkvist, "Large-scale storage of hydrogen," *International Journal of Hydrogen Energy*, vol. 44, no. 23, pp. 11901 – 11919, 2019.

[47] S. Niaz, T. Manzoor, and A. H. Pandith, "Hydrogen storage: Materials, methods and perspectives," *Renewable and Sustainable Energy Reviews*, vol. 50, pp. 457 – 469, 2015.

[48] T. N. Veziroglu, S. Sherif, and F. Barbir, "Hydrogen energy solutions," in *Environmental solutions*, pp. 143–180, Elsevier, 2005.

[49] F. Barbir, "Chapter ten - fuel cell applications," in *PEM Fuel Cells (Second Edition)* (F. Barbir, ed.), pp. 373 – 434, Boston: Academic Press, second edition ed., 2013.

[50] J. J. Minnehan and J. W. Pratt, "Practical application limits of fuel cells and batteries for zero emission vessels," tech. rep., Sandia National Lab.(SNL-NM), Albuquerque, NM (United States), 2017.

[51] J. J. de Troya, C. Alvarez, C. Fernández-Garrido, and L. Carral, "Analysing the possibilities of using fuel cells in ships," *International Journal of Hydrogen Energy*, vol. 41, no. 4, pp. 2853–2866, 2016.

[52] A. M. Helmenstine, "The chemical composition of air," Sep 2018.

[53] N. Sammes, R. Bove, and K. Stahl, "Phosphoric acid fuel cells: Fundamentals and applications," *Current Opinion in Solid State and Materials Science*, vol. 8, no. 5, pp. 372 – 378, 2004.

[54] "Fuelcelltoday - the leading authority on fuel cells." http://www.fuelcelltoday.com/technologies/pafc, Accessed: 2019-06-06.

[55] S. Mekhilef, R. Saidur, and A. Safari, "Comparative study of different fuel cell technologies," *Renewable and Sustainable Energy Reviews*, vol. 16, no. 1, pp. 981–989, 2012.

[56] A. S. Patil, T. G. Dubois, N. Sifer, E. Bostic, K. Gardner, M. Quah, and C. Bolton, "Portable fuel cell systems for america's army: technology transition to the field," *Journal of Power Sources*, vol. 136, no. 2, pp. 220 – 225, 2004. Selected papers presented at the International Power Sources Symposium.

[57] S. Alkaner and P. Zhou, "A comparative study on life cycle analysis of molten carbon fuel cells and diesel engines for marine application," *Journal of power sources*, vol. 158, no. 1, pp. 188–199, 2006.

[58] A. Choudhury, H. Chandra, and A. Arora, "Application of solid oxide fuel cell technology for power generation—a review," *Renewable and Sustainable Energy Reviews*, vol. 20, pp. 430 – 442, 2013.

[59] "Hoe waait de wind, https://www.knmi.nl/over-het-knmi/nieuws/hoe-waait-de-wind." Accessed: 2019-11-05.

[60] A. Brand, "Offshore wind atlas of the dutch part of the north sea," *China/Global Wind Power*, 2008.

[61] J. Coelingh, A. van Wijk, and A. Holtslag, "Analysis of wind speed observations over the north sea," *Journal of Wind Engineering and Industrial Aerodynamics*, vol. 61, no. 1, pp. 51 – 69, 1996.

[62] T. Sowell, *Say's law: An historical analysis*. Princeton University Press, 2015.

[63] M. T. ÇOBAN and E. Cüneyt, "Design and analysis of nato f-76 diesel fuelled solid oxide fuel cell system onboard surface warship," *Journal of Naval Science and Engineering*, 2010.

[64] T. Smith, J. Jalkanen, B. Anderson, J. Corbett, J. Faber, S. Hanayama, E. O'Keeffe, S. Parker, L. Johansson, L. Aldous, C. Raucci, M. Traut, S. Ettinger, D. Nelissen, D. Lee, S. Ng, A. Agrawal, J. Winebrake, M. Hoen, S. Chesworth, and A. Pandey, *Third IMO Greenhouse Gas Study 2014*. international maritime organization, 2015.

[65] V. P. McConnell, "Now, voyager? the increasing marine use of fuel cells," *Fuel cells bulletin*, vol. 2010, no. 5, pp. 12–17, 2010.

[66] C. H. Choi, S. Yu, I.-S. Han, B.-K. Kho, D.-G. Kang, H. Y. Lee, M.-S. Seo, J.-W. Kong, G. Kim, J.-W. Ahn, *et al.*, "Development and demonstration of pem fuel-cell-battery hybrid system for propulsion of tourist boat," *International Journal of Hydrogen Energy*, vol. 41, no. 5, pp. 3591–3599, 2016.

[67] *Perspectives for the Use of Hydrogen as Fuel in Inland Shipping*. MariGreen, 2018.

[68] J. Pike, "Military." https://www.globalsecurity.org/military/world/europe/type-212.htm, Accessed: 2019-08-2.

[69] L. Van Biert, M. Godjevac, K. Visser, and P. Aravind, "A review of fuel cell systems for maritime applications," *Journal of Power Sources*, vol. 327, pp. 345–364, 2016.

[70] K.-T. Hammou, "One hundred passengers and zero emissions the first ever passenger vessel to sail propelled by fuel cells."

[71] J. J. de Troya, C. Álvarez, C. Fernández-Garrido, and L. Carral, "Analysing the possibilities of using fuel cells in ships," *International Journal of Hydrogen Energy*, vol. 41, no. 4, pp. 2853 – 2866, 2016.

[72] N. Manthey, "Joint call on eu to provide framework for h2 infrastructure," Oct 2019.

[73] *Evolution: Electric vehicles in Europe: gearing up for a new phase?* Mar 2014. McKinsey and Amsterdam Round Tables, Accessed: 2019-08-08.

[74] "Rozenburg klaar voor verwarming met 100% waterstof, https://www.stedin.net/." Accessed: 2019-11-07.

[75] F. Brito, J. Martins, D. D. R. Pedrosa, V. D. F. Monteiro, and J. L. Afonso, "Real-life comparison between diesel and electric car energy consumption," *Grid electrified vehicles: performance, design and environmental impacts (Editor: Carla Alexandra Monteiro da Silva)*, pp. 209–232, 2013.

[76] S. Dijksma, *Actieplan Schone Lucht*. 2019.

[77] J. Koot, "Amsterdam en utrecht krijgen meerdere tankstations voor waterstof," *fd*, Jan 2019.

[78] "Personenautoverkeer," tech. rep., CBS, 2017.

[79] "Development of business cases for fuel cells and hydrogen," 2017. Roland Berger.

[80] R. Segers, R. Oever, R. Niessink, and M. Menkveld, "Warmtemonitor 2017," tech. rep., CBS TNO, 2019.

[81] Nordex Acciona Windpower, "Delta Generation: Proven Technology - At a New Stage of Evolution,"

[82] H. C. Gils and S. Simon, "Carbon neutral archipelago–100% renewable energy supply for the canary islands," *Applied energy*, vol. 188, pp. 342–355, 2017.

[83] K. Nath and D. Das, "Production and storage of hydrogen: Present scenario and future perspective," 2007.

[84] N. Qin, P. Brooker, and S. Srinivasan, "Hydrogen fueling stations infrastructure," tech. rep., 2014.

[85] J. Kurtz, S. Sprik, and T. H. Bradley, "Review of transportation hydrogen infrastructure performance and reliability," *International Journal of Hydrogen Energy*, vol. 44, no. 23, pp. 12010 – 12023, 2019.

[86] V. Oldenbroek, L. A. Verhoef, and A. J. Van Wijk, "Fuel cell electric vehicle as a power plant: Fully renewable integrated transport and energy system design and analysis for smart city areas," *International Journal of Hydrogen Energy*, vol. 42, no. 12, pp. 8166–8196, 2017.

[87] J. F. Manwell, J. G. McGowan, and A. L. Rogers, "Wind Energy Explained: Theory, Design and Application," tech. rep., 2010.

[88] C. Tang, M. Pathmanathan, W. Soong, and N. Ertugrul, "Effects of inertia on dynamic performance of wind turbines," in *2008 Australasian Universities Power Engineering Conference*, pp. 1–6, IEEE, 2008.

[89] C. Tang, W. L. Soong, P. Freere, M. Pathmanathan, and N. Ertugrul, "Dynamic wind turbine output power reduction under varying wind speed conditions due to inertia," *Wind Energy*, vol. 16, no. 4, pp. 561–573, 2013.

[90] Ø. Ulleberg, "Modeling of advanced alkaline electrolyzers: a system simulation approach," *International journal of hydrogen energy*, vol. 28, no. 1, pp. 21–33, 2003.

[91] R. García-Valverde, N. Espinosa, and A. Urbina, "Simple PEM water electrolyser model and experimental validation," *International Journal of Hydrogen Energy*, vol. 37, no. 2, pp. 1927–1938, 2012.

[92] M. Ni, M. K. H. Leung, and D. Y. C. Leung, "Electrochemistry Modeling of Proton Exchange Membrane (PEM) Water Electrolysis for Hydrogen Production," *Whec*, vol. 16, no. June, pp. 13–16, 2006.

[93] F. Barbir, "Fuel Cell Electrochemistry," in *PEM Fuel Cells*, pp. 33–72, Elsevier, 9 2012.

[94] B. Han, S. M. Steen, J. Mo, and F.-Y. Zhang, "Electrochemical performance modeling of a proton exchange membrane electrolyzer cell for hydrogen energy," *International Journal of Hydrogen Energy*, vol. 40, no. 22, pp. 7006 – 7016, 2015.

[95] T. Yigit and O. F. Selamet, "Mathematical modeling and dynamic simulink simulation of high-pressure pem electrolyzer system," *International Journal of Hydrogen Energy*, vol. 41, no. 32, pp. 13901 – 13914, 2016.

[96] A. S. Tijani, N. A. B. Yusup, and A. A. Rahim, "Mathematical modelling and simulation analysis of advanced alkaline electrolyzer system for hydrogen production," *Procedia Technology*, vol. 15, pp. 798–806, 2014.

[97] J. O. Jensen, A. P. Vestbø, Q. Li, and N. Bjerrum, "The energy efficiency of onboard hydrogen storage," *Journal of Alloys and Compounds*, vol. 446, pp. 723–728, 2007.

[98] B. Sliz-Szkliniarz, J. Eberbach, B. Hoffmann, and M. Fortin, "Assessing the cost of onshore wind development scenarios: Modelling of spatial and temporal distribution of wind power for the case of poland," *Renewable and Sustainable Energy Reviews*, vol. 109, pp. 514–531, 2019.

[99] M. de Simón-Martín, Á. de la Puente-Gil, D. Borge-Diez, T. Ciria-Garcés, and A. González-Martínez, "Wind energy planning for a sustainable transition to a decarbonized generation scenario based on the opportunity cost of the wind energy: Spanish iberian peninsula as case study," *Energy Procedia*, vol. 157, pp. 1144–1163, 2019.

[100] M. Taylor, P. Ralon, and A. Ilas, "The power to change: solar and wind cost reduction potential to 2025," *International Renewable Energy Agency (IRENA)*, 2016.

[101] J. Pratt, D. Terlip, C. Ainscough, J. Kurtz, and A. Elgowainy, "H2first reference station design task: Project deliverable 2-2," tech. rep., National Renewable Energy Lab.(NREL), Golden, CO (United States), 2015.

[102] U. DOE, "The fuel cell technologies office multi-year research, development, and demonstration plan," tech. rep., Tech. rep., US Department of Energy, 2016.

[103] Ø. Ulleberg and R. Hancke, "Techno-economic calculations of small-scale hydrogen supply systems for zero emission transport in norway," *International Journal of Hydrogen Energy*, 2019.

[104] T. Nguyen, Z. Abdin, T. Holm, and W. Mérida, "Grid-connected hydrogen production via large-scale water electrolysis," *Energy Conversion and Management*, vol. 200, p. 112108, 2019.

[105] G. Parks, R. Boyd, J. Cornish, and R. Remick, "Hydrogen station compression, storage, and dispensing technical status and costs: Systems integration," tech. rep., National Renewable Energy Lab.(NREL), Golden, CO (United States), 2014.

[106] T. A. Gunawana, A. Singliticoa, P. Blount, J. G. Carton, and R. F. Monaghan, "Towards techno-economic evaluation of renewable hydrogen production from wind curtailment and injection into the irish gas network,"

[107] C. F. Guerra, M. J. Caparrós, B. N. Calderón, V. S. Carbonero, E. N. Gallego, L. Reyes-Bozo, A. Godoy-Faundez, C. Clemente-Jul, and E. Vyhmeister, "Viability analysis of centralized hydrogen generation plant for use in mobility sector," *International Journal of Hydrogen Energy*, vol. 43, no. 26, pp. 11793–11802, 2018.

[108] D. Baldwin, "Development of high pressure hydrogen storage tank for storage and gaseous truck delivery," tech. rep., Hexagon Lincoln LLC, Lincoln, NE (United States), 2017.

[109] C. Chardonnet, V. Giordano, L. De Vos, F. Bart, and T. De Lacroix, "Study on early business cases for h2 in energy storage and more broadly power to h2 applications," *FCH-JU: Brussels, Belgium*, vol. 228, 2017.

[110] R. H. Wiser, M. Bolinger, and E. Lantz, "Benchmarking wind power operating costs in the united states: Results from a survey of wind industry experts," 2019.

[111] M. Fasihi and C. Breyer, "Baseload electricity and hydrogen supply based on hybrid pv-wind power plants," *Journal of Cleaner Production*, p. 118466, 2019.

[112] M. F. Andrea, R. H. Sara, S. S. Giovanni, B. Enrico, *et al.*, "Techno-economic analysis of in-situ production by electrolysis, biomass gasification and delivery systems for hydrogen refuelling stations: Rome case study," *Energy Procedia*, vol. 148, pp. 82–89, 2018.

[113] "Aandeel hernieuwbare energie naar 7,4 procent," May 2019. Centraal Bureau voor de Statistiek.

[114] "Electricity price statistics," May 2019. Electricity price statistics - Statistics Explained, Accessed: 2019-05-04.

[115] M. Afman, S. Hers, and T. Scholten, *Energy and electricity price scenarios 2020-2023-2030.* 2017.

[116] "Kosten met watermeter." https://www.waternet.nl/service-en-contact/drinkwater/kosten/met-watermeter/, Accessed: 11-11-2019.

[117] J. Adolf, C. H. Balzer, J. Louis, U. Schabla, M. Fischedick, K. Arnold, A. Pastowski, and D. Schüwer, "Energy of the future?: Sustainable mobility through fuel cells and h2; shell hydrogen study," 2017.

[118] G. Saur and C. Ainscough, "Us geographic analysis of the cost of hydrogen from electrolysis," tech. rep., National Renewable Energy Lab.(NREL), Golden, CO (United States), 2011.

[119] O. J. Guerra Fernandez, J. D. Eichman, B. S. Hodge, and J. M. Kurtz, "Cost-competitive electrolysis-based hydrogen under current us electric utility rates," tech. rep., National Renewable Energy Lab.(NREL), Golden, CO (United States), 2018.

[120] *Hydrogen: A renewable energy perspective.* 2019. International Renewable Energy Agency.

[121] N. Popovich, "Us department of energy hydrogen and fuel cells program 2016 annual merit review and peer evaluation report: June 6-10, 2016, washington, dc," tech. rep., National Renewable Energy Lab.(NREL), Golden, CO (United States), 2016.

[122] W. Zhang, F. Ren, Z. Feng, and J. Wang, ""manufacturing cost analysis of novel steel/concrete composite vessel for stationary storage of high-pressure hydrogen," *no. September*, 2012.

[123] Z. Feng, J. Wang, and W. Zhang, "Vessel design and fabrication technology for stationary high-pressure hydrogen storage," *ORNL*, 2012.

[124] "Innovation center for energy and transportation (icet), fuel economy in major car markets," tech. rep., 2019. IEA, Paris (2019), www.iea.org/topics/transport/gfei/report/.

[125] Nov 2019. https://opendata.cbs.nl/statline//CBS/nl/dataset/80416NED/table?fromstatweb, Accessed: 19-11-2019.

[126] P. Larscheid, L. Lück, and A. Moser, "Potential of new business models for grid integrated water electrolysis," *Renewable Energy*, vol. 125, pp. 599 – 608, 2018.